

Marc Arriaza i Bosch

Concrete delamination detection using the impulse response method

Bachelor's project in Industrial Engineering

Supervisor: Daniel Cantero

December 2019

NTNU
Norwegian University of Science and Technology
Faculty of Engineering
Department of Structural Engineering



Marc Arriaza i Bosch

Concrete delamination detection using the impulse response method

Bachelor's project in Industrial Engineering
Supervisor: Daniel Cantero
December 2019

Norwegian University of Science and Technology
Faculty of Engineering
Department of Structural Engineering

Table of contents

Abstract	III
Sammendrag	III
Preface	IV
Acknowledgments	IV
List of figures	V
List of equations	VII
List of tables	VII
1. Introduction	1
1.1. Motivation	1
1.2. Objectives.....	1
1.3. Thesis structure	1
2. Theoretical background	2
2.1. Delamination	2
2.1.1. Delamination, causes and effects	2
2.1.2. Detecting methods.....	3
2.1.2.1. Visual inspection	6
2.1.2.2. Ultrasonic methods	7
2.1.2.2.1. Ultrasonic pulse echo	7
2.1.2.2.2. Ultrasonic pulse velocity	8
2.1.2.3. Infrared thermography.....	10
2.1.2.4. Ground penetrating radar	10
2.1.2.5. Impact testing.....	12
2.1.2.5.1. Acoustic impact test	12
2.1.2.5.2. Impact echo test.....	13
2.1.2.5.3. Frequency response functions	15
2.1.2.5.3.1. Impulse response test	15
2.1.2.5.3.1.1. Data processing.....	16
2.1.2.5.3.1.2. Interpretation of results.....	17
2.1.2.5.3.1.3. Factors affecting the response.....	19
2.1.2.5.3.1.4. Advantages and limitations.....	19
3. Implementation of the impulse response method	20
3.1. Hardware.....	22
3.1.1. Instrumented hammer	22

3.1.2.	Accelerometer	23
3.1.3.	Central unit.....	24
3.2.	Software	24
4.	Experimental setup	27
4.1.	Artificial delamination.....	27
4.1.1.	3D printed piece.....	27
4.1.2.	Moulds.....	29
4.1.3.	Concrete casting.....	31
4.1.4.	Test setup	35
5.	Results and discussion.....	38
6.	Future recommendations	50
7.	Conclusion	51
8.	References.....	52
Appendix	55
Appendix A: Results.....	55
Appendix A.1: Accelerance plots for the measurements done with the hard plastic tip with the blue cover	55
Appendix A.2: Accelerance plots for the measurements done with the metal tip.....	58
Appendix B: <i>MATLAB</i> scripts	62
Appendix B.1: Main script and functions	62
Appendix B.2: Accelerance script.....	71
Appendix C: Concrete recipe.....	74
Appendix D: Concrete weight and strength measurements.....	82
Appendix E: Drawings of the 3D printed pieces and the moulds.....	85

Abstract

Concrete is known for being a reliable construction material for building all kind of structures. Nevertheless, internal defects such as delamination can reduce significantly the service life of concrete.

Delamination is a type of internal defect that affects concrete structures causing a separation in the layers of concrete that produces an internal void. If not detected prematurely, delamination could lead to a loss of mechanical properties of the structure.

The purpose of this thesis is to develop an automatic software for detecting delamination in concrete structures.

For better understanding and increasing the knowledge on this field, an overview of the main non-destructive testing methods has been made. The impulse response test has been the one chosen for detecting delamination in this research. A delamination detecting method has been developed using the *MATLAB* software.

In the experimental part, artificial delamination was simulated with 3D printed pieces placed inside the concrete slabs at different depths.

The results from the experimental tests are represented with the mobility plot obtained with the impulse response method. Due to that it hasn't been possible to detect delamination in the mobility plot, results are also given with the accelerance function, where delamination could have been detected in two different depths.

Sammendrag

Betongdelaminering er en type indre defekter som påvirker betongkonstruksjoner og forårsaker en separasjon i lagene i betongen som forårsaker et indre tomrom. Hvis det ikke oppdages, kan delaminering føre til at strukturen taper mekaniske egenskaper.

Hensikten med denne oppgaven er å utvikle programvare som automatisk oppdager delaminering i betongkonstruksjoner. I den eksperimentelle delen ble kunstig delaminering simulert med 3D-printede elementer plassert inne i betongplatene på forskjellige dybder.

Resultatene fra eksperimentene er representert ved bruk av impulsresponsmetoden med et mobilitetsplott.

Preface

This bachelor thesis has been written at the Norwegian University of Science and Technology (NTNU) during an Erasmus programme. It is the final work of my Bachelor Degree in Industrial Engineering at Universitat Politècnica de Barcelona (UPC).

From the personal side, structural engineering is one of the topics inside the Bachelor Degree that I have more interest for. This project will help me to expand my knowledge in this field and also will help me to apply what I have learnt in my further master studies and also in the professional field.

Acknowledgments

First of all, I would like to give my appreciation to my supervisor Daniel Cantero, for all the feedback and help received during the semester. I would also like to thank Terje Kanstad for being my first contact at NTNU and for assigning me this thesis and supervisor.

Secondly, I would like to thank all the technical staff at the NTNU concrete laboratory who helped me with the experimental work, in special to Per Øystein Nordtug.

I would also like to thank Assís Aranó, PhD candidate at NTNU, who has been one of the most important people during my stay in Trondheim.

Finally, I would like to extend my appreciation to my family and friends, for the visits received in Trondheim, for supporting me in the personal side but also giving me feedback on the thesis.

List of figures

Figure 1: Concrete delamination due to reinforcement corrosion [1]	2
Figure 2: Delaminated surface [4]	4
Figure 3: Operating process of the ultrasonic pulse echo [5]	4
Figure 4: Operating process of the ultrasonic pulse velocity [6]	4
Figure 5: Operating process of the infrared thermography [7]	5
Figure 6: Operating process of the ground penetrating radar [8]	5
Figure 7: Operating process of the acoustic impact test [9]	5
Figure 8: Operating process of the impact echo test [10]	6
Figure 9: Operating process of the Impulse response test [11]	6
Figure 10: Delaminated concrete surface [12]	7
Figure 11: Ultrasonic pulse echo method [5]	8
Figure 12: Types of recording the signals with the ultrasonic pulse velocity method [13]	8
Figure 13: Internal imperfections detection with ultrasonic velocity pulse method [14]	9
Figure 14: Operating principle of the ground penetrating radar [15]	11
Figure 15: Data acquisition on a bridge deck using air-coupled GPR [15]	11
Figure 16: Data acquisition on a bridge deck using ground- coupled GPR [15]	11
Figure 17: Acoustic impact test performed a with hammer [16]	12
Figure 18: Chain drag tool [16]	12
Figure 19: Operating diagram of the impact echo test [17]	13
Figure 20: Frequency spectrum for a slab in good condition [18]	13
Figure 21: Frequency spectrum for a slab in fair condition [18]	14
Figure 22: Frequency spectrum for slabs in poor and serious condition respectively [18]	14
Figure 23: Typical mobility plot [19]	16
Figure 24: Mobility plot of concrete with a void below the slab [21]	17
Figure 25: Mobility plot for honeycombed concrete [21]	18
Figure 26: Instrumented hammer PCB 086C03 [24]	22
Figure 27: Frequency response of the different types of tips [25]	23
Figure 28: Accelerometer PCB 352C03 [26]	23
Figure 29: NI 9234 [27]	24
Figure 30: NI cDAQ 9174 [28]	24
Figure 31: 3D printing process	27
Figure 32: Design in <i>Solidworks</i> for the 3D printed piece	28
Figure 33: 3D printed piece	28
Figure 34: 3D printed part attached with screws	29
Figure 35: 3D printed parts attached with glue	29
Figure 36: Position of the 3D printed pieces inside the mould in <i>Solidworks</i>	30
Figure 37: Position of the 3D printed pieces (represented in black) inside the mould.	30
Figure 38: Ingredients for the concrete mix	31
Figure 39: Mixing machine	31
Figure 40: Mixing procedure (Blandeprosedyre)	32
Figure 41: Wet blending process	32
Figure 42: Concrete mix	33
Figure 43: Concrete poured inside the moulds	33
Figure 44: Concrete slabs covered with plastic for curing	33
Figure 45: Lateral view of the healthy slab	34

Figure 46: Lateral view and detailed view of the 15mm depth slab.....	34
Figure 47: Lateral view and detailed view of the 30mm depth slab.....	34
Figure 48: Compressive strength test	35
Figure 49: Fractured test specimen	35
Figure 50: Drawing of the impact points and accelerometers position.....	36
Figure 51: Hitting points on one of the test slabs	37
Figure 52: Attachment of the accelerometer	37
Figure 53: Mobility plot obtained from a test hit	38
Figure 54: Mobility plot for the slab 1 and position 1.....	39
Figure 55: Mobility plot for the slab 2 and position 1.....	39
Figure 56: Mobility plot for the slab 3 and position 1.....	40
Figure 57: Frequency measurement range depending on the type of mount of the accelerometer [35].....	41
Figure 58: Force time history of five measurements done in one position.....	42
Figure 59: Acceleration time history of five measurements done in one position.....	42
Figure 60: Force frequency spectrum for 5 measurements of the same position	43
Figure 61: Acceleration frequency spectrum for 5 measurements of the same position	43
Figure 62: Comparison of the acceleration frequency spectrum between the three slabs in position 1.....	44
Figure 63: Comparison of the acceleration frequency spectrum between three slabs in position 4.....	45
Figure 64: accelerance plot for the four positions in slab 1.....	46
Figure 65: Accelerance plot for the four positions in slab 2	46
Figure 66: Accelerance plot for the four positions in slab 3	47
Figure 67: accelerance plot for the three slabs in position 1.....	47
Figure 68: Accelerance plot for the three slabs in position 2	48
Figure 69: Accelerance plot for the three slabs in position 3	48
Figure 70: Accelerance plot for the three slabs in position 4	49
Figure 71: Types of mounts for the accelerometer and their sensitivity deviations [26].....	50
Figure 72: Accelerance plot of the average of five hits on the four positions in slab 1.....	55
Figure 73: Accelerance plot of the average of the five hits on the four positions in slab 2	55
Figure 74: Accelerance plot of the average of the five hits on the four positions in slab 3	56
Figure 75: Accelerance plot of the average of the five hits on position 1 for the three slabs....	56
Figure 76: Accelerance plot of the average of the five hits on position 2 for the three slabs....	57
Figure 77: Accelerance plot of the average of the five hits on position 3 for the three slabs....	57
Figure 78: Accelerance plot of the average of the five hits on position 4 for the three slabs....	58
Figure 79: Accelerance plot of the average of the five hits on the four positions of slab 1	58
Figure 80: Accelerance plot of the average of the five hits on the four positions of slab 2	59
Figure 81: Accelerance plot of the average of the five hits on the four positions of slab 3	59
Figure 82: Accelerance plot of the average of the five hits on position 1 for the three slabs....	60
Figure 83: Accelerance plot of the average of the five hits on position 2 for the three slabs....	60
Figure 84: Accelerance plot of the average of the five hits on position 3 for the three slabs....	61
Figure 85: Accelerance plot of the average of the five hits on position 4 for the three slabs....	61

List of equations

Equation 1: Pulse velocity calculation	9
Equation 2: Compliance function	15
Equation 3: Mobility function	15
Equation 4: Accelerance function	15
Equation 5: Mobility plot calculation	16

List of tables

Table 1: Summary of the main non-destructive testing methods for delamination	6
Table 2: Concrete quality based on the pulse velocity recorded	9
Table 3: Concrete condition corresponding to values of average mobility	18

1. Introduction

1.1. Motivation

Concrete delamination is affecting a great number of concrete structures from bridge decks to concrete floors. Detection of delamination in these structures is usually done using an acoustic impact echo test. This test is performed by tapping with a hammer on the concrete surface and hearing variation in the pitch of the sound emitted by the impact. Although this method is valid and widely used, it is very subjective, effectivity depends on the experience of the operator, it's impossible to know the depth of the delaminated part, it is very difficult to find deep delamination and can't be used in noisy environments.

1.2. Objectives

The main objectives for this thesis are:

- Developing an automatic method for detecting delamination that solves some of the problems seen in the acoustic impact echo test.
- Selecting a method for analysing the data recorded and being able to detect delamination based on the selected method.
- Creating artificial delamination inside the concrete in order to test the program developed.

1.3. Thesis structure

The thesis is divided in four main parts:

- In the first part, the delamination problem is presented and a review of the main non-destructive testing methods is done.
- In the second part, how the selected method for detecting delamination will be applied is explained.
- In the third part, the experimental work is presented, from creating artificial delamination to the testing setup.
- Finally, the results are shown and discussed.

2. Theoretical background

2.1. Delamination

2.1.1. Delamination, causes and effects

Delamination is a type of internal defect that affects concrete structures where a layer of concrete is separated from the base slab, normally parallel and near the surface, causing a void inside the structure filled with air or water.

Delamination is most of the times produced by climatic and exposure conditions. Four of the main causes why delamination occurs are:

- Freeze-thaw successive cycles: This phenomenon happens with porous concrete that is able to absorb water. When water flows inside the concrete structure and freezes due to climatic conditions, the water will expand causing little cracks and tensions inside the concrete.
- Bleeding: This process is caused by a non-uniform composition of the concrete at different depths. When concrete is compacted, the solids settle, causing lighter materials like air and water to migrate near the surface. If the concrete surface is densified or sealed prematurely while bleeding is occurring, the materials that should migrate upwards are trapped under the surface, causing voids inside the concrete slab.
- Corrosion in the reinforcement: This is the main reason why delamination appears in concrete structures. When corrosion affects the concrete reinforcement, it will expand generating forces towards the concrete. If these forces are bigger than the tensile strength of concrete, cracking will appear around the reinforcement. When these cracks propagate and meet other neighbour cracks, a fracture plane is formed running through all the rebars (figure 1).

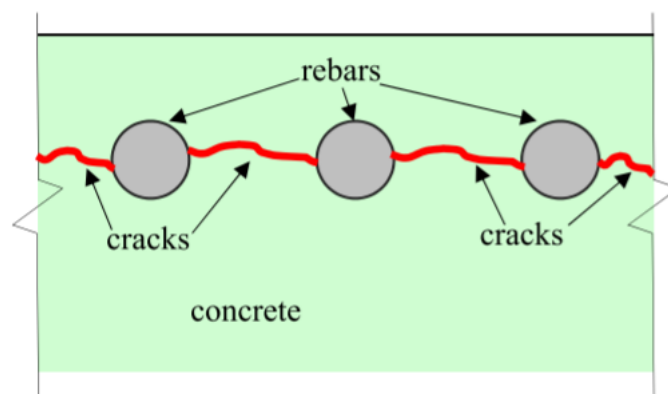


FIGURE 1: CONCRETE DELAMINATION DUE TO REINFORCEMENT CORROSION [1]

- Alkali-aggregates reactions: These reactions take place when certain aggregates containing reactive forms of silica react with sodium, potassium and calcium hydroxide from the cement paste, forming gel around the aggregates. With the presence of moisture, the gel will expand creating little cracks in the concrete and also making it less impermeable.
- Sulphate reactions: In this group we find all the reactions where the sulphate ions (SO_4) are present. When reacting with the cement compounds, ettringite and thaumasite are formed. Ettringite formation is a very expansive reaction that will result in cracking. Thaumasite is not expansive but causes concrete disaggregation. Some examples of sulphate sources would be atmospheric pollution, decomposition of organic matter or maritime environments.

If not detected prematurely, delamination could cause a loss of adhesion between the steel reinforcement and the concrete and could affect at the stability and properties of the structure, as we can see in the following studies:


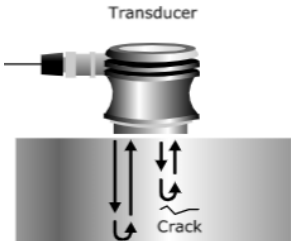
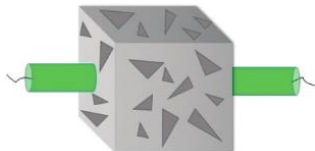
- [2] reported that delamination caused a decrease in the initial stiffness of the structure in the punching shear test. Progressive delamination produced a 3% decrease in the punching shear capacity and critical delamination reduced it a 12%.
- [3] found that concrete with delamination sustained between a 9% and 32% lower load before punching shear failure than concrete with delamination¹. Also, reinforced concrete with delamination had a lower pre punching stiffness and post punching stiffness in the punching shear test.

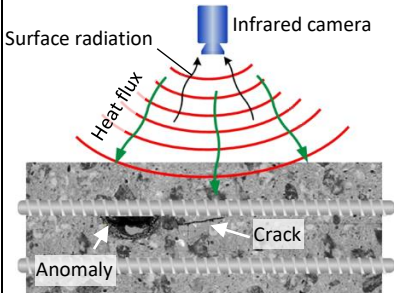
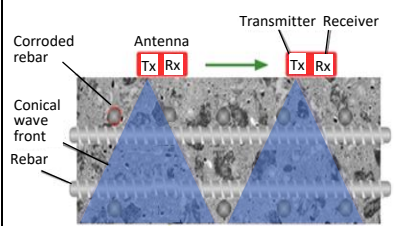
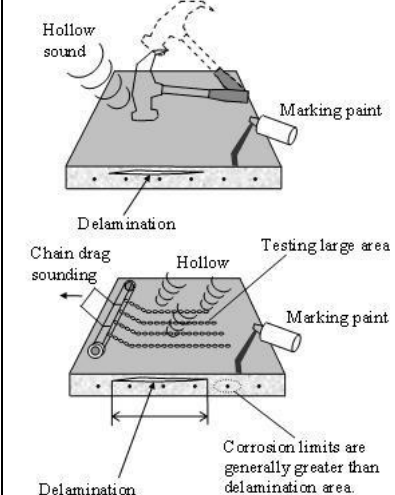
2.1.2. Detecting methods

Detecting methods for delamination are divided in destructive and non-destructive. De-assembling the structure and looking inside is the most reliable way for looking at internal defects in concrete. Nevertheless, that isn't always the optimal solution due to the high cost and time consumed. Non-destructive methods offer a fast and also reliable way for searching at imperfections inside the structure.

In the table 1, we can see a summary of the most used non-destructive methods for detecting delamination in concrete, with the advantages and disadvantages of each one. Also, all these techniques will be explained further down in more detail, especially the impulse response test, that will be the one developed in the experimental part.

¹ Values depend on the type of reinforcement built in each specimen tested.

Name and picture	Technology used	Advantages	Disadvantages
<p>Visual inspection</p>  <p>FIGURE 2: DELAMINATED SURFACE [4]</p>	<p>Examination of the surface performed by a human eye looking for imperfections on the concrete surface.</p>	<ul style="list-style-type: none"> - Simple and inexpensive instrumentation. - Effective for delamination seen from the surface. 	<ul style="list-style-type: none"> - Well trained-eye required. - Impossible to detect internal delamination.
<p>Ultrasonic pulse echo</p>  <p>FIGURE 3: OPERATING PROCESS OF THE ULTRASONIC PULSE ECHO [5]</p>	<p>Reflected ultrasonic waves generated by an electro-acoustical transducer.</p>	<ul style="list-style-type: none"> - Well-known and widely used method for detecting delamination. - Immediate results. - Determination of the depth and orientation of the delamination. - Also used for measuring the slab thickness. 	<ul style="list-style-type: none"> - Requires a coupling gel between the transducer and the testing surface. - Difficulty in rough parts, irregular or not homogeneous shapes. - Expert technicians required.
<p>Ultrasonic pulse velocity</p>  <p>FIGURE 4: OPERATING PROCESS OF THE ULTRASONIC PULSE VELOCITY [6]</p>	<p>Ultrasonic waves generated by an electro-acoustical transducer and converted into electrical signal by a second transducer.</p>	<ul style="list-style-type: none"> - Portable equipment, fast and reliable. - Apart from locating internal imperfections, it can also measure the concrete quality. 	<ul style="list-style-type: none"> - Requires a coupling gel between the transducer and the testing surface. - Difficulty of measuring in rough and irregular parts or in not homogeneous shapes. - Expert technicians required.

<p>Infrared thermography</p>  <p>FIGURE 5: OPERATING PROCESS OF THE INFRARED THERMOGRAPHY [7]</p>	<p>Reflection of infrared radiation of materials caused by different temperatures of the different materials inside the concrete while heated.</p>	<ul style="list-style-type: none"> - Fast method suitable for big structures, especially the passive thermography. -Fast and easy equipment setup. 	<ul style="list-style-type: none"> - Doesn't provide information about the depth of the defect. - Measurements affected by changes in external conditions such as temperature and wind speed. - High cost of the equipment.
<p>Ground penetrating radar (GPR)</p>  <p>FIGURE 6: OPERATING PROCESS OF THE GROUND PENETRATING RADAR [8]</p>	<p>Reflection of short electromagnetic pulses in materials that have different electromagnetic properties.</p>	<ul style="list-style-type: none"> -Fast method, suitable for inspecting large areas. -Reliable and repeatable 	<ul style="list-style-type: none"> - Requires advanced training for data collection and interpretation. - Data collection negatively affected in very cold climates, also de-icing agents can compromise signal penetration.
<p>Acoustic impact test</p>  <p>FIGURE 7: OPERATING PROCESS OF THE ACOUSTIC IMPACT TEST [9]</p>	<p>Changes in sound pitch heard by the operator while tapping the concrete surface with a hammer for small areas or dragging chains for large areas.</p>	<ul style="list-style-type: none"> - Simple and inexpensive equipment. - No post-processing of the data is required. 	<ul style="list-style-type: none"> - Not suitable for noisy environments. - Accuracy may depend on the experience of the operator. - Very deep delamination can't be detected. - No possibility of knowing the depth of the delamination.

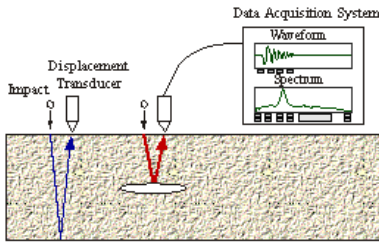
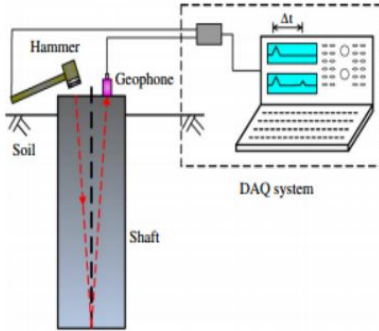
<p>Impact echo</p>  <p>FIGURE 8: OPERATING PROCESS OF THE IMPACT ECHO TEST [10]</p>	<p>P-waves (compression waves), created by an impact on the surface, reflect on the slab boundaries as well as in internal imperfections. The frequency spectrum of the response of the excited structure is analysed to locate any internal defects.</p>	<ul style="list-style-type: none"> - Easy to perform by a single operator. - The depth of the delamination can be determined. - The depth of the tested structure can be also determined. 	<ul style="list-style-type: none"> - Only used in small areas, because it can only measure the structure below the impact point.
<p>Impulse response</p>  <p>FIGURE 9: OPERATING PROCESS OF THE IMPULSE RESPONSE TEST [11]</p>	<p>Flexibility of the structure in the area around the impact point. An instrumented hammer collects the time history of the force, while a geophone collects velocity time history. With these data recorded, a mobility plot is obtained.</p>	<ul style="list-style-type: none"> - Robust, fast and repeatable. - A small area is measured with one hit, what results in faster analysis of the structure. 	<ul style="list-style-type: none"> - Can't provide information about the depth of delamination. - Requires skilled data interpretation.

TABLE 1: SUMMARY OF THE MAIN NON-DESTRUCTIVE TESTING METHODS FOR DELAMINATION

2.1.2.1. Visual inspection

Visual inspection is the first check that should be done before using other destructive or non-destructive methods. This test can be very useful to detect shallower delamination that can be seen from the surface. Instrumentation for this method is very simple and cheap (e.g. rulers, markers, binoculars...) but it requires a well-trained eye for doing the inspection.



FIGURE 10: DELAMINATED CONCRETE SURFACE [12]

2.1.2.2. Ultrasonic methods

2.1.2.2.1. Ultrasonic pulse echo

The ultrasonic pulse echo method is based on the use of ultrasonic waves for locating internal defects in concrete. These waves are generated by an electro-acoustical transducer in contact with one surface of the concrete tested, usually at a frequency between 2 and 5 MHz. The pulse is transmitted to the concrete structure through a liquid coupling material such as cellulose paste or grease. Once the pulse is generated, a complex system of longitudinal and transversal waves develops inside the concrete tested. If there is some kind of internal defect such as delamination, part of the energy of the wave will be reflected back from the internal imperfection. The sound energy is converted to an electrical signal by the transducer and then is displayed on a screen.

In case a delamination is located, we can get several information about it, such as the location, size or orientation. If desired, the thickness of the concrete slab could also be measured.

One of the main limitations for this method is the difficulty to inspect rough parts, very thin or small, due to the need of coupling the transducer in a flat surface. Also, expensive technical knowledge is required for manual operation and getting accurate measurements without added noise.

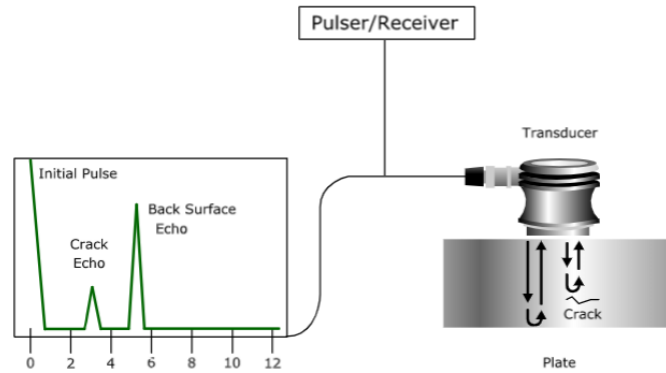


FIGURE 11: ULTRASONIC PULSE ECHO METHOD [5]

2.1.2.2.2. Ultrasonic pulse velocity

This method also uses ultrasonic waves that go through the tested concrete structure. Two transducers are used: the first one is generating the signal and the second one is collecting the signal, instead of recording the echo of the generated signal with the same transducer like in the ultrasonic pulse echo. The second transducer also converts the recorded signal into an electrical signal. Signals can be received with a direct, semi-direct or indirect way. The direct way is the most sensitive while the indirect way is the least, so indirect transmission should be used when only one face of the concrete structure is accessible.

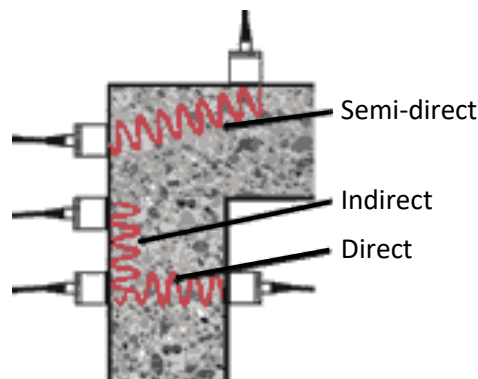


FIGURE 12: TYPES OF RECORDING THE SIGNALS WITH THE ULTRASONIC PULSE VELOCITY METHOD [13]

Internal defects such as delamination or cracks can also be detected with this method due to the fact that the transmission of the signal through voids with air is negligible compared to the transmission through solid concrete. Then, the first pulse to arrive to the receiving transducer will take more time to go around the periphery of the void. In case the void is very large, the signal may not arrive at the receiving transducer (figure 13).

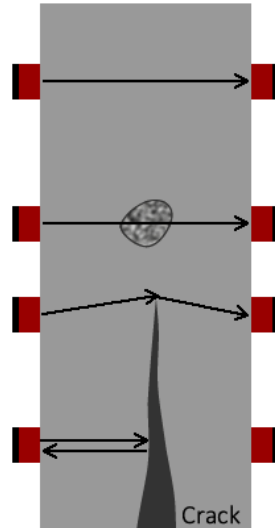


FIGURE 13: INTERNAL IMPERFECTIONS DETECTION WITH ULTRASONIC VELOCITY PULSE METHOD [14]

With this method, the concrete quality can also be measured by knowing the pulse velocity, which can be obtained with equation 1, and looking at the reference table (table 2).

$$v = \frac{1}{t}$$

EQUATION 1: PULSE VELOCITY CALCULATION

Where t is the time between the signal leaves the first transducer and arrives to the second one.

Pulse velocity	Concrete quality
>4.0 km/s	Very good to excellent
3.5 – 4.0 km/s	Good to very good, slight porosity may exist
3.0 – 3.5 km/s	Satisfactory but loss of integrity is suspected
<3.0 km/s	Poor and loss of integrity exist.

TABLE 2²: CONCRETE QUALITY BASED ON THE PULSE VELOCITY RECORDED

The ultrasonic pulse velocity test is usually applied using a portable equipment, offering a very fast and reliable way for detecting internal imperfections in concrete. However, like in the ultrasonic pulse echo test, it requires experienced technicians, it might be difficult to inspect structures with rough surface and a coupling gel between the transducers and the concrete is also required.

² Table from: IS 1331 (Part 1), Table 2

2.1.2.3. Infrared thermography

The infrared thermography test is based on the Law of Planck and the principle that all objects above absolute zero emit infrared radiation. For the human eye, radiation becomes visible only when the temperature is above 500°C. The infrared thermography equipment can detect reflected radiations at lower temperatures and represent it as a visible image. The method is based on heating up the test surface to create thermal contrasts between the internal defects and the rest of the structure. These imperfections are normally filled with water or air and have a different thermal capacity than concrete, what results in different times for heating up the areas on top of delamination and the rest of the structure. Infrared thermography is divided in passive and active: in passive infrared thermography, natural heating sources like the sun are used, while in active other artificial heating sources are used such as halogen lamps. Active thermography may produce better controlled and quality results, but it is not suitable for testing big structures like bridge decks.

The equipment consists of:

- Infrared camera: It has a similar appearance to a video camera, normally can be used with interchangeable lenses and has a precision of 0.1°C. The different recorded temperatures in the image are transformed into a colour code creating a thermogram.
- Data acquisition and analysis equipment: It consists on a software for data storage and analysis.
- Recording and retrieving devices: Used to record visual and thermal images. Video tape recorders, cameras and computer printed images are included inside this group. In modern setups, these additional recording devices are not used because the infrared camera is capable of recording infrared radiation and high-resolution video images simultaneously.

This method is widely used for fast and reliable inspection of concrete structures, being capable of analysing big structures instantaneously. Nevertheless, it has some disadvantages such as the high cost for the instrumentation and the variation in the results due to external factors while recording such as the surface quality, wind speed or ambient temperature, especially when the passive thermography is used. Also, it doesn't provide information about the depth of the defect.

2.1.2.4. Ground penetrating radar

Ground penetrating radar (GPR) is the electromagnetic analogue of the ultrasonic pulse echo method. It is based on the propagation of short electromagnetic impulses, with a duration of $\leq 1\text{ns}$ ($1 \cdot 10^{-9}\text{s}$) inside the tested structure. An emitter antenna creates these very short pulses that reflect on the interfaces between materials with different electromagnetic properties (figure 14). The reflected signal travels back to the surface and there it is registered by a receiver antenna. The presence of internal defects or rebars is determined by knowing some properties of the signal received such as the speed of the returning signal, amplitude, attenuation, signal polarity or wave length.

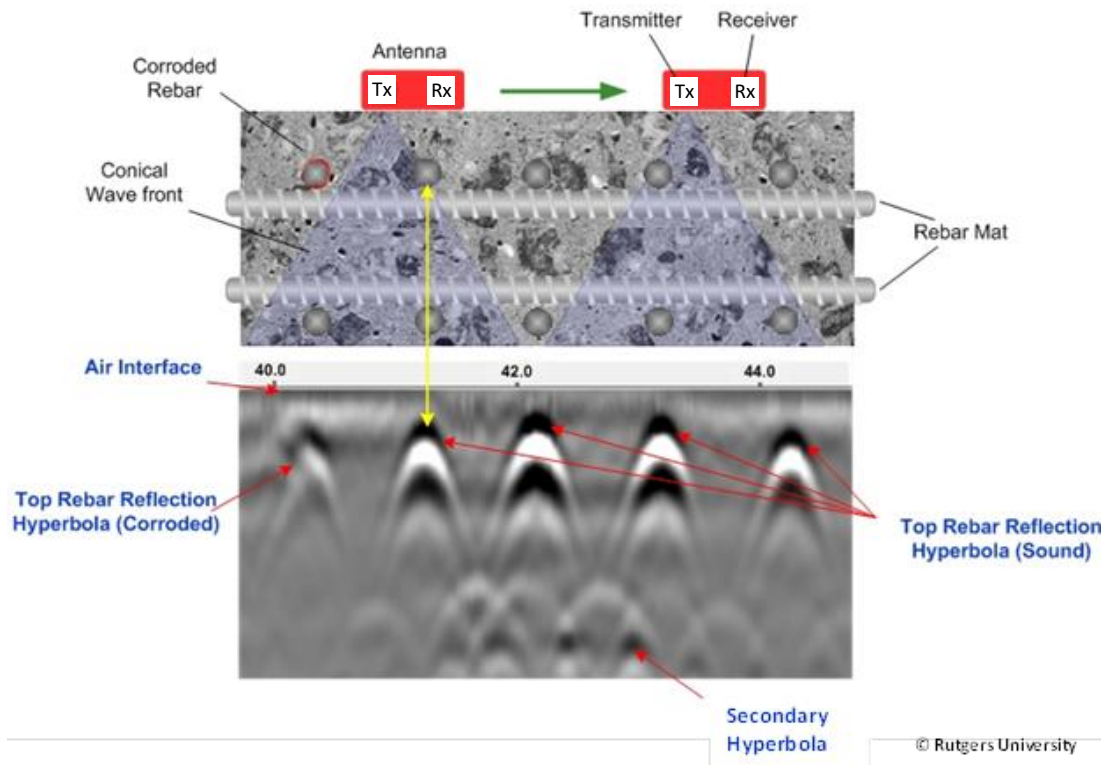


FIGURE 14: OPERATING PRINCIPLE OF THE GROUND PENETRATING RADAR [15]

This method is used for searching internal defects in big structures such as highway pavements and its foundations or bridge decks. It is also used in ice studies as well as archaeological research.

One of the main advantages is that it can map large areas of big structures in a short time due to the fact that it could be performed either air-coupled (figure 15) or ground-coupled (figure 16).



FIGURE 15: DATA ACQUISITION ON A BRIDGE DECK USING AIR-COUPLED GPR [15]



FIGURE 16: DATA ACQUISITION ON A BRIDGE DECK USING GROUND- COUPLED GPR [15]

On the other hand, it requires advanced training for data processing and interpretation and it is not suitable for cold environments, because data could be negatively influenced by cold conditions and de-icing agents can decrease signal penetration.

2.1.2.5. Impact testing

2.1.2.5.1. Acoustic impact test

Detecting delamination through sound is probably one of the most used methods for detecting delamination. This test is usually performed with a hammer for small areas (figure 17) or with chains for larger areas (figure 18). Delamination is detected based on the change of pitch in the sound of the impact.

The main advantages of this method are that is cheap, uses very basic instrumentation and no post processing of the data acquired is required. On the other hand, its main disadvantages are that very deep delamination can't be detected as well as it is not possible to know the depth of the delamination found. Moreover, this method can't be done in very noisy environments and the exactitude may depend on the experience of the operator.



© Rutgers University

FIGURE 17: ACOUSTIC IMPACT TEST PERFORMED A WITH HAMMER [16]



© Rutgers University

FIGURE 18: CHAIN DRAG TOOL [16]

2.1.2.5.2. Impact echo test

This method is based on producing an impact on the concrete surface which creates P-waves (compression waves) that propagate through the structure and are reflected by internal imperfections and external surfaces. When the reflected waves return to the surface, they produce displacements which are measured by the transducer. The time-displacement response recorded is transformed to frequency domain using a Fast Fourier Transform algorithm.

The necessary equipment includes a mechanical spherical impactor source (from 3 to 12mm of diameter), a transducer located approximately 5cm away from the impact point and a data acquisition system for saving and post processing the signals.

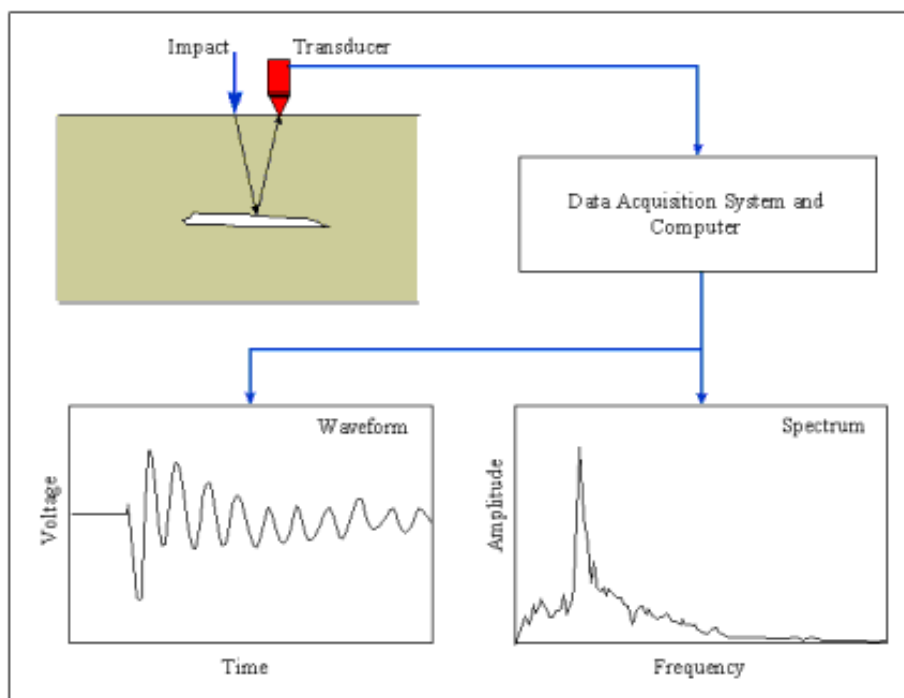


FIGURE 19: OPERATING DIAGRAM OF THE IMPACT ECHO TEST [17]

For structures without any internal defect, only one peak will appear in the frequency spectrum, corresponding to the bottom part of the structure tested.

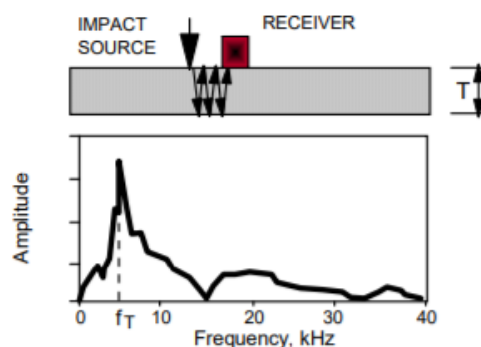


FIGURE 20: FREQUENCY SPECTRUM FOR A SLAB IN GOOD CONDITION [18]

For an initial delamination, the frequency spectrum will show two peaks. This will happen because the internal defect is not very developed yet, so it will reflect some waves as well as letting pass the others left. Therefore, one of the peaks will correspond to the internal defect, and the other to the bottom of the slab.

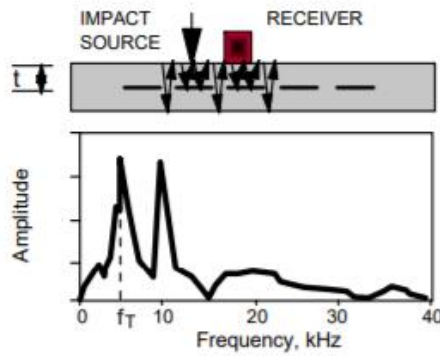


FIGURE 21: FREQUENCY SPECTRUM FOR A SLAB IN FAIR CONDITION [18]

For more severe delamination, the waves will not be able to go through the delaminated part, causing only one peak in the frequency spectrum corresponding to that delamination.

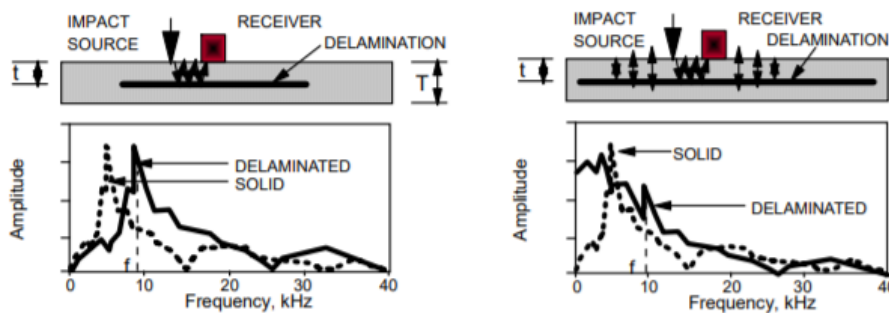


FIGURE 22: FREQUENCY SPECTRUM FOR SLABS IN POOR AND SERIOUS CONDITION RESPECTIVELY [18]

With this method it is possible to determine the depth of the internal defect by measuring the speed and frequency of the reflected waves. Another great advantage is that the test could be performed by only one operator in a short period of time (15-20 seconds/test).

The main disadvantage of the test is that it can only measure the depth immediately below the impact point, so it's mostly used for small areas.

2.1.2.5.3. Frequency response functions

The frequency response functions are obtained by recording the force signal produced by the impact of an instrumented hammer and the response of the structure to that excitement. There are three different types of frequency response functions: compliance, mobility and acceleration. The difference between them is the way the response of the structure is recorded. In the compliance function, the response is the displacement of the structure $X(w)$ (equation 2). Velocity $\dot{X}(w)$ is used in the mobility function (equation 3), and acceleration $\ddot{X}(w)$ is used in the acceleration function (equation 4). The most used frequency response function for detecting delamination is the mobility function inside the impulse response test, which will be explained below.

$$H(w) = \frac{X(w)}{F(w)} \left[\frac{m}{N} \right]$$

EQUATION 2: COMPLIANCE FUNCTION

$$H(w) = \frac{\dot{X}(w)}{F(w)} \left[\frac{ms^{-1}}{N} \right]$$

EQUATION 3: MOBILITY FUNCTION

$$H(w) = \frac{\ddot{X}(w)}{F(w)} \left[\frac{ms^{-2}}{N} \right]$$

EQUATION 4: ACCELERANCE FUNCTION

2.1.2.5.3.1. Impulse response test

The impulse response test measures the relative flexibility of the structure at the point tested. The test slab is excited by tapping with an instrumented hammer on the concrete surface. The response (movement) of the structure is measured by a transducer located at an adjacent point to the impact point. The instrumented hammer, which usually weighs 1kg, collects the force time history while the transducer collects the velocity time history. The hammer size, length, weight, material and velocity of the impact determine the amplitude and frequency from the force impulse. The tips of the hammer are made of different materials and are interchangeable. The material of the tip allows you to change the pulse width and frequency content of the force signal. On the other side of the head of the hammer an extended mass can be installed which allows to concentrate more energy at lower frequencies. Each impact has an area of influence around the hitting point around, so it's not only measuring the area below the sensor like in most of the previous tests we've seen.

2.1.2.5.3.1.1. Data processing

With the force and velocity data recorded we can obtain the mobility plot, which is the basic output for the test, as follows:

$$M(\omega) = \frac{v(\omega) * F^*(\omega)}{F(\omega) * F^*(\omega)}$$

EQUATION 5: MOBILITY PLOT CALCULATION

Where:

$M(\omega)$ = mobility spectrum.

$v(\omega)$ = velocity spectrum.

$F^*(\omega)$ = complex conjugate of force spectrum.

$F(\omega)$ = impact force spectrum.

The mobility function is multiplied by the complex conjugate of the force spectrum for minimizing the effect of the noise in the mobility plot.

The mobility plot (figure 23) represents the response velocity amplitude per unit of force in the frequency domain.

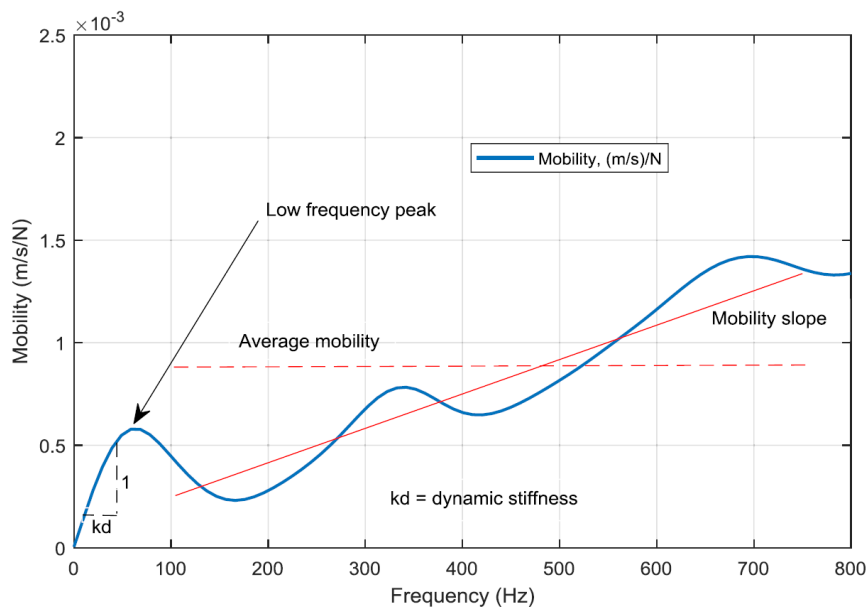


FIGURE 23: TYPICAL MOBILITY PLOT [19]

We can extract some important parameters from the mobility plot that will be useful for the interpretation of results:

- Low frequency peak: Peak value of mobility below 100Hz.
- Dynamic stiffness: Inverse of the linear fit of the mobility spectrum from 0 to 40 Hz. This property depends on the elastic modulus, thickness, support conditions and the presence of internal defects.
- Average mobility: Mean value for the mobility spectrum within the frequency range of 100 to 800Hz.
- Mobility slope: Linear fit of the mobility spectrum from 100 to 800 Hz.
- Peak-mean mobility ratio or voids index: Ratio between the low frequency peak and the average mobility.

2.1.2.5.3.1.2. Interpretation of results

In general terms, high mobility plots will indicate that the structure is more flexible at that point, which could be potentially caused by an internal defect. Nevertheless, analysing some of the parameters found in the mobility plot we can obtain more specific information:

- Peak-mean mobility ratio or voids index: High values of peak-mean mobility ratio indicate the presence of internal defects such as delamination or debonding. Based on experience, the research [20] reported that if the peak-mean mobility ratio is higher than 2.5 the concrete tested has delamination.
- Low frequency peak: High values for the low frequency peak indicate a void below the slab [21]. High values of the low frequency peak are normally much higher than the average mobility, what results in a high peak-mean mobility ratio.

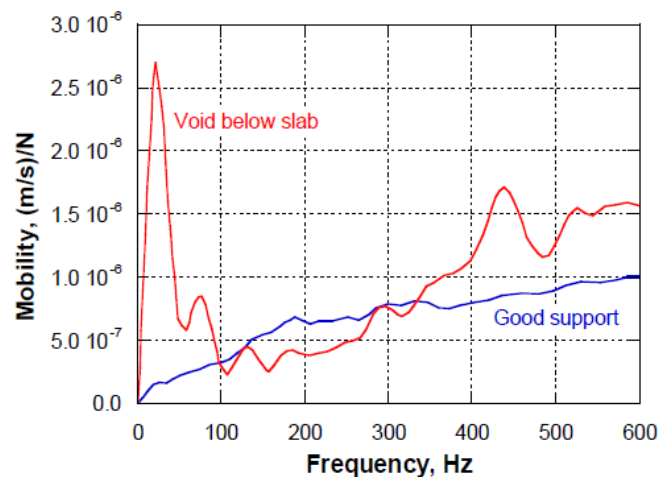


FIGURE 24: MOBILITY PLOT OF CONCRETE WITH A VOID BELOW THE SLAB [21]

- Average mobility: It is directly related to the thickness of the slab and the density of concrete [22]. Then, a reduction of the plate thickness, probably caused by delamination or other defects, will be followed by an increase of the average mobility.

In the research [23] statistical analysis was applied to measurements of average mobility of dozens of different projects, reporting some general guidelines for identifying internal imperfections in concrete, resumed in the following table:

Type of defect	Values for average mobility
Healthy slab	Within 2 standard deviations of the mean
Lower strength, surface deterioration or other minor localized defects	Between 2 and 4 standard deviations of the mean
Significant concrete deficiencies	Greater than 4 standard deviations of the mean

TABLE 3: CONCRETE CONDITION CORRESPONDING TO VALUES OF AVERAGE MOBILITY

- Mobility slope: High values of the mobility slope (red dashed line) compared to the solid concrete (blue dashed line) indicate honeycombed concrete according to the research [21].

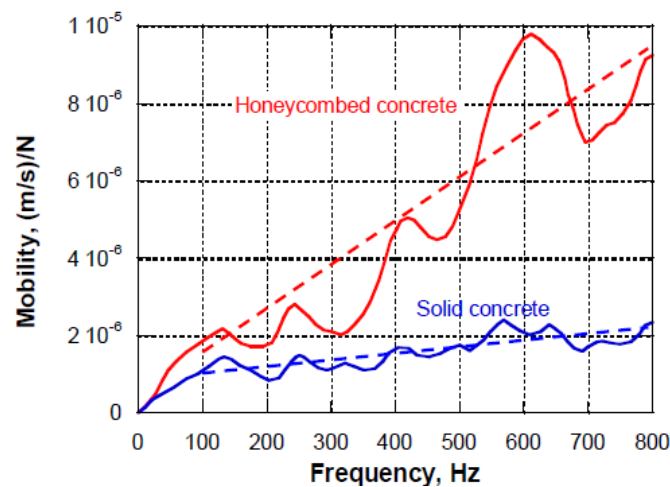


FIGURE 25: MOBILITY PLOT FOR HONEYCOMBED CONCRETE [21]

2.1.2.5.3.1.3. Factors affecting the response

Changes in the response measured by the transducer may be caused by several factors:

- Primary factors. Structural thickness and support conditions:
 - o Presence of delamination or other internal defects such as voids or cracks.
 - o Edges of slabs or columns.
- Secondary factors. Concrete condition:
 - o Smooth and undamaged surface.
 - o Surface erosion or cracks near the surface.
 - o Repairs made adding new materials to the structure that have a different response.
- Tertiary factors. Equipment and operator (may be considered in large projects):
 - o Use of the same equipment for all of the test.
 - o Repeat testing, with multiple times for each location and sets of equipment.

2.1.2.5.3.1.4. Advantages and limitations

One of the main advantages of the impulse response test in front of the impulse echo test for instance, is that you can measure a wider area with only one hit. This area depends on the weight added to the hammer. Also, it is a robust, fast and repeatable test.

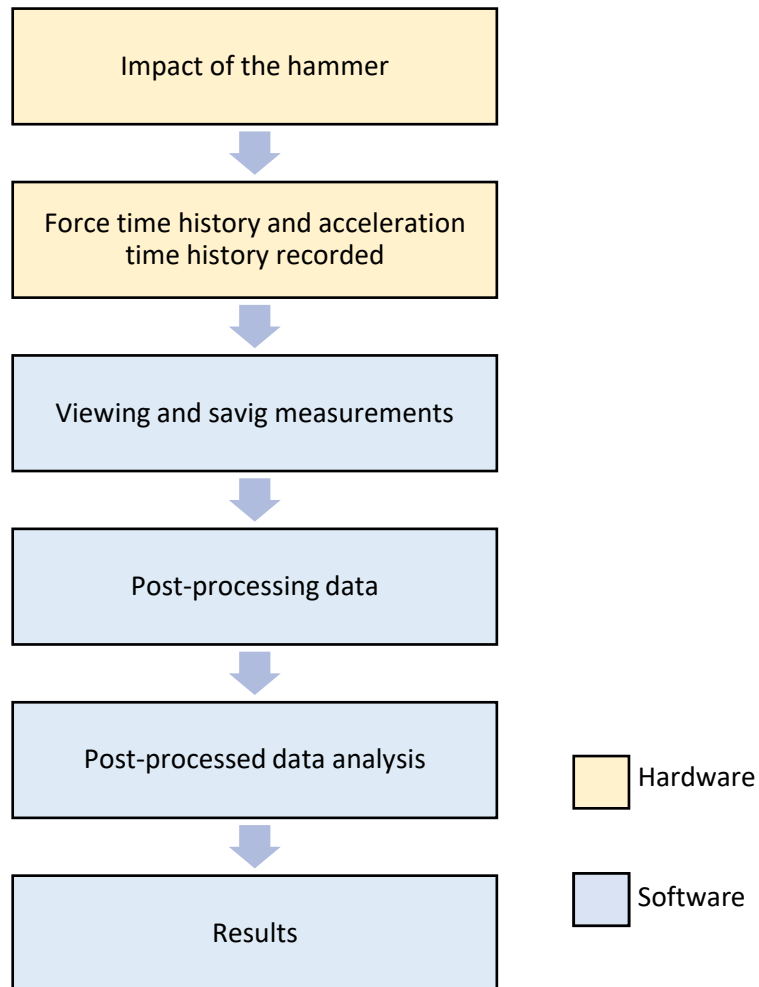
On the other hand, with the impulse response method you can't determine the depth of the internal defect and requires a skilled data interpretation.

3. Implementation of the impulse response method

As we have seen, the impulse response method offers a fast, robust and repeatable tool for finding internal imperfections in concrete structures. These applications added to the fact that it is a well-known technique and that there is even a commercial equipment called “*s’MASH*” using this method were key for choosing the impulse response method for detecting delamination in this project.

In the theoretical background, we have seen there are two main ways for finding delamination with the impulse response method: through the average mobility or through the peak-mean mobility ratio. The peak-mean mobility ratio will be chosen for finding delamination because there are several references in other papers about delamination found analysing this parameter as well as it is a fast way without involving very complex data post processing. As it was mentioned before, based on experience the minimum peak-mean mobility ratio number for finding delamination is 2,5. Nevertheless, we will have to calibrate this number based on our tests.

The solution applied for finding delamination can be divided in two parts: hardware and software. With the following flow diagram, a full overview of the full process is represented, from impacting the structure with the hammer to knowing whether there is delamination or not. Note that the steps involving the hardware are represented in light orange and the ones involving software are represented in light blue. Both hardware and software will be explained further down in more detail.



As we can see in the flow diagram, the process will start with an impact of the hammer on the test surface. Then, as explained in the theoretical background, the hammer will record the force time history of the impact and the transducer will record the structure vibration. As it will be described in a further section, the transducer used for collecting the structure response will be an accelerometer, so the structure response will be recorded in form of acceleration.

Until here, only the hardware has been used. Then, the next step will be using the software for representing the signals recorded and saving the measurements.

Finally, the last step is post-processing the data in order to obtain the mobility plot. Once we have the mobility plot and its significant parameters, an analysis of the peak-mean mobility ratio is done to get a final result that will indicate the presence of delamination.

3.1. Hardware

3.1.1. Instrumented hammer

The instrumented hammer used is the 086C03 of PCB electronics³.



FIGURE 26: INSTRUMENTED HAMMER PCB 086C03 [24]

This hammer consists on a sensor mounted on the striking end of the hammer head. The function of the sensor is transforming the impact force into electrical signal for further display and analysis.

As we've seen previously, the tip and the mass extender can change the frequency range of the measurement. For higher frequency response, a harder tip should be used without extended mass. For lower frequency response, a softer tip with the extender mass should be used. This hammer comes with four types of tips:

- Hard tip: Metal tip with a maximum peak of force of 355,86N⁴.
- Medium tip: Hard plastic white tip with a maximum peak force of 355,86N. A vinyl cover (blue cover) could be added on top of the tip to make the tip softer and lower the range of frequencies recorded.
- Soft tip: Soft plastic black tip with a maximum peak force of 88,96N.
- Super soft tip: Soft plastic red tip with a maximum peak force of 88,96N.

³ Detailed specifications of the hammer can be found in: PCB Piezotronics, "Impact Hammer Model 086D05 Installation and Operating Manual," 2007.

⁴ 1N= 0,224809 lbf

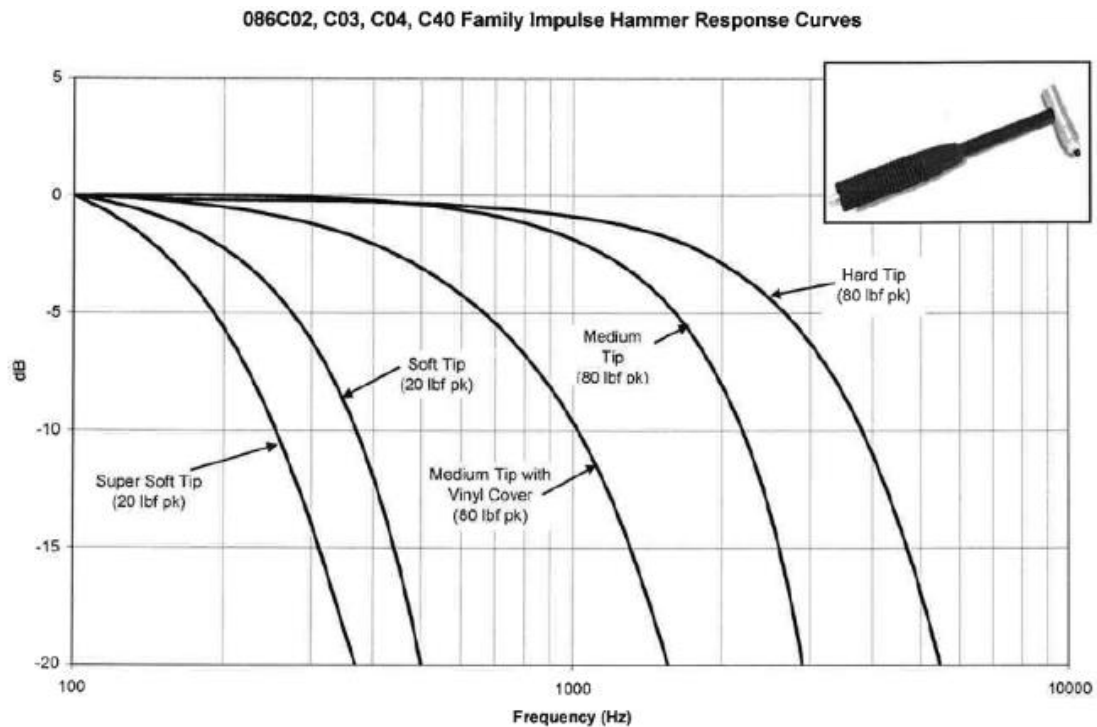


FIGURE 27: FREQUENCY RESPONSE OF THE DIFFERENT TYPES OF TIPS [25]

The three hardest tips (hard tip, medium tip and medium tip with cover) are suitable for the testing we want to perform due to the range of frequencies represented in the mobility plot is between 0 and 800 Hz.

3.1.2. Accelerometer

The accelerometer used is the 352C03 from PCB electronics⁵. It records the response of the structure in form of acceleration, that will be later transformed into velocity by the software.



FIGURE 28: ACCELEROMETER PCB 352C03 [26]

⁵ Detailed specifications of the accelerometer can be found in: P. C. B. Piezotronics, "Model 352C04 General purpose, ceramic shear ICP[®] accel., 10 mV / g, 0.5 to 10k Hz, 10-32 Installation and Operating Manual," 2007.

3.1.3. Central unit

The central unit is the connection between the sensors and the computer. It is formed by two parts:

- NI 9234⁶: Signal acquisition module from National Instruments. It has four input channels and allows the connection of the instrumented hammer and the accelerometers.



FIGURE 29: NI 9234 [27]

- NI cDAQ 9174⁷: Controls the timing and synchronisation of the signals and the data transfer from the inputs to the output.



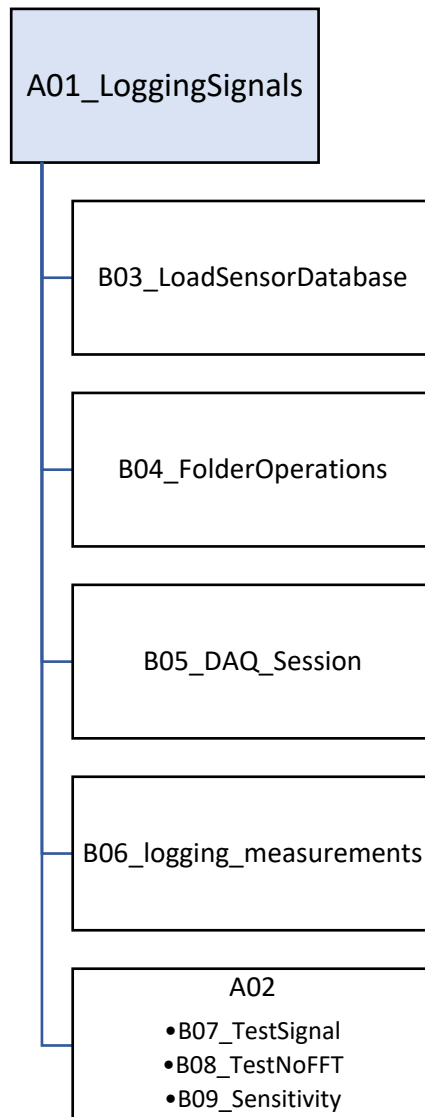
FIGURE 30: NI cDAQ 9174 [28]

3.2. Software

The software allows to view, save and post process the signals following the impulse response method. The main program built in *MATLAB* is running several functions. A scheme of the program is represented below. The full program is included in the appendix B1.

⁶ Detailed specifications of the signal acquisition module can be found in: “NI-9234 - National Instruments.” [Online]. Available: <https://www.ni.com/en-no/support/model.ni-9234.html>. [Accessed: 28-Nov-2019].

⁷ Detailed specifications of the *NI cDAQ 9174* can be found in: “NI-9234 - National Instruments.” [Online]. Available: <https://www.ni.com/en-no/support/model.ni-9234.html>. [Accessed: 28-Nov-2019].



An initial script including A01_LoggingSignals, B03_LoadSensorDatabase, B04_FolderOperations, B05_DAQ_Session and B06_logging_measurements was given before starting this project in order to be able to record signals. Nevertheless, A01 has been converted into the main program and some changes have been made to B06_logging_measurements that will be explained below.

Description of the functions:

- B03_LoadSensorDatabase: Loads the database with the properties of the sensors.
- B04_FolderOperations: Checks if “.mat” files are existing in the destination folder.
- B05_DAQ_Session: Creates a session in the DAQ session-based interface.
- B06_logging_measurements: Logs the signals from the channels defined in the session. In order to have a better classification of the measurements, the date and time of the measurements have been included in the file name.

- A02: Post processes the signals and obtains the mobility plot. Also saves automatically all the mobility plots of each measurement made in one session. Inside the function A02, we have the following sub-functions:
 - B07_TestSignal: Calculates the FFT of a given signal and plots the real and imaginary parts, the module and the phase.
 - B08_TestNoFFT: Does the same as the B07_TestSignal function but without doing the FFT of the signal.
 - B09_Sensitivity: Divides the sensitivity of the sensors used to obtain the right magnitude in the force and acceleration data recorded.

The post-processing of the signals for obtaining the desired results consists of:

- Cleaning the signals: Cropping the first 0,5 seconds of the recorded signal and doing the mean of the cropped signal. Then removing the mean of the cropped signal to the original one for placing the signal at the 0 value of the y axis.
- Lengthen the signals: Zeroing the signal (adding zeros at the end of the clean signals) in order to make a longer signal of 15 seconds. Longer signals allow better calculations of the FFT.
- Sensitivity: Using the B09_Sensitivity function for obtaining the expected magnitude of the signals.
- Velocity: Integrating acceleration to get velocity.
- Filtering: Applying a high pass filter to the velocity signal to remove frequencies lower than 20Hz (noise that will affect to the mobility plot).
- FFT: Transforming into frequency domain the force, acceleration and velocity signals and plotting the resulting signals using B07_TestSignal.
- Complex conjugate: Calculating the complex conjugate of the force.
- Mobility plot: Operating and plotting the mobility function.
- Delamination indicators: Calculating the dynamic stiffness, average mobility, mobility slope and peak-mean mobility ratio of the previous mobility plot. Also comparing the peak-mean mobility ratio with the limit value in order to detect delamination.
- Results: Plotting and saving the final mobility plot.

4. Experimental setup

The purpose of the experimental work is to simulate delamination inside a concrete slab and being able to detect it with the hardware and software explained previously. For this research, three different concrete slabs have been built. In two of the slabs, delamination has been tested at different depths: 15mm and 30mm. The other slab was used as reference without any internal defects.

4.1. Artificial delamination

The main idea behind simulating delamination is to create a void inside the concrete slab in order to replicate the displacement of the concrete layers and the void of air created by the delamination process. We can find many studies that have simulated delamination using different materials such as polystyrene [29], foam [30] or bubble wrap [31] and also different shapes from the most common sheets [31] squares [30], circles [32] or even an “A” shape [33]. These plastic materials are used because of their similar conductivity to the air [34]. Although there's a great variety of materials and shapes used, all of the artificial delamination materials are made with plastic materials.

4.1.1. 3D printed piece

For our research, a plastic 3D printed hollow prism will be placed inside the concrete slab for simulating delamination (figure 32). The 3D printing technique has been used in order to guarantee that the prism stays always at the same position while pouring the concrete.

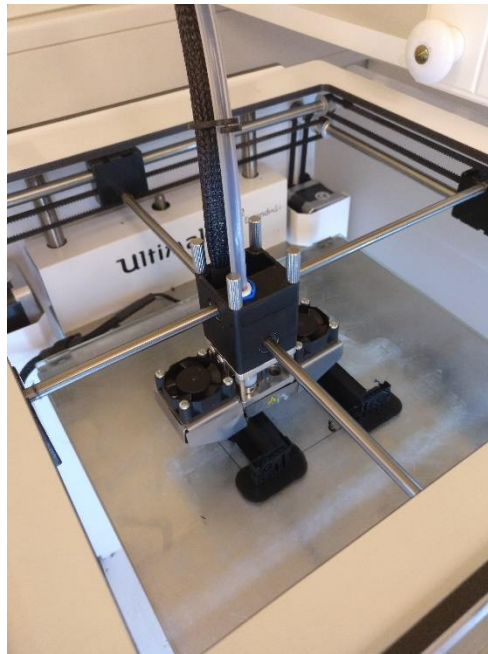


FIGURE 31: 3D PRINTING PROCESS

The 3D printed parts have been designed in *Solidworks* and then printed using the *Ultimaker 2+* 3D printer and the *Cura* software. Two different pieces have been designed for the two different depths. We can divide the piece in two parts:

- Prism: Void prism measuring 100x100x10mm. It simulates delamination by creating an internal void full of air. The prism is the same for the two different types of 3D printed pieces. The open lateral parts were taped before pouring the concrete so the concrete didn't flow inside the void. It hasn't been designed completely because it was more difficult to remove the excess of material printed inside the hollow part.
- Legs: Allows the prism to stay at the same height while pouring the concrete and fixes the structure to the base of the mould. The legs have different lengths for each type of 3D printed piece.

Complete drawings of the piece are included in the appendix E.

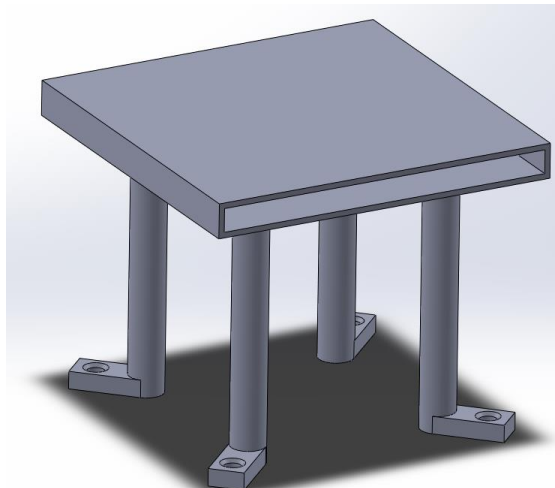


FIGURE 32: DESIGN IN *SOLIDWORKS* FOR THE 3D PRINTED PIECE



FIGURE 33: 3D PRINTED PIECE

4.1.2. Moulds

To ensure the desired shape and measures of the slab, concrete will be poured inside three wooden moulds. All the moulds will be a square of 310x310x10 mm. The first mould will be a healthy mould, meaning that it will not have any type of internal defect. The second mould, will have 3D printed pieces at a depth of 15mm. The third mould will also have two 3D printed pieces but at a depth of 30 mm. At first, the 3D printed pieces were designed for being attached to the moulds with four screws (figure 34). Nevertheless, due to the difficulty to the difficulty of putting screws near the corners, the 3D pieces were finally attached with glue (figure 35).



FIGURE 34: 3D PRINTED PART ATTACHED WITH SCREWS

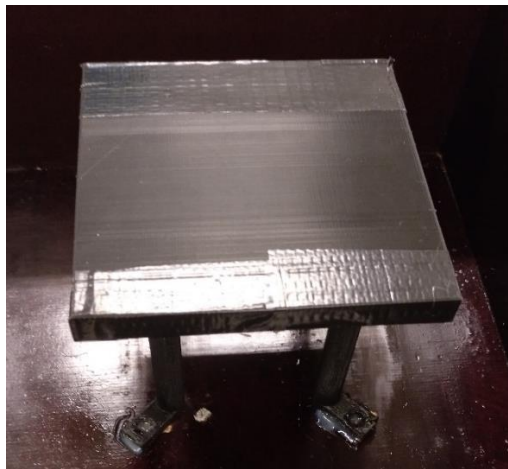


FIGURE 35: 3D PRINTED PARTS ATTACHED WITH GLUE

The location of the 3D printed parts is shown in figures 36 and 37. Again, the complete drawings of the assembly of the moulds with the 3D printed pieces for each depth are included in the appendix E.

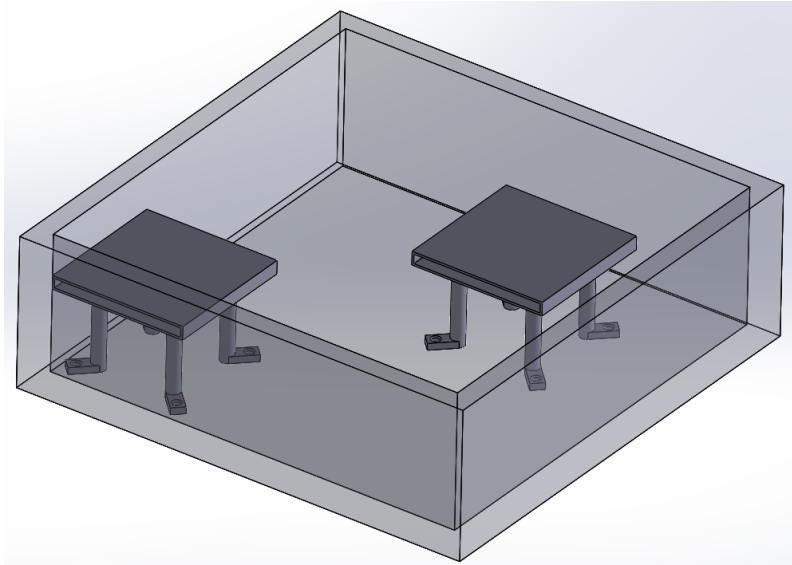


FIGURE 36: POSITION OF THE 3D PRINTED PIECES INSIDE THE MOULD IN *SOLIDWORKS*

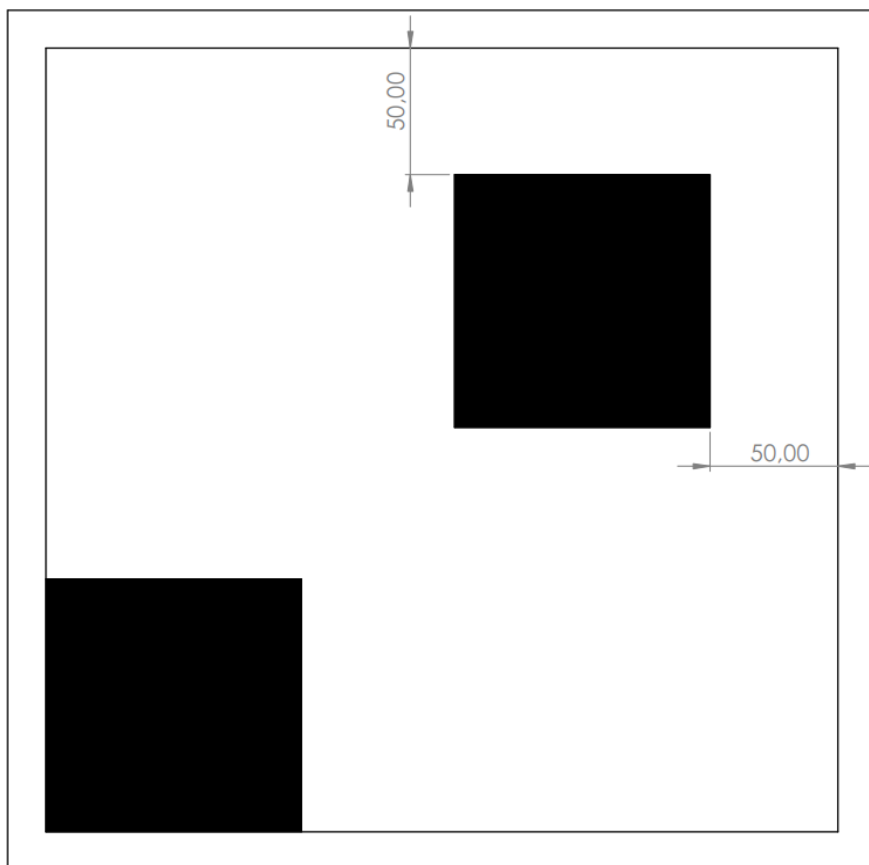


FIGURE 37: POSITION OF THE 3D PRINTED PIECES (REPRESENTED IN BLACK) INSIDE THE MOULD.

4.1.3. Concrete casting

For making the concrete slabs, the concrete mix had first to be prepared and then poured into the moulds. In parallel to the concrete slabs, three concrete cube samples were also made for knowing the weight and testing the compressive strength. The information about the weight and compressive strength of the concrete made is included in the appendix D.

In order to make the concrete mix, we had the following 3 ingredients: cement, gravel and sand, seen in the figure 38 in the mentioned order. All of them were put together inside the mixing machine (figure 39). More details about the concrete recipe can be found at the appendix C.



FIGURE 38: INGREDIENTS FOR THE CONCRETE MIX



FIGURE 39: MIXING MACHINE

Then, the following mixing procedure was followed (figure 40):

1. 1 minute dry blending (cement + aggregates).
2. 2 minutes wet blending (add the water gradually during the first 30 seconds) (figure 41).
3. 2 minutes pause.
4. 1 minute blending.

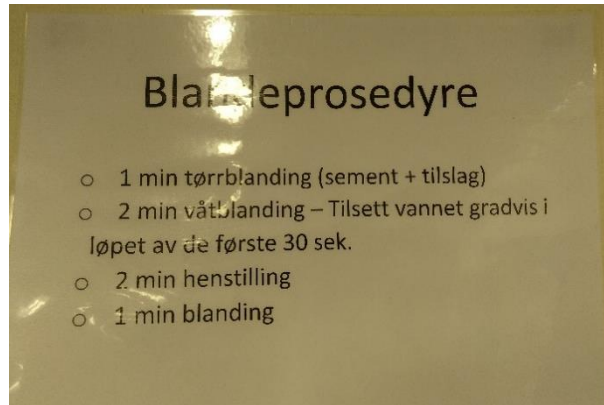


FIGURE 40: MIXING PROCEDURE (BLANDEPROSEDYRE)



FIGURE 41: WET BLENDING PROCESS

After finishing with the process, the concrete mix was obtained (figure 42) and then poured inside the three moulds (figure 43). The slabs were covered with a wet towel and plastic for curing before beginning with the tests (figure 44).



FIGURE 42: CONCRETE MIX

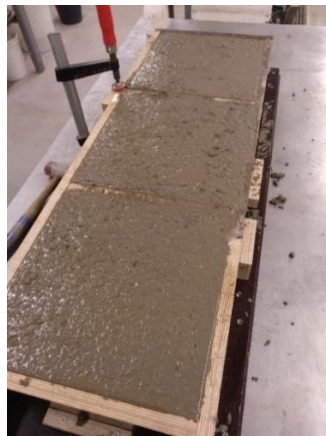


FIGURE 43: CONCRETE POURED INSIDE THE MOULDS



FIGURE 44: CONCRETE SLABS COVERED WITH PLASTIC FOR CURING

In the following figures we can see the final result of the concrete slabs. In the detailed view of the 15 mm slab we can see that the concrete didn't flow all the way to the corner and a void under the 3D printed part was formed (figure 46).

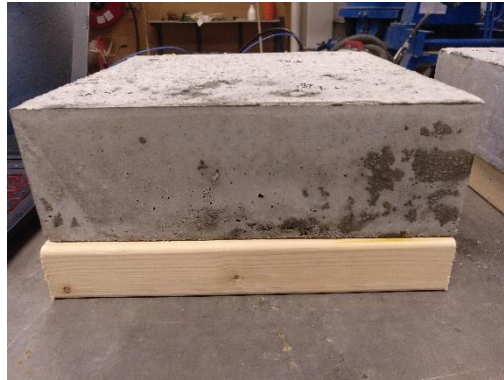


FIGURE 45: LATERAL VIEW OF THE HEALTHY SLAB



FIGURE 46: LATERAL VIEW AND DETAILED VIEW OF THE 15MM DEPTH SLAB



FIGURE 47: LATERAL VIEW AND DETAILED VIEW OF THE 30MM DEPTH SLAB

4.1.4. Test setup

All the measurements are performed on the 9th day after the concrete casting. In that day, a compressive strength test for the hardened concrete was done. For performing the test, the standard NS-EN 12390-3:2019 was followed, except from the number of samples measured. Two of the three samples were tested, leaving the third one in case of another test day was needed. The concrete had a compressive strength after 9 days of 42,18MPa.



FIGURE 48: COMPRESSIVE STRENGTH TEST



FIGURE 49: FRACTURED TEST SPECIMEN

Four different impact points have been set in each slab. The accelerometer has been attached 1,5 cm next to each impact point with duct tape. The location of the impact points and the accelerometers are shown in figure 50. Five hammer hits with the same tip will be performed in each impact point, for better consistency in the final results. The measurements will be done with the three hardest tips available (metal, hard plastic and hard plastic with cover).

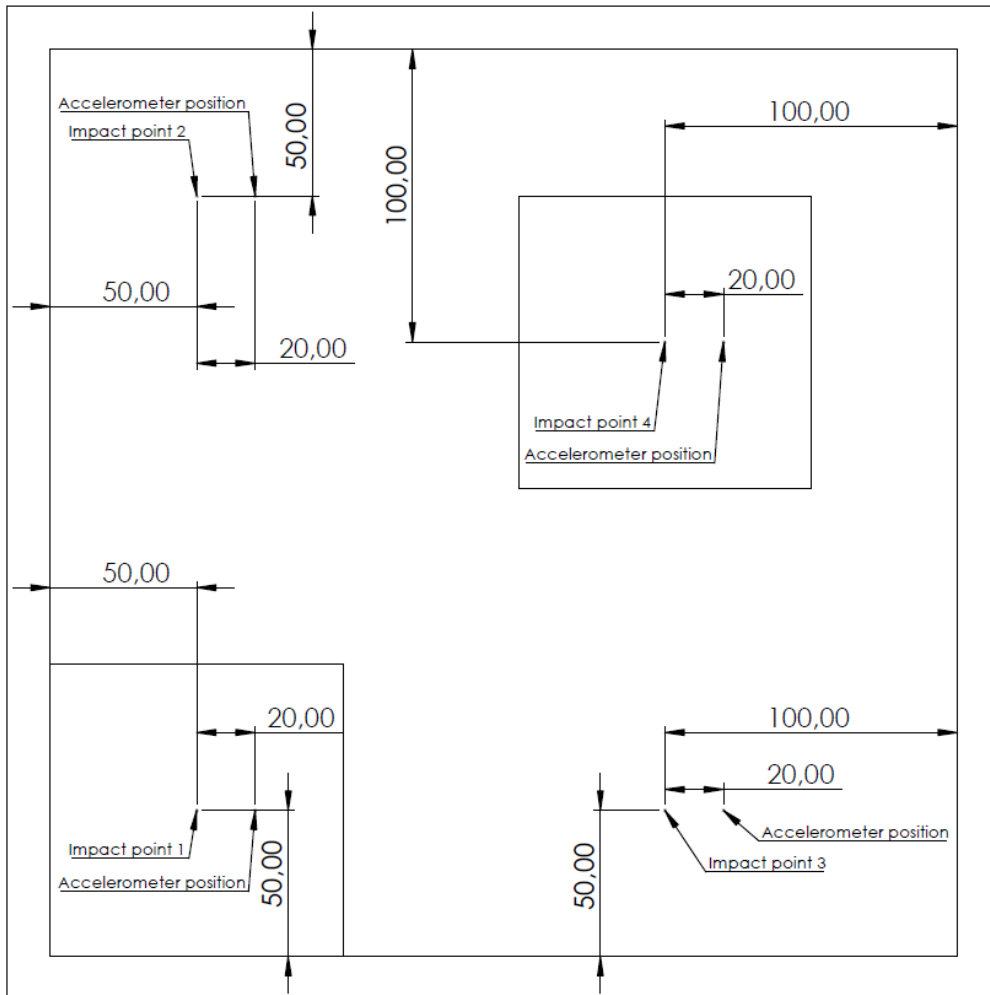


FIGURE 50: DRAWING OF THE IMPACT POINTS AND ACCELEROMETERS POSITION

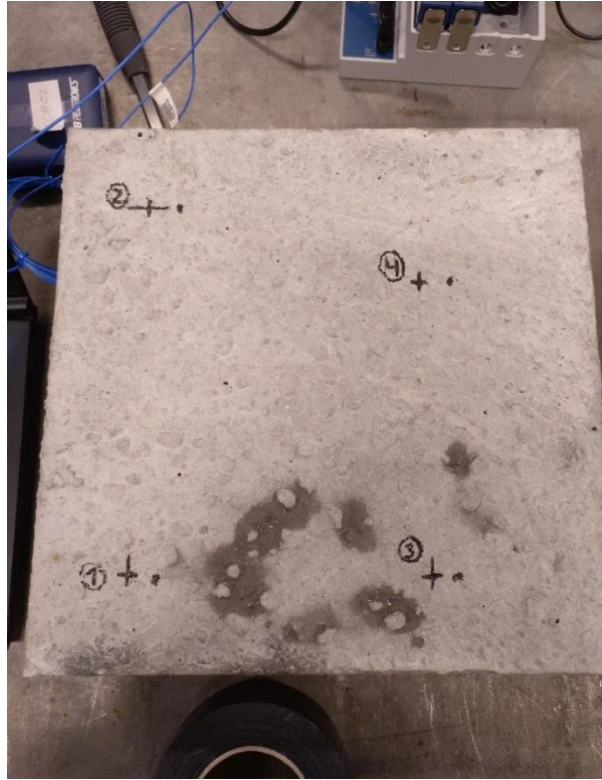


FIGURE 51: HITTING POINTS ON ONE OF THE TEST SLABS

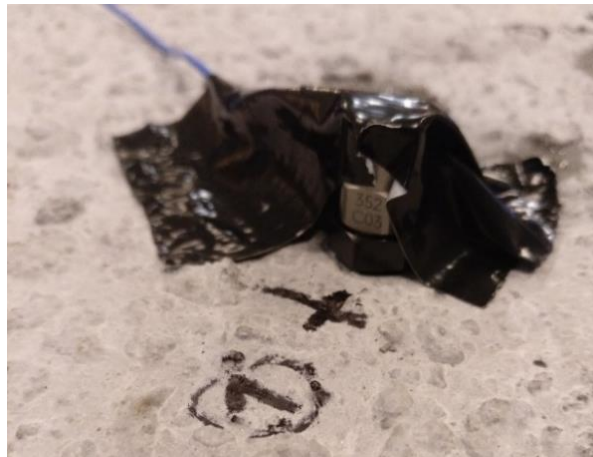


FIGURE 52: ATTACHMENT OF THE ACCELEROMETER

5. Results and discussion

The expected final result was obtaining a mobility plot using the impulse response method for each hit and calculating the peak-mean mobility ratio that will indicate whether the tested concrete had delamination or not. Based on our tests, we wanted to know the minimum peak-mean mobility ratio value for detecting delamination, that would be around 2,5 following what was written in other papers. So, the MATLAB post-processing code was programmed for obtaining the mobility plot with all its parameters, as it can be seen in the following plot obtained from a test hit done before building the concrete slabs.

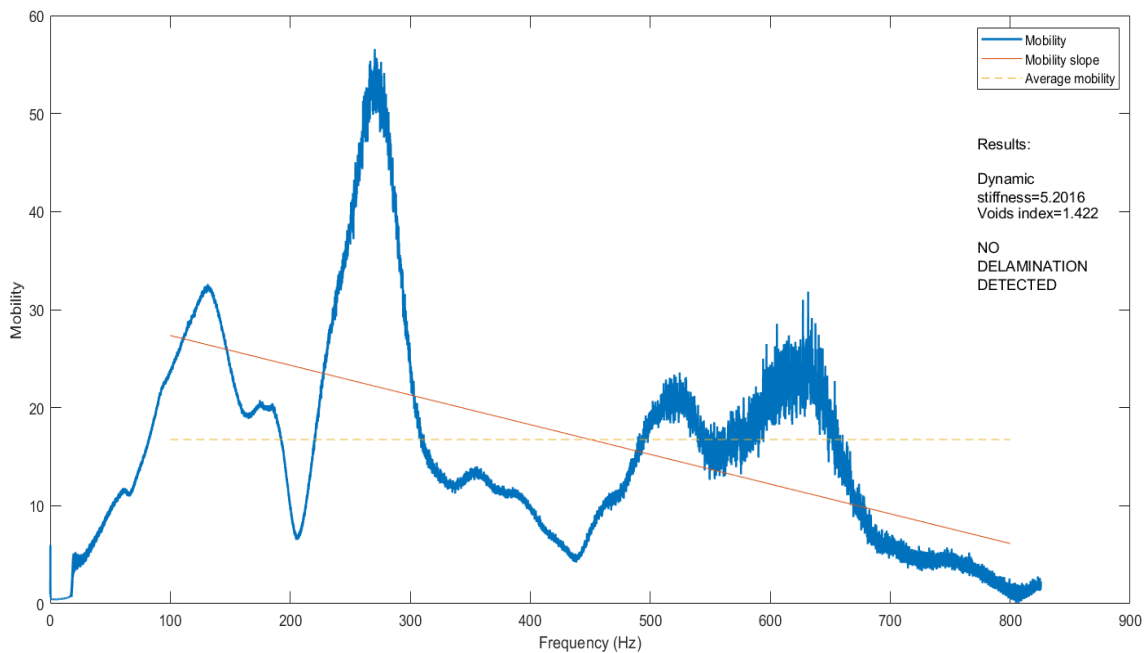


FIGURE 53: MOBILITY PLOT OBTAINED FROM A TEST HIT

Nevertheless, the mobility plots obtained from the tests done on the concrete slabs were not as expected. We will start looking at the measurements done with the hard plastic tip (white tip), which allowed to record the frequency range desired and was narrower than the metal tip, so potentially better for hitting on a rough surface always in the same point. From 200Hz, the mobility had very low values in all the measurements, so it wasn't possible to get a reliable value for the average mobility, the mobility slope and consequently for the voids index. Moreover, any relevant similitudes or differences could be found in the same position for the three different slabs (figures 54,55,56).

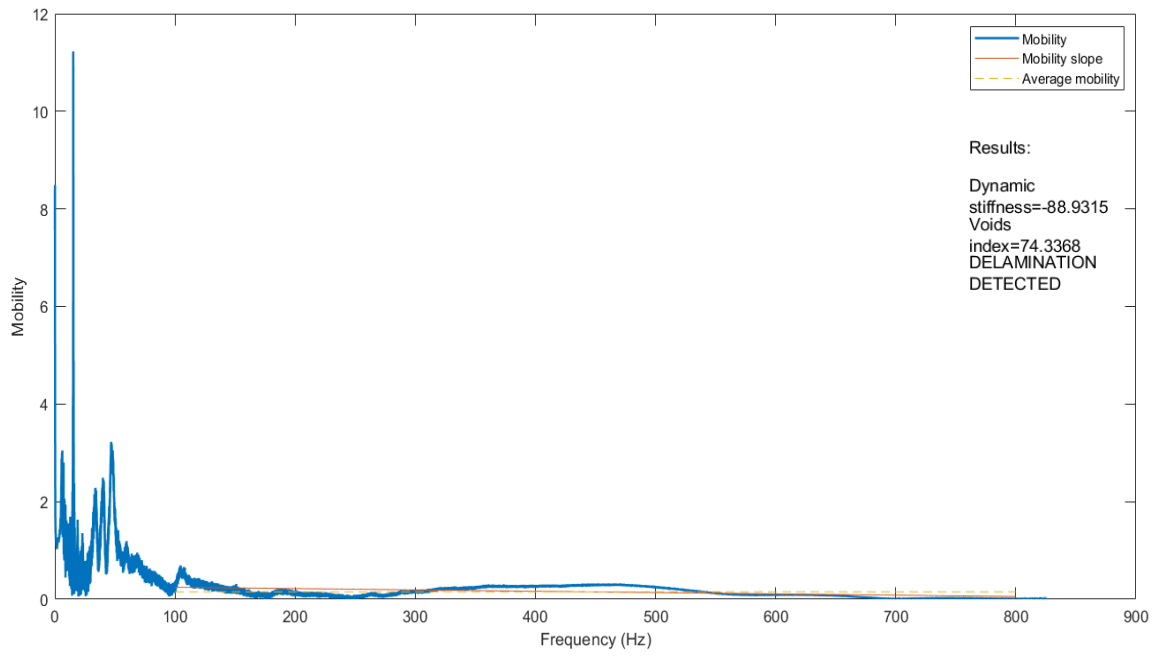


FIGURE 54: MOBILITY PLOT FOR THE SLAB 1 AND POSITION 1

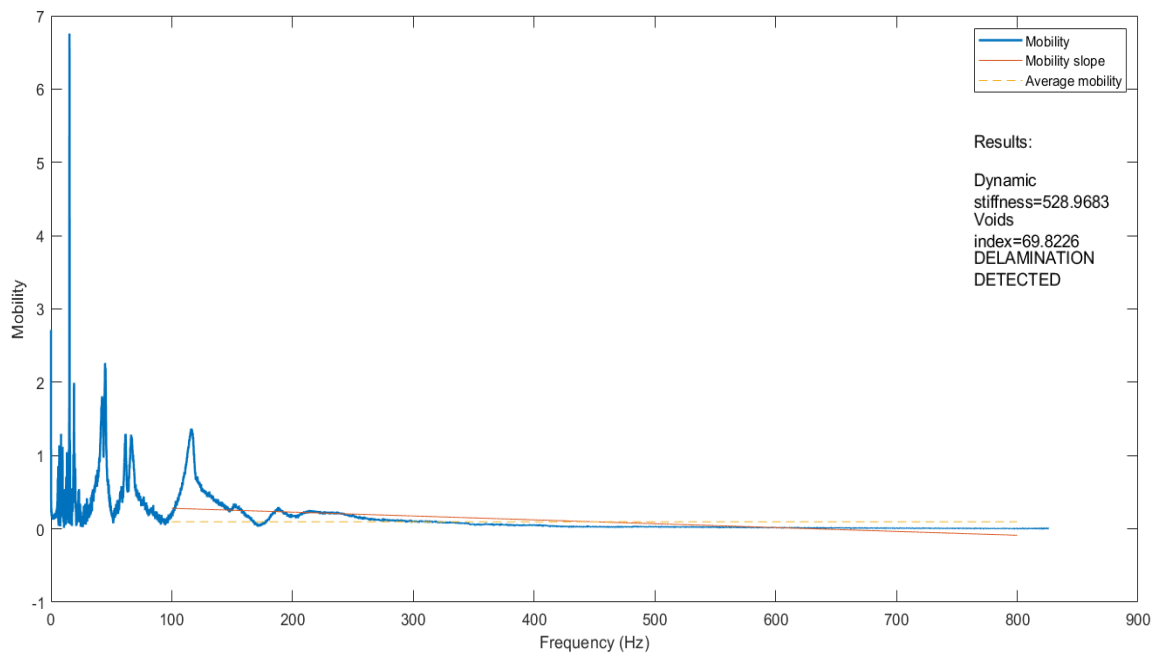


FIGURE 55: MOBILITY PLOT FOR THE SLAB 2 AND POSITION 1

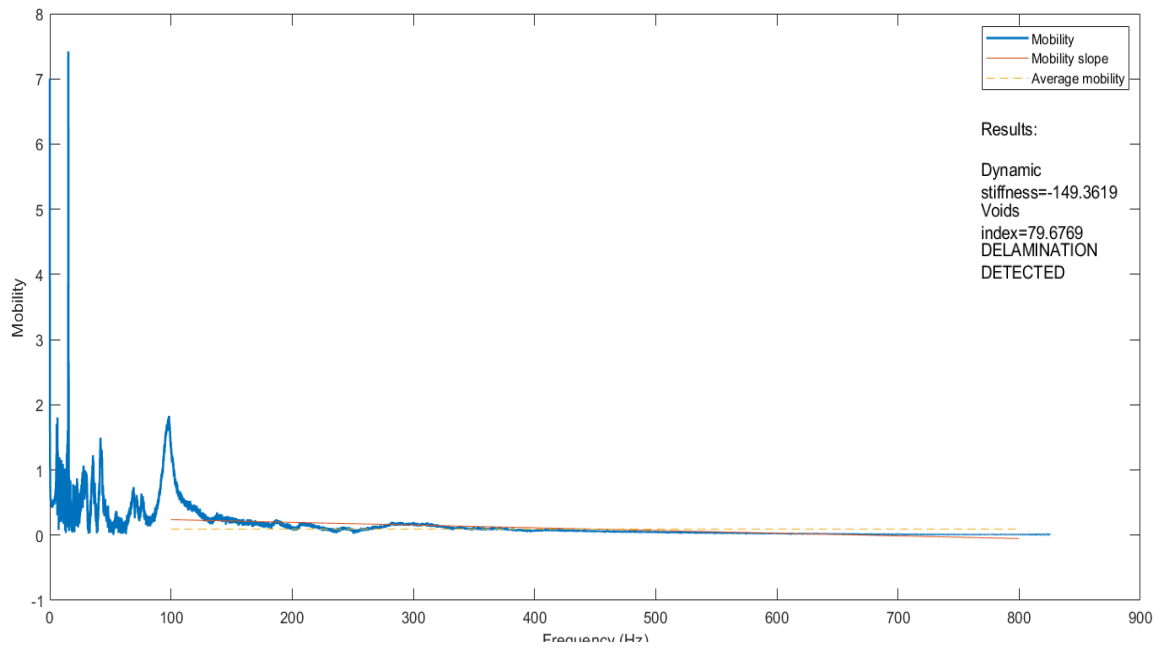


FIGURE 56: MOBILITY PLOT FOR THE SLAB 3 AND POSITION 1

The possible causes why the mobility plot isn't as expected could be a combination of different factors. First of all, the reason why higher frequencies are not represented in the mobility plot may be due to the way of attaching the accelerometer. According to [35], frequencies higher than 600 Hz can't be detected with an accelerometer attached with thick tape (figure 57). Another factor that should be considered is the roughness of the surface. The slabs didn't have a perfectly flat top surface, which could have produced errors on the signals recorded. On the one hand, the accelerometer couldn't be placed exactly forming 90 degrees with the surface, which could have caused some alteration in the measurements according to the accelerometer manual [36]. On the other hand, the fact that we didn't have a homogeneous surface could lead to hitting on different materials in the concrete: e.g. hitting on an aggregate. This could cause irregularity in the measurements done and also different response of the structure depending on the material hit by the hammer.

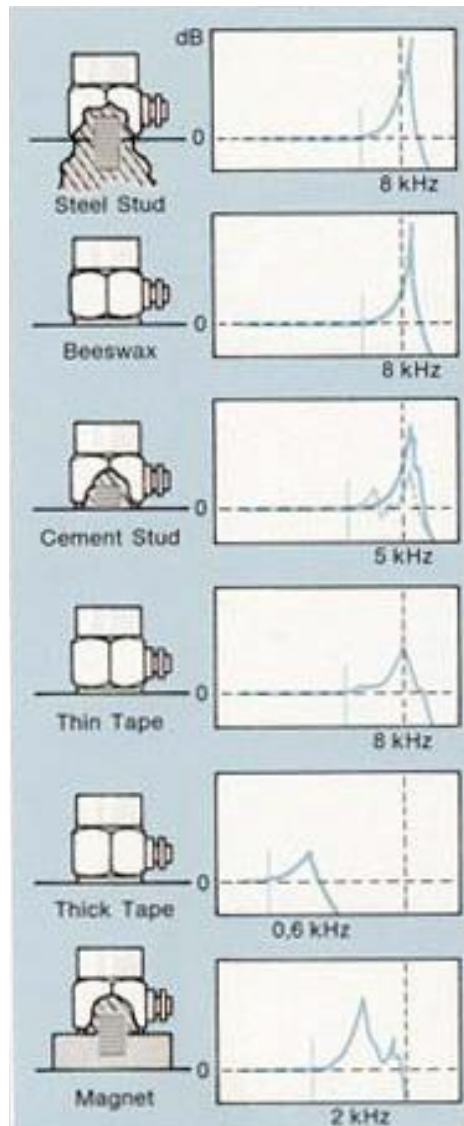


FIGURE 57: FREQUENCY MEASUREMENT RANGE DEPENDING ON THE TYPE OF MOUNT OF THE ACCELEROMETER [35]

Having seen that the mobility plot wasn't giving the expected results, the other two frequency response functions were taken into consideration for detecting delamination: compliance and accelerance. The accelerance function was chosen as an alternative method because, as we've seen in the theoretical background, this function is dividing acceleration over force, which were the two signals that had already been recorded. With these two signals the compliance function could also be calculated, but it involved more post-processing of the results because the acceleration signal should be integrated twice for getting the displacement, which meant more sources of possible errors. A second post-processing MATLAB program was built for calculating and plotting the accelerance function and it's included in the appendix B.2.

First, the signals obtained from the measurements recorded have been analysed in the time and frequency domain.

Analysing the force, acceleration and velocity time history we can see that, once the signals were calibrated and filtered, we had very small amount of noise in the signals.

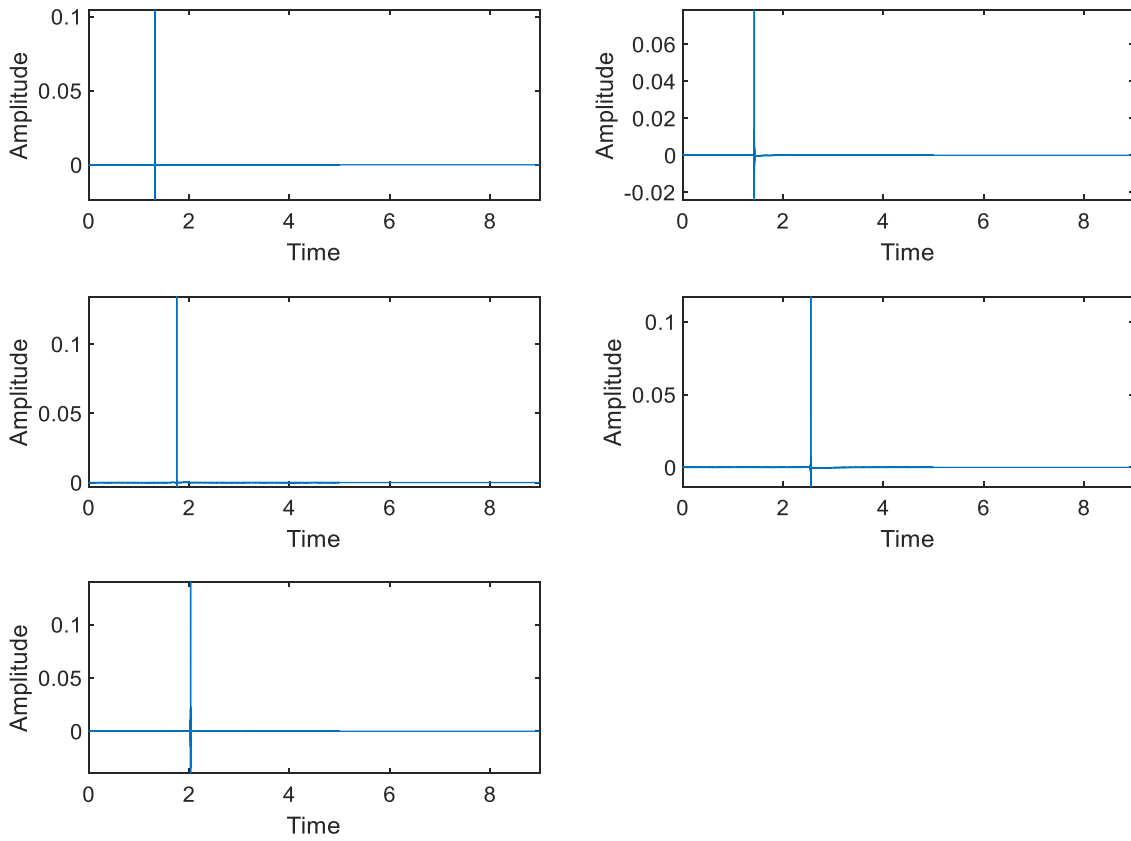


FIGURE 58: FORCE TIME HISTORY OF FIVE MEASUREMENTS DONE IN ONE POSITION

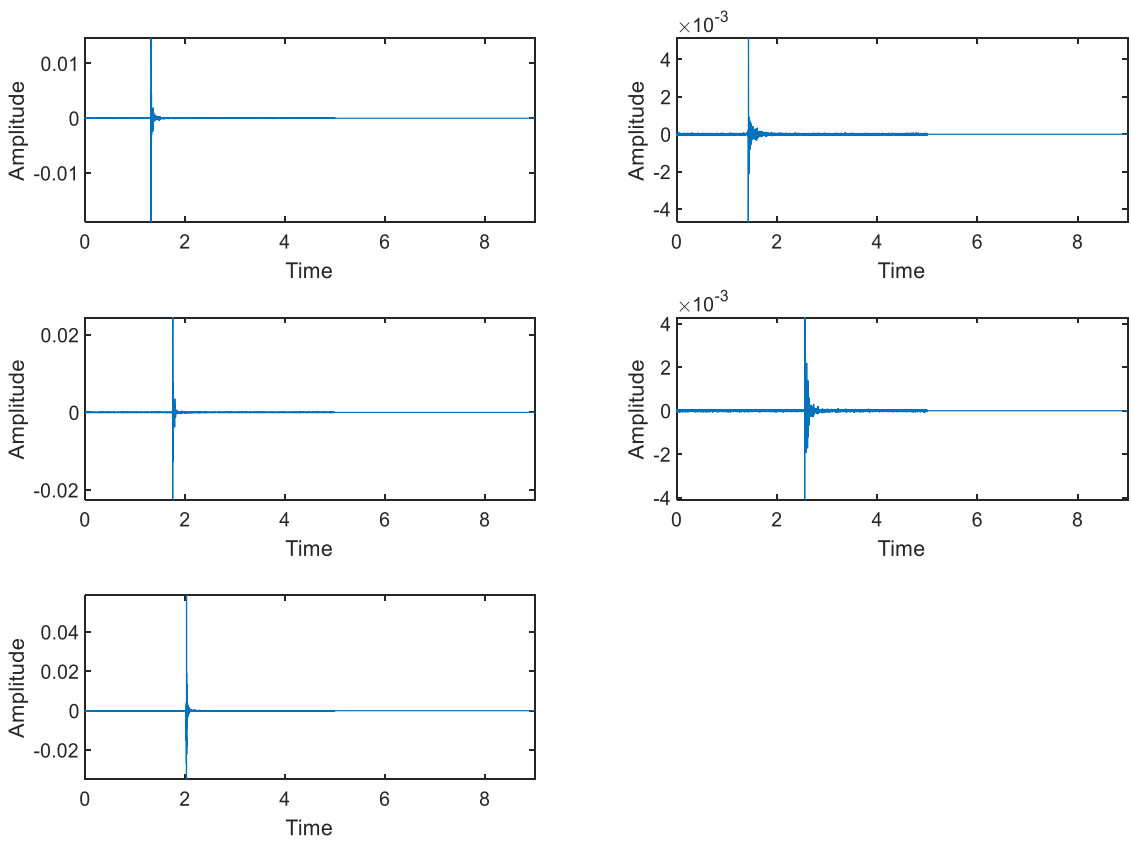


FIGURE 59: ACCELERATION TIME HISTORY OF FIVE MEASUREMENTS DONE IN ONE POSITION

The next step done is transforming the signals to frequency domain. We can see that the force is behaving almost constant through the frequency spectrum, with different amplitudes for each hit (figure 60). In the acceleration signal we can see a consistent response of the structure on the five hits performed at the same position (figure 61). We can also see some peaks below 300 Hz that can help us determine how the slab is vibrating in each hit. For higher frequencies the signal is remaining constant or with random peaks, so we will focus on the frequencies below 300Hz. The random behaviour of the signal for higher frequencies is directly related to the way the accelerometer was attached.

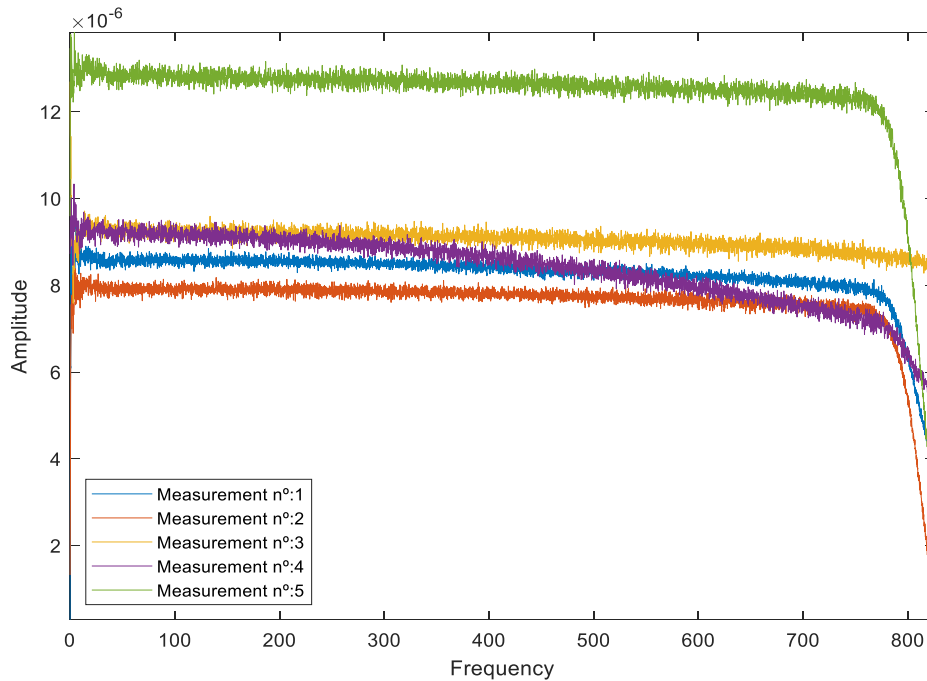


FIGURE 60: FORCE FREQUENCY SPECTRUM FOR 5 MEASUREMENTS OF THE SAME POSITION

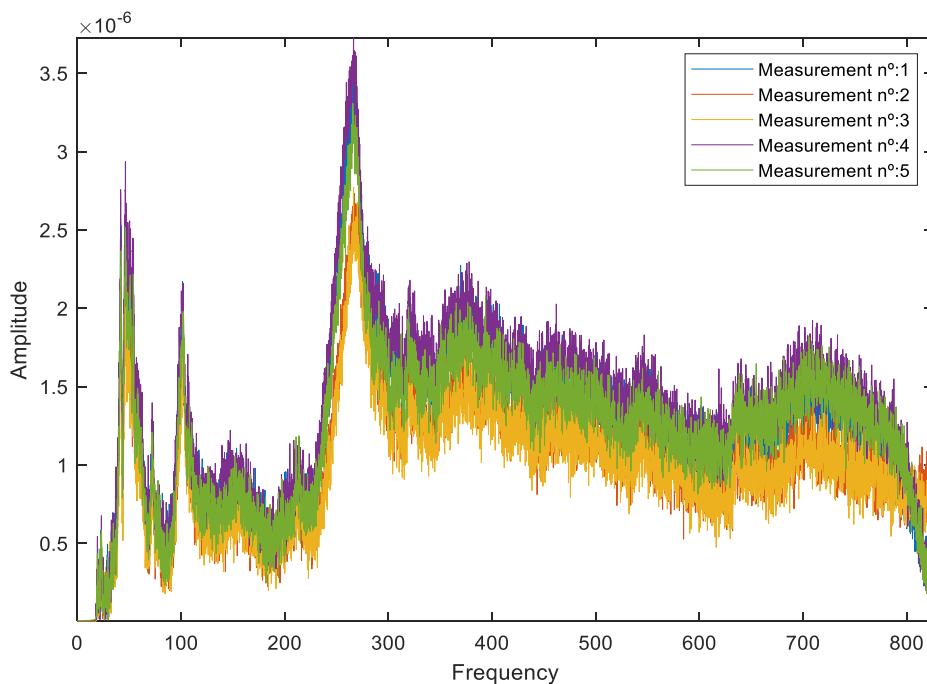


FIGURE 61: ACCELERATION FREQUENCY SPECTRUM FOR 5 MEASUREMENTS OF THE SAME POSITION

Regarding at the comparison of the acceleration frequency spectrum for position 1 in the three slabs, we can see three main peaks below 300 Hz. The peak at 117 Hz corresponds to the healthy slab, the peak at 98,49 Hz corresponds to the slab with the internal defect at 30mm of depth and the final peak at 47,18 Hz corresponds to the slab with the internal defect at 15mm. This plot is showing us the expected behaviour of the three concrete slabs depending on whether they had or not the internal defect. The healthy slab has the peak amplitude at a higher frequency than the slabs with the 3D printed parts. Also, the difference in the depth of the defects could be seen in the plot. We could say that the slab 3 is less damaged than slab 2, because in slab 3 the internal defect is deeper than in slab two. Then, we can see that the most damaged slab has a lower frequency peak than the less damaged. This difference between the signals in the frequency domain could also be heard during the testing. When the hammer impacted the concrete, the slab with the shallower defect sounded with a lower pitch than the other two slabs.

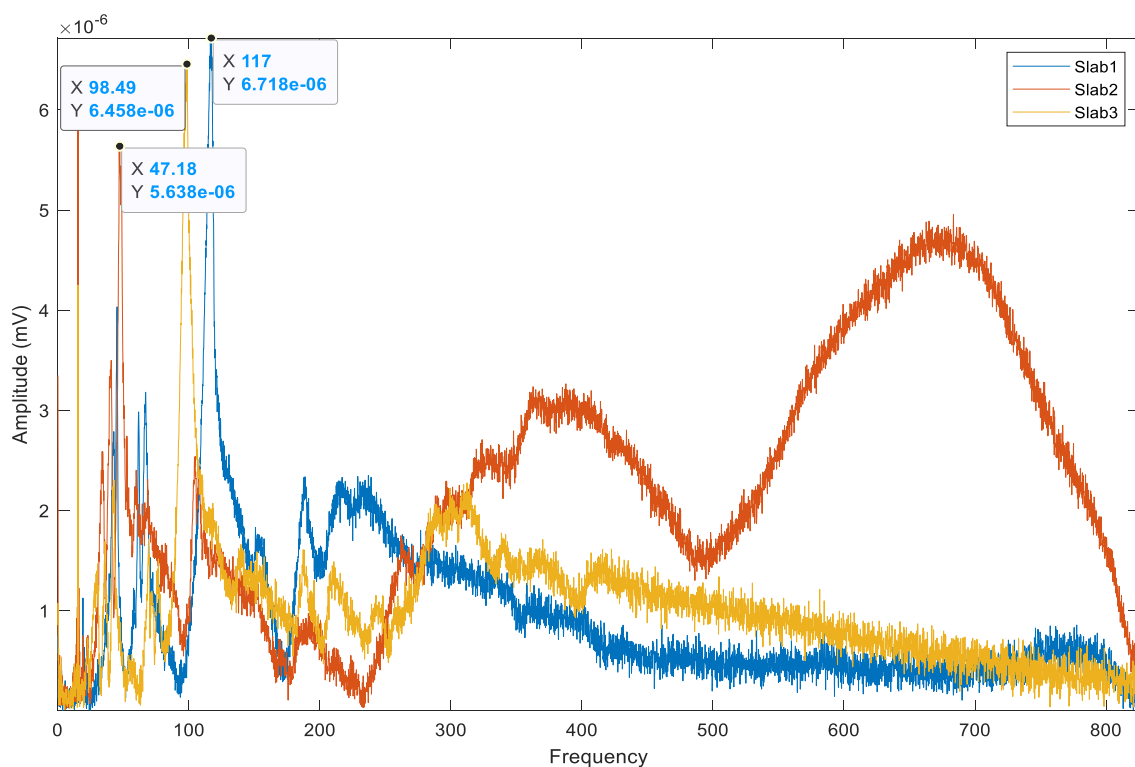


FIGURE 62: COMPARISON OF THE ACCELERATION FREQUENCY SPECTRUM BETWEEN THE THREE SLABS IN POSITION 1

Nevertheless, this expected behaviour of the concrete slab was only happening for position 1. In the other position with delamination, the peaks in the acceleration frequency spectrum don't follow that expected pattern or any other recognizable pattern. This may occur due to the fact that the slab number 2 had an area below the 3D printed part without concrete, because the concrete didn't flow all the way to the corner. Then, the delamination in position number 1 became more evident than in position number 4.

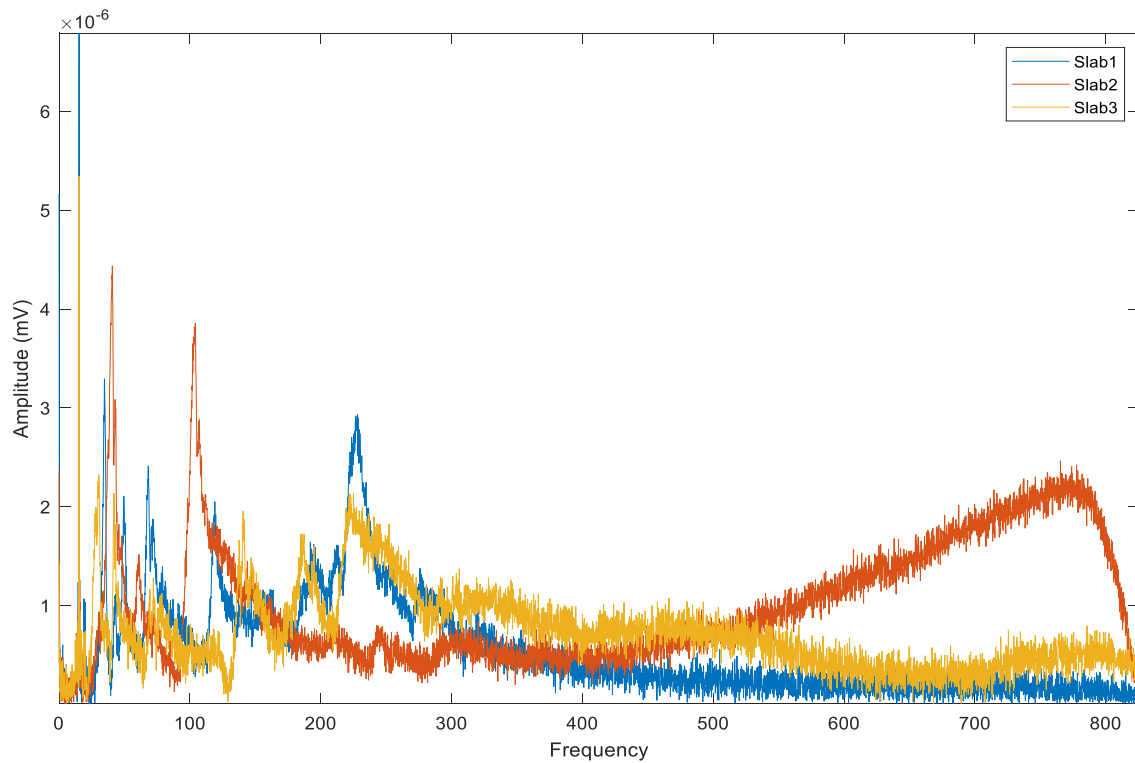


FIGURE 63: COMPARISON OF THE ACCELERATION FREQUENCY SPECTRUM BETWEEN THREE SLABS IN POSITION 4

The next step is obtaining the accelerance function from the signals analysed previously. We expect the accelerance function to have the same shape as the acceleration frequency spectrum, because we are dividing the acceleration frequency spectrum by the force spectrum which is almost constant.

For each position, the average of the five hits has been done, as well as removing the fourth measurement for slab 2 and position 1 because there was an error in the measurement. Below, we can see the comparison between the average accelerance function for each position and each slab. As it was explained previously, we are going to focus on the frequencies below 300Hz, so the x axis has been limited to 300Hz.

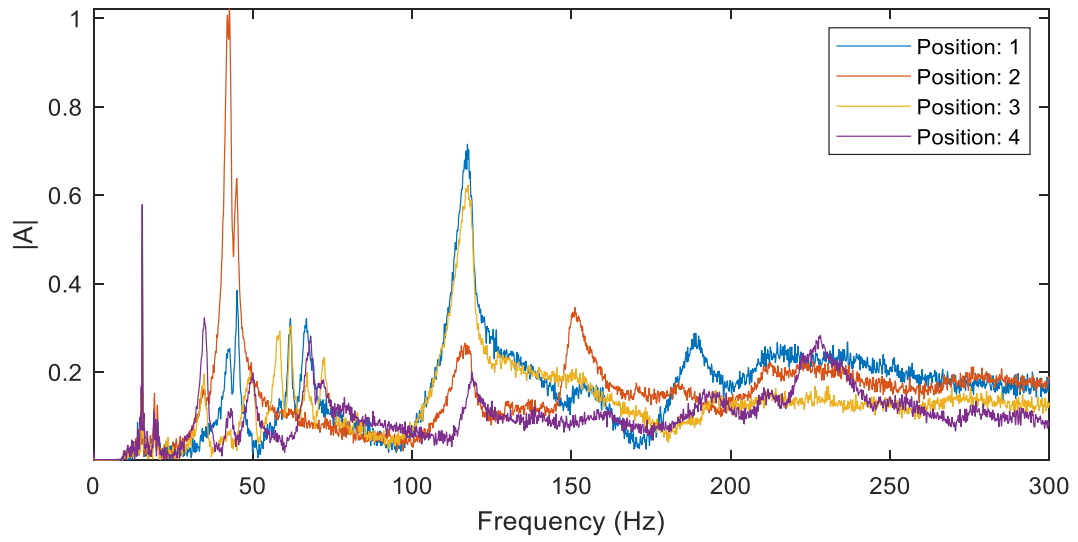


FIGURE 64: ACCELERANCE PLOT FOR THE FOUR POSITIONS IN SLAB 1

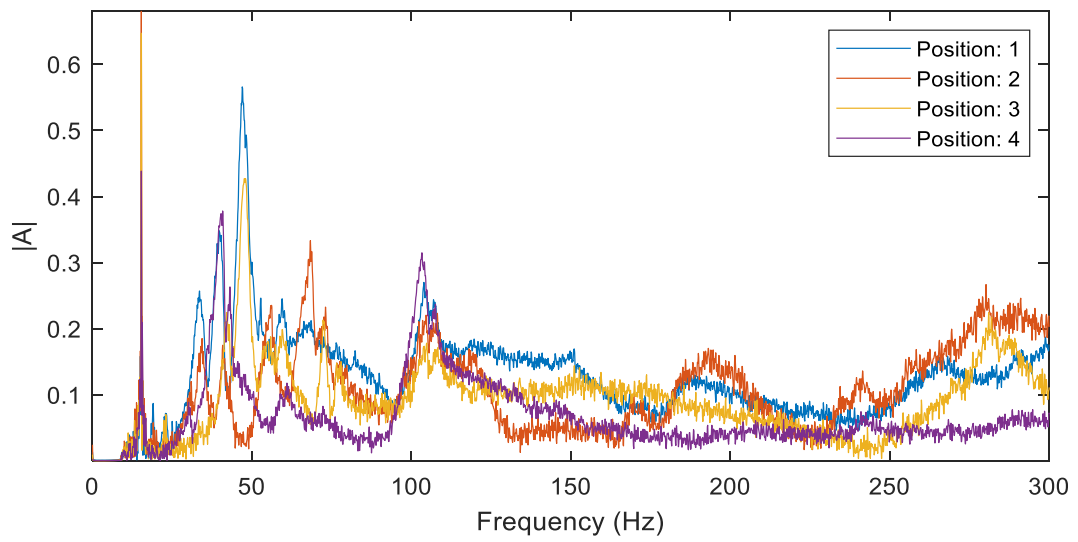


FIGURE 65: ACCELERANCE PLOT FOR THE FOUR POSITIONS IN SLAB 2

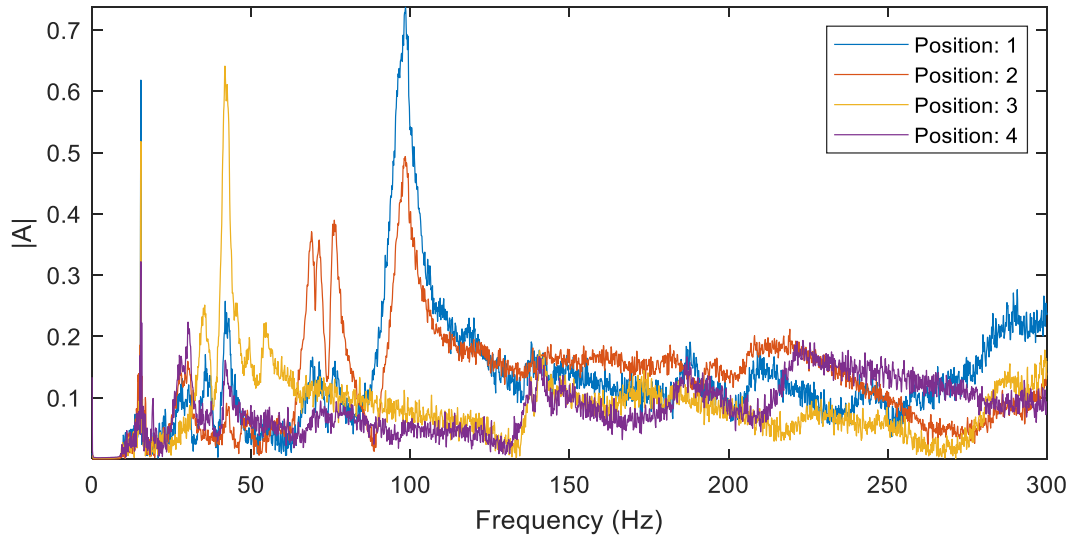


FIGURE 66: ACCELERANCE PLOT FOR THE FOUR POSITIONS IN SLAB 3

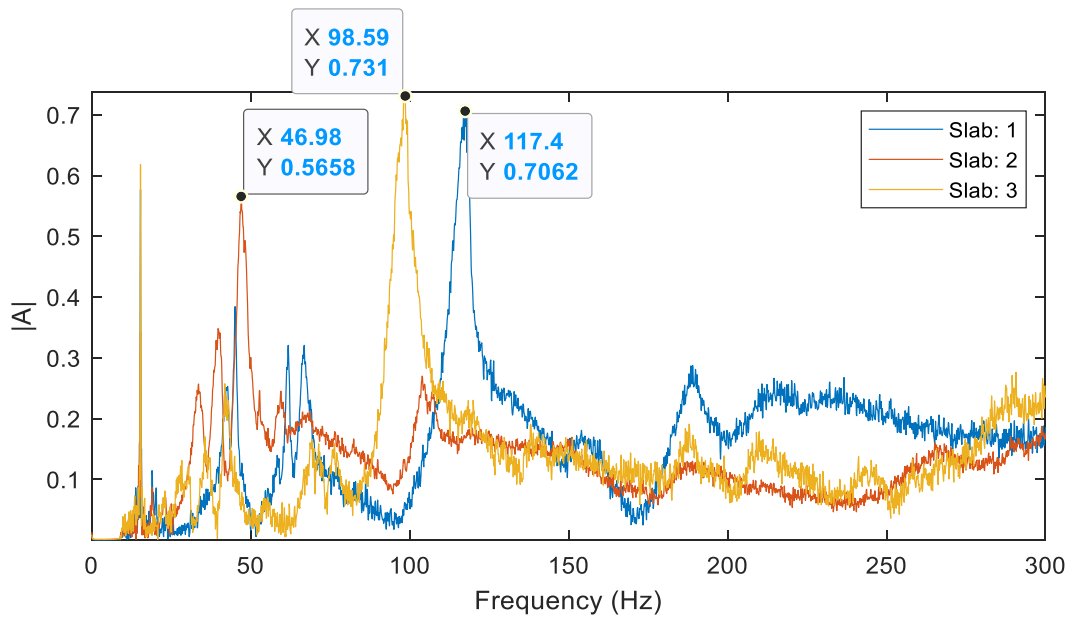


FIGURE 67: ACCELERANCE PLOT FOR THE THREE SLABS IN POSITION 1

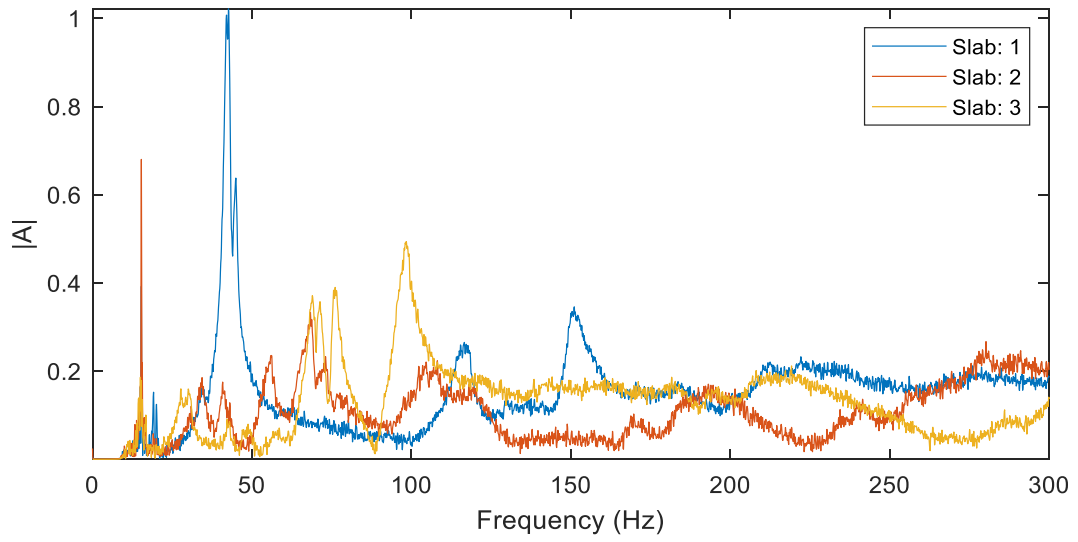


FIGURE 68: ACCELERANCE PLOT FOR THE THREE SLABS IN POSITION 2

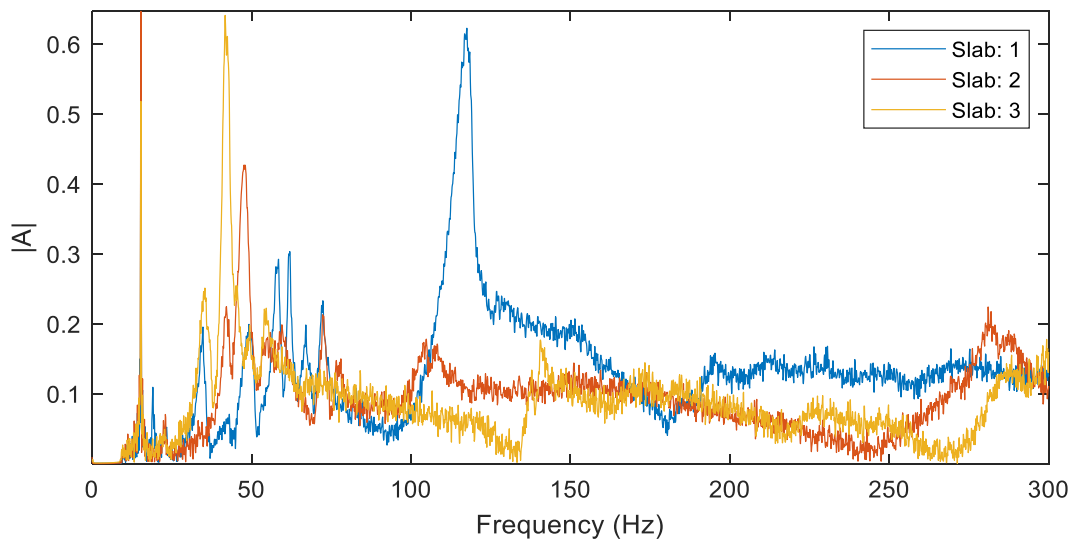


FIGURE 69: ACCELERANCE PLOT FOR THE THREE SLABS IN POSITION 3

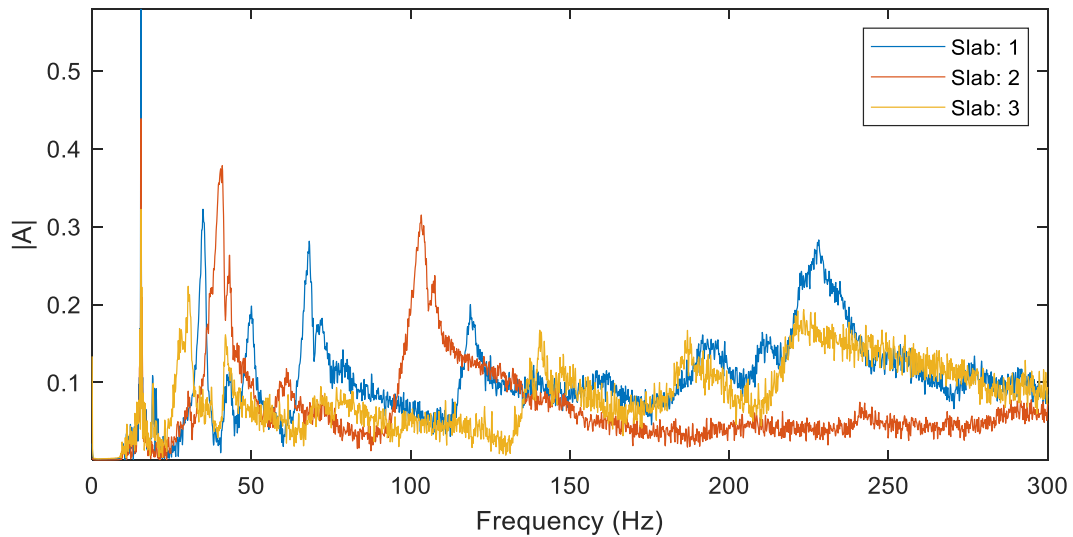


FIGURE 70: ACCELERANCE PLOT FOR THE THREE SLABS IN POSITION 4

As expected, the accelerance function is behaving the same way as the acceleration frequency spectrum. In the plot of the average accelerance functions for position 1, we can see again the expected frequency peaks for each slab, like it was happening with the acceleration frequency spectrum. For the other comparisons of the position and slabs, we can't see this pattern due to the same reasons explained previously for the acceleration frequency spectrum.

Analysing the measurements done with the other tips we can see that the hard-plastic tip with the blue cover is behaving the same way as the measurements done with the same tip without the cover. As expected, this tip had more noise in higher frequencies because it was the softer of the three tips tested. Looking at the measurements done with the metal tip we can't see that the accelerance plot in position 1 for the slab 2 is not behaving the expected way (figure 82). This may be happening because the metal tip was slightly wider than the plastic tip, so this may cause that with a rough surface the impact point may not be exactly the same as in the other slabs.

All the accelerance plots for the hard plastic tip with cover and the metal tip are included in the appendix A.

6. Future recommendations

First of all, for future projects where the frequency response has to be measured, the surface where the tests are performed should be ideally completely flat. That will guarantee good quality in the measurements, allowing the hammer to hit on a homogeneous surface and allowing the accelerometer to be placed completely flat on the surface.

Secondly, the boundary conditions of the slab should be considered, meaning that the support below the slabs should be placed in the same position and the material used should not have any influence on the response of the slab. In our tests, the slabs were put on two wood strips, but these were not placed in exactly the same position in the three slabs and the material chosen was probably absorbing some of the impact waves, which could have led to a narrower frequency range of the response.

Another point to consider is the attachment of the accelerometer, which should be appropriate for recording frequencies up to 800 Hz at least. Looking at the accelerometer manual, we can see that for a rough surface like we had, a hand probe mount would have been the best option for attaching the accelerometer, although the measurements may have a slight deviation from higher frequencies than 700 Hz approximately. Nevertheless, the perfect scenario would be to have a flat surface like it was mentioned previously, where the accelerometer could be attached with a magnet, a mounting pad, an adhesive mount or a stud mount.

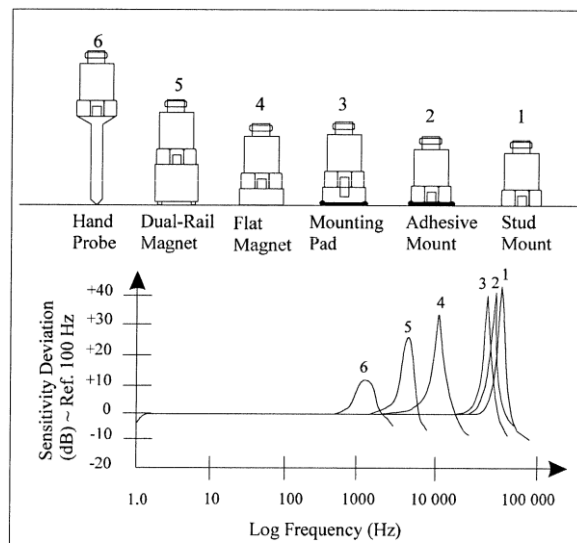


FIGURE 71: TYPES OF MOUNTS FOR THE ACCELEROMETER AND THEIR SENSITIVITY DEVIATIONS [26]

Finally, thinking about future projects following this thesis, the impulse response method could be combined with the impact echo test in order to be able to determine the depth of the delamination found. One possible option would be first doing the impulse response test in order to search for a possible delamination, and in case of finding it, then analysing the acceleration signal following the impact echo test in order to calculate the depth of the delaminated part.

7. Conclusion

Although the results weren't as expected, we can obtain some valuable conclusions from this project.

Firstly, we can affirm that the impulse response test can be a potentially good method for detecting delamination because it can be computed in *MATLAB* obtaining instant results.

Secondly, looking at the experimental part, it has been possible to simulate delamination and find it for one position using the accelerance function.

Thirdly, thinking about a more practical or even commercial version of this project, one of the main challenges for implementing this project is finding a system for measuring the response of the structure with the accelerometer that doesn't affect the quality of the measurement as well as being able to make fast measurements in different points of the structure and also in rough surfaces.

Finally, having seen the main non-destructive delamination testing methods, other methods for detecting delamination could be also considered in case of not being possible to achieve some of the advantages that make the impulse response method more versatile than the others non-destructive methods, such as being able to measure in rough surfaces. A good alternative will be detecting delamination with ultrasonic waves using the ultrasonic pulse echo test or the ultrasonic pulse velocity test. These two tests are widely used in delamination detection in real applications and are probably the fastest way to detect delamination on a flat surface and finding its depth.

8. References

- [1] Y. Zhang and R. K. L. Su, "Concrete cover delamination model for non-uniform corrosion of reinforcements," *Constr. Build. Mater.*, 2019.
- [2] H. Aoude, W. D. Cook, and D. Mitchell, "Effects of Simulated Corrosion and Delamination on Response of Two-Way Slabs," *J. Struct. Eng.*, vol. 140, no. 1, p. 04013023, Jan. 2014.
- [3] J. L. Reilly, W. D. Cook, J. Bastien, and D. Mitchell, "Effects of Delamination on the Performance of Two-Way Reinforced Concrete Slabs," *J. Perform. Constr. Facil.*, vol. 28, no. 4, p. 04014001, Aug. 2014.
- [4] "What Is Concrete Delamination & How Can I Prevent It? | CTI Ready Mix." [Online]. Available: <https://cti-ia.net/what-is-concrete-delamination-how-can-i-prevent-it/>. [Accessed: 21-Nov-2019].
- [5] "Introduction to Ultrasonic Testing." [Online]. Available: <https://www.nde-ed.org/EducationResources/CommunityCollege/Ultrasonics/Introduction/description.htm>. [Accessed: 20-Nov-2019].
- [6] F. Khademi, M. Akbari, and S. M. Jamal, "Measuring Compressive Strength of Pozzolanic Concrete by Ultrasonic Pulse Velocity Method," *i-manager's J. Civ. Eng.*, vol. 5, no. 3, pp. 23–30, Aug. 2015.
- [7] "NDE Technology." [Online]. Available: https://fhwaapps.fhwa.dot.gov/ndep/DisplayTechnology.aspx?tech_id=14. [Accessed: 21-Nov-2019].
- [8] "NDE Technology." [Online]. Available: https://fhwaapps.fhwa.dot.gov/ndep/DisplayTechnology.aspx?tech_id=9. [Accessed: 21-Nov-2019].
- [9] "Non Destructive Evaluation." [Online]. Available: <http://www.theconcreteportal.com/nde.html>. [Accessed: 22-Nov-2019].
- [10] "GEOVision." [Online]. Available: <http://www.geovision.com/impactecho.php>. [Accessed: 23-Nov-2019].
- [11] "(PDF) An investigative study into the application of non-destructive testing techniques for integrity assessment of RC piles." [Online]. Available: https://www.researchgate.net/publication/283623493_An_investigative_study_into_the_application_of_non-destructive_testing_techniques_for_integrity_assessment_of_RC_piles/figures?lo=1. [Accessed: 23-Nov-2019].
- [12] "Delamination Repair | Forest Contractors Vaughan Asphalt Toronto." [Online]. Available: <http://forestcontractors.com/services/building-restoration/delamination-repair/>. [Accessed: 07-Nov-2019].
- [13] "Ultrasonic Pulse Velocity Tester | Concrete Testing | PCTE." [Online]. Available: <https://www.pcte.com.au/pundit-lab-ultrasonic-tester>. [Accessed: 20-Nov-2019].
- [14] "Ultrasonic Testing of Concrete | FPrimeC Solutions." [Online]. Available: <https://www.fprimec.com/ultrasonic-testing-of-concrete/>. [Accessed: 22-Nov-2019].

- [15] "NDE Technology." [Online]. Available: https://fhwaapps.fhwa.dot.gov/ndep/DisplayTechnology.aspx?tech_id=9. [Accessed: 22-Nov-2019].
- [16] "NDE Technology." [Online]. Available: https://fhwaapps.fhwa.dot.gov/ndep/DisplayTechnology.aspx?tech_id=16. [Accessed: 09-Nov-2019].
- [17] "The Impact-Echo Method." [Online]. Available: <https://www.ndt.net/article/0298/streett/streett.htm>. [Accessed: 09-Nov-2019].
- [18] N. Gucunski, G. Slabaugh, Z. Wang, T. Fang, A. Maher, and P. Manager, "VISUALIZATION AND INTERPRETATION OF IMPACT ECHO DATA FROM BRIDGE DECK TESTING."
- [19] S. Sajid and L. Chouinard, "Impulse response test for condition assessment of concrete: A review," *Construction and Building Materials*, vol. 211. Elsevier Ltd, pp. 317–328, 30-Jun-2019.
- [20] A. G. and B. H. H. Davis, *Nondestructive Testing of Concrete Pavement Slabs and Floors with the Transient Dynamic Response Method*. 1987.
- [21] C. Ndt, "Catalog NDT 2014," 2014.
- [22] M. Andrzej and M. Marta, "Modern NDT Systems for Structural Integrity Examination of Concrete Bridge Structures," *Procedia Eng.*, vol. 91, pp. 418–423, 2014.
- [23] E. C. Dodge and S. V. Chapa, "Impulse Response Testing-Analysis of Relative Test Data."
- [24] "PCB Model 086C03." [Online]. Available: <https://www.pcb.com/products?model=086c03>. [Accessed: 13-Dec-2019].
- [25] PCB Piezotronics, "Impact Hammer Model 086D05 Installation and Operating Manual," 2007.
- [26] P. C. B. Piezotronics, "Model 352C04 General purpose , ceramic shear ICP[®] accel ., 10 mV / g , 0 . 5 to 10k Hz , 10-32 Installation and Operating Manual," 2007.
- [27] "NI-9234 - National Instruments." [Online]. Available: <https://www.ni.com/en-no/support/model.ni-9234.html>. [Accessed: 13-Dec-2019].
- [28] "CompactDAQ Chassis - National Instruments." [Online]. Available: <https://www.ni.com/en-no/shop/select/compactdaq-chassis?modelId=125698>. [Accessed: 13-Dec-2019].
- [29] J. Huh, V. Mac, Q. Tran, K.-Y. Lee, J.-I. Lee, and C. Kang, "Detectability of Delamination in Concrete Structure Using Active Infrared Thermography in Terms of Signal-to-Noise Ratio," *Appl. Sci.*, vol. 8, no. 10, p. 1986, Oct. 2018.
- [30] J. White, S. Hurlebaus, and A. Wimsatt, "Concrete Bridge Deck Condition Assessment using Multi-Method Nondestructive Testing Techniques."
- [31] L. M. Linton, "Delaminations in Concrete : A comparison of two common nondestructive testing methods," vol. 36, no. 2, pp. 21–27, 2010.
- [32] "Impact Acoustic Methods for defect evaluation in concrete." [Online]. Available: <https://www.ndt.net/article/ndtce03/papers/v040/v040.htm>. [Accessed: 25-Nov-2019].

- [33] "Utilization of NDI to Inspect Internal Defects in Reinforced Concrete Structures." [Online]. Available: <https://www.ndt.net/article/ndtce03/papers/v028/v028.htm>. [Accessed: 25-Nov-2019].
- [34] Q. H. Tran, D. Han, C. Kang, A. Haldar, and J. Huh, "Effects of ambient temperature and relative humidity on subsurface defect detection in concrete structures by active thermal imaging," *Sensors (Switzerland)*, vol. 17, no. 8, Aug. 2017.
- [35] O. Døssing and B. & Kjae, "Part I: Mechanical Mobility Measurements," *See*, pp. 789–794, 2014.
- [36] "PCB Model 352C03." [Online]. Available: <https://www.pcb.com/products?m=352C03>. [Accessed: 13-Dec-2019].

Appendix

Appendix A: Results

Appendix A.1: Accelerance plots for the measurements done with the hard plastic tip with the blue cover

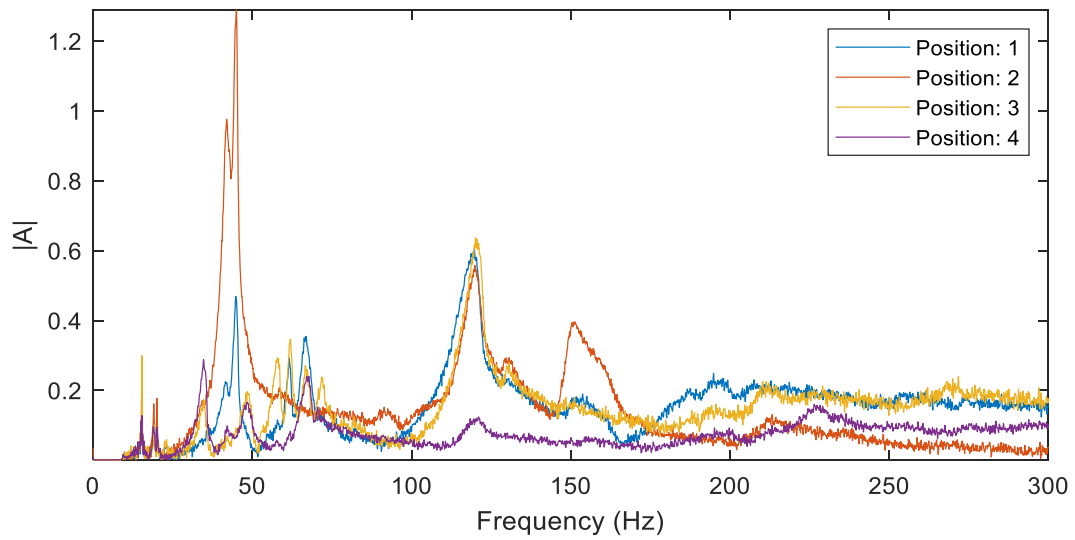


FIGURE 72: ACCELERANCE PLOT OF THE AVERAGE OF FIVE HITS ON THE FOUR POSITIONS IN SLAB 1

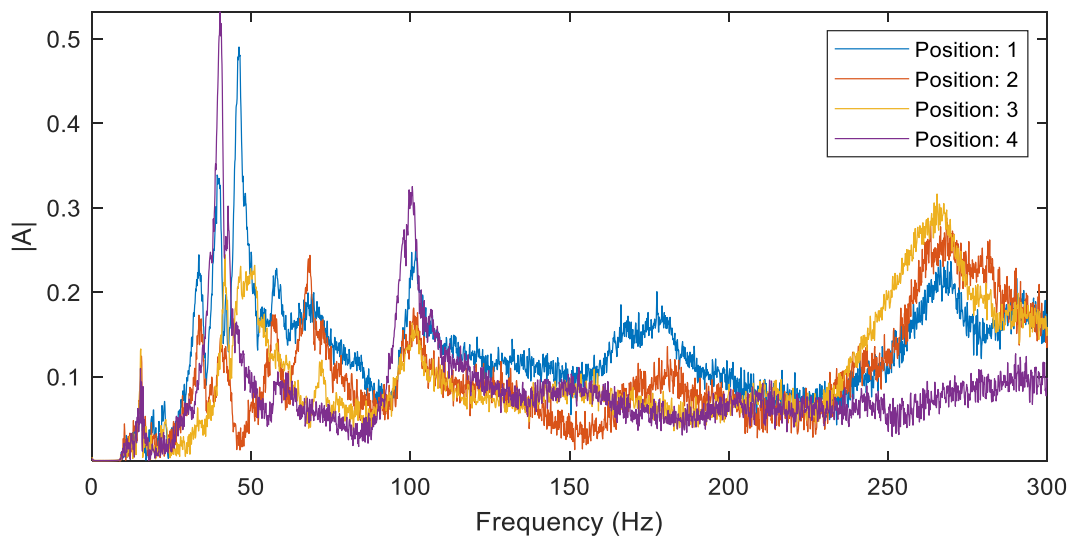


FIGURE 73: ACCELERANCE PLOT OF THE AVERAGE OF THE FIVE HITS ON THE FOUR POSITIONS IN SLAB 2

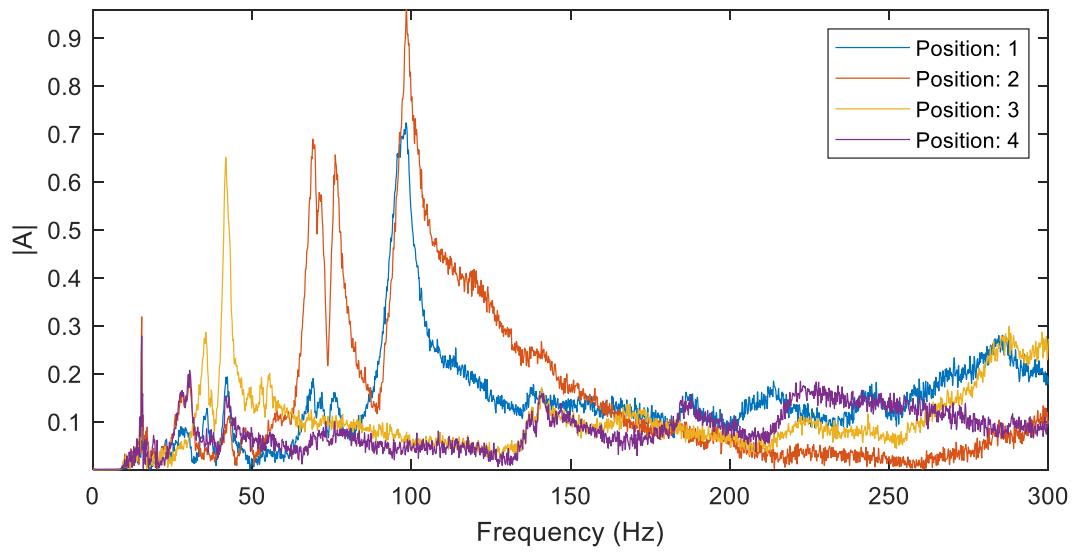


FIGURE 74: ACCELERANCE PLOT OF THE AVERAGE OF THE FIVE HITS ON THE FOUR POSITIONS IN SLAB 3

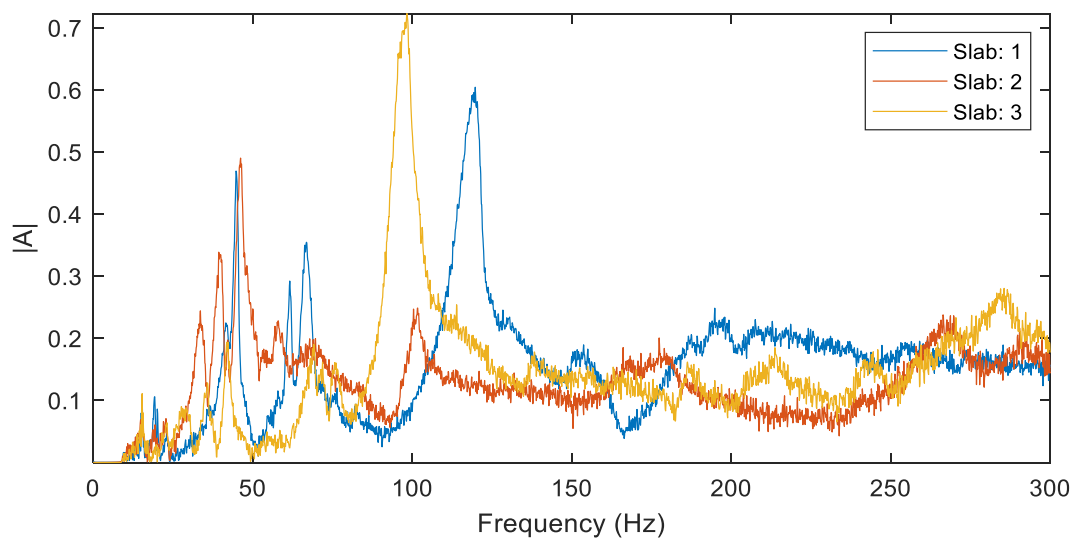


FIGURE 75: ACCELERANCE PLOT OF THE AVERAGE OF THE FIVE HITS ON POSITION 1 FOR THE THREE SLABS

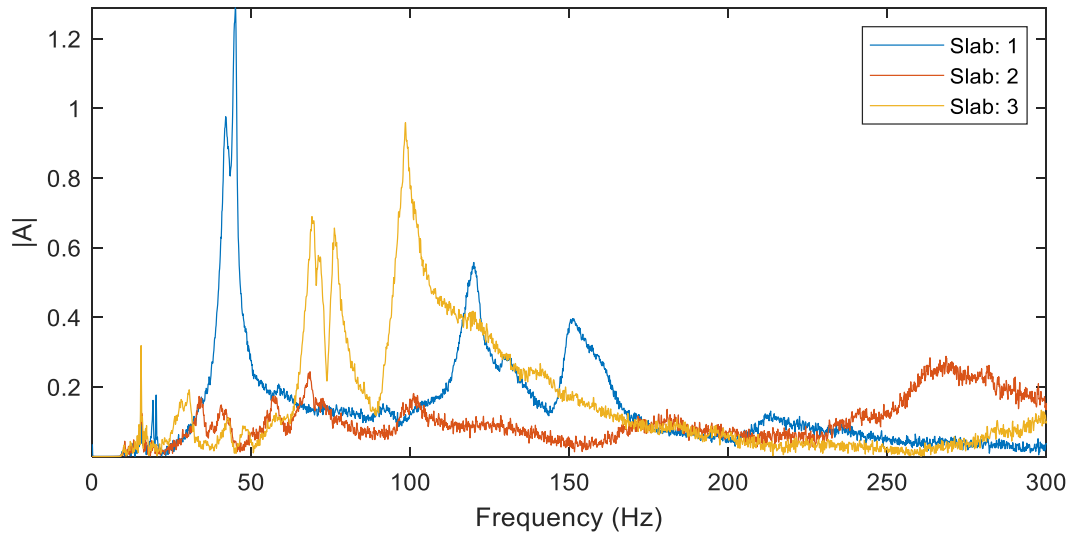


FIGURE 76: ACCELERANCE PLOT OF THE AVERAGE OF THE FIVE HITS ON POSITION 2 FOR THE THREE SLABS

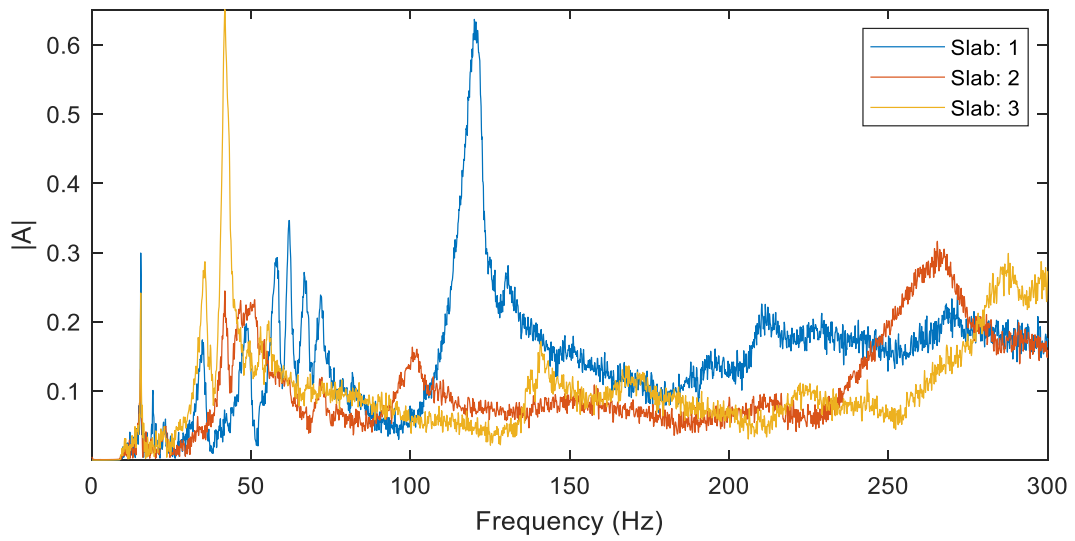


FIGURE 77: ACCELERANCE PLOT OF THE AVERAGE OF THE FIVE HITS ON POSITION 3 FOR THE THREE SLABS

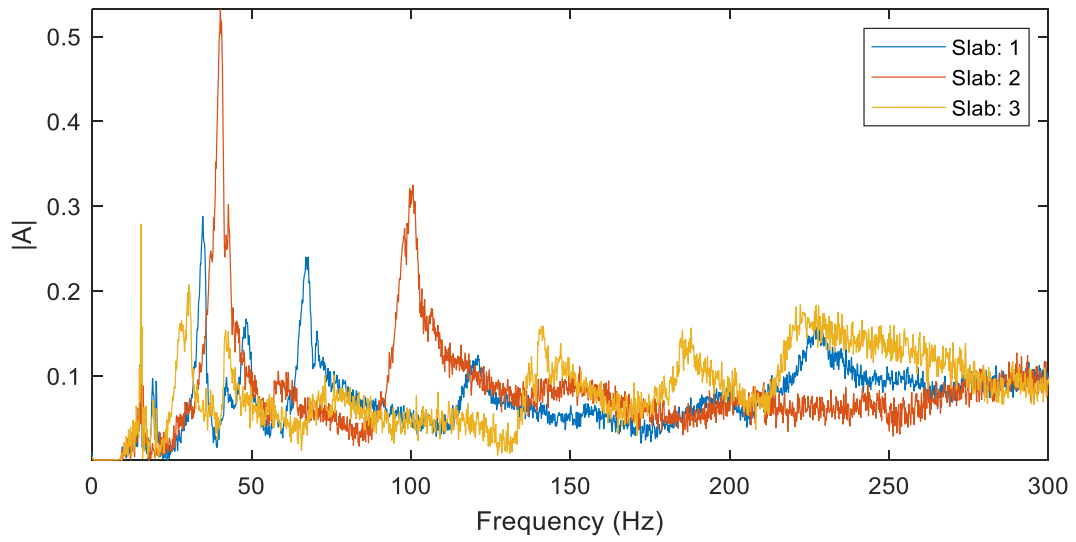


FIGURE 78: ACCELERANCE PLOT OF THE AVERAGE OF THE FIVE HITS ON POSITION 4 FOR THE THREE SLABS

Appendix A.2: Accelerance plots for the measurements done with the metal tip

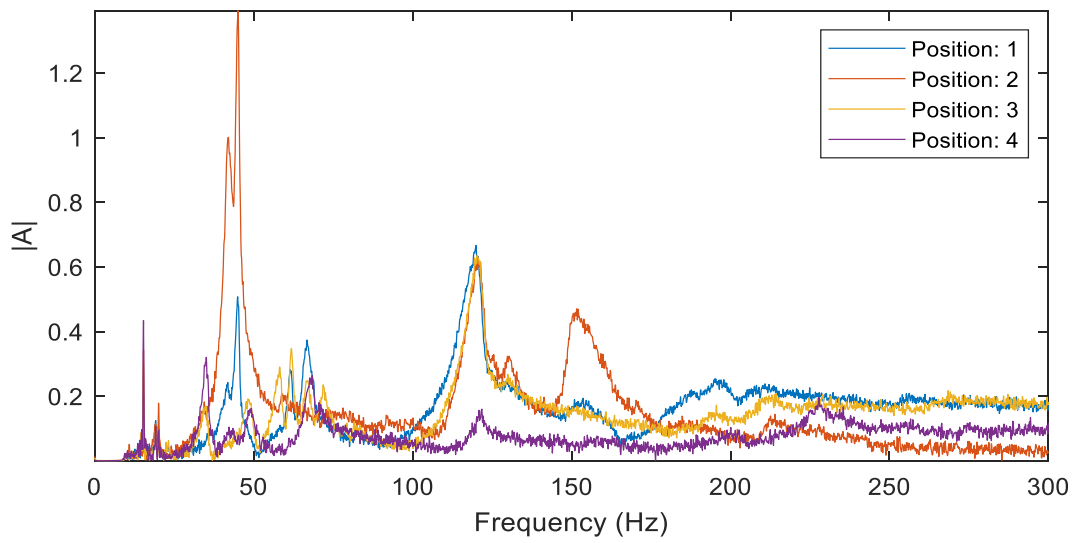


FIGURE 79: ACCELERANCE PLOT OF THE AVERAGE OF THE FIVE HITS ON THE FOUR POSITIONS OF SLAB 1

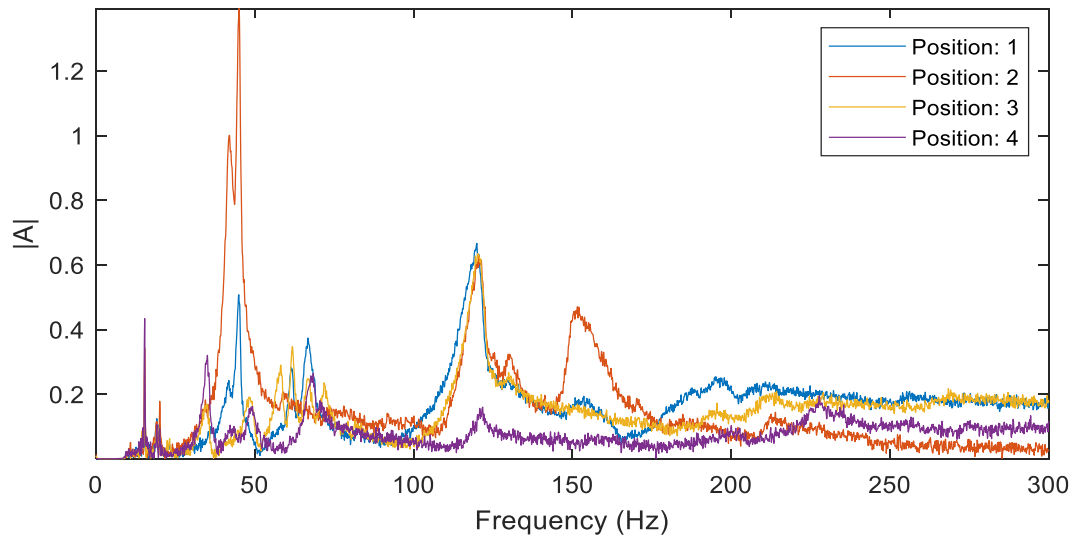


FIGURE 80: ACCELERANCE PLOT OF THE AVERAGE OF THE FIVE HITS ON THE FOUR POSITIONS OF SLAB 2

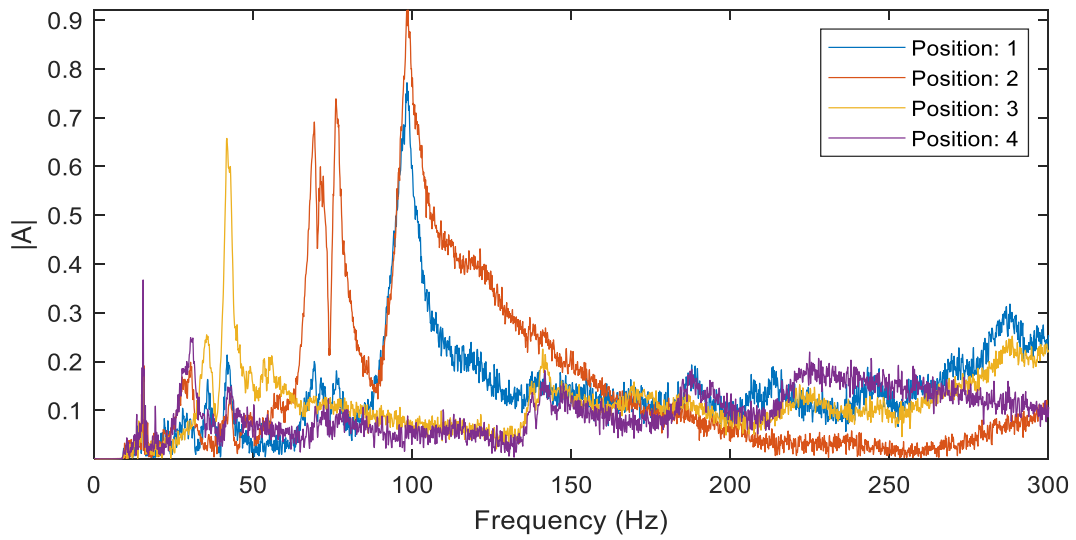


FIGURE 81: ACCELERANCE PLOT OF THE AVERAGE OF THE FIVE HITS ON THE FOUR POSITIONS OF SLAB 3

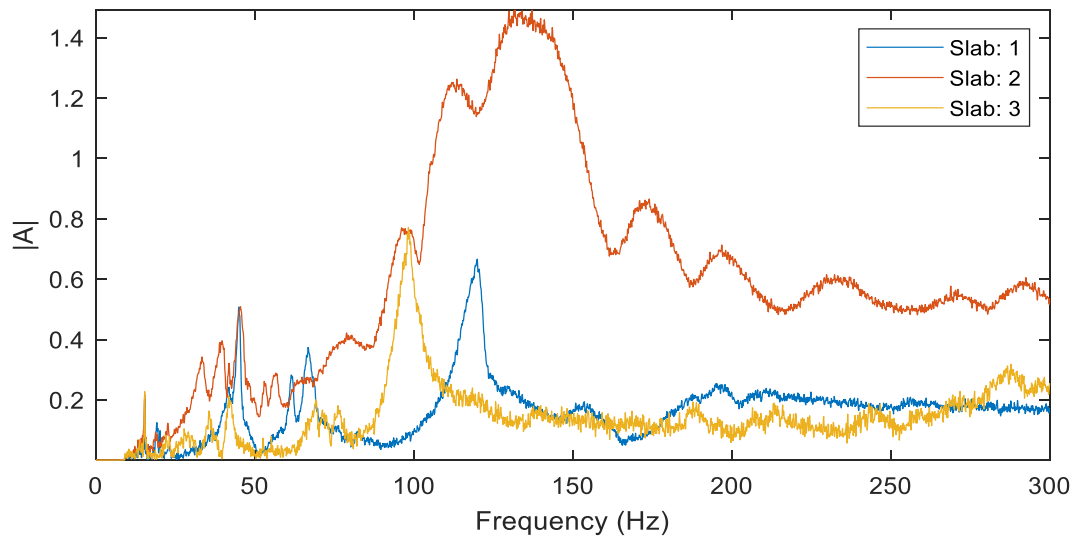


FIGURE 82: ACCELERANCE PLOT OF THE AVERAGE OF THE FIVE HITS ON POSITION 1 FOR THE THREE SLABS

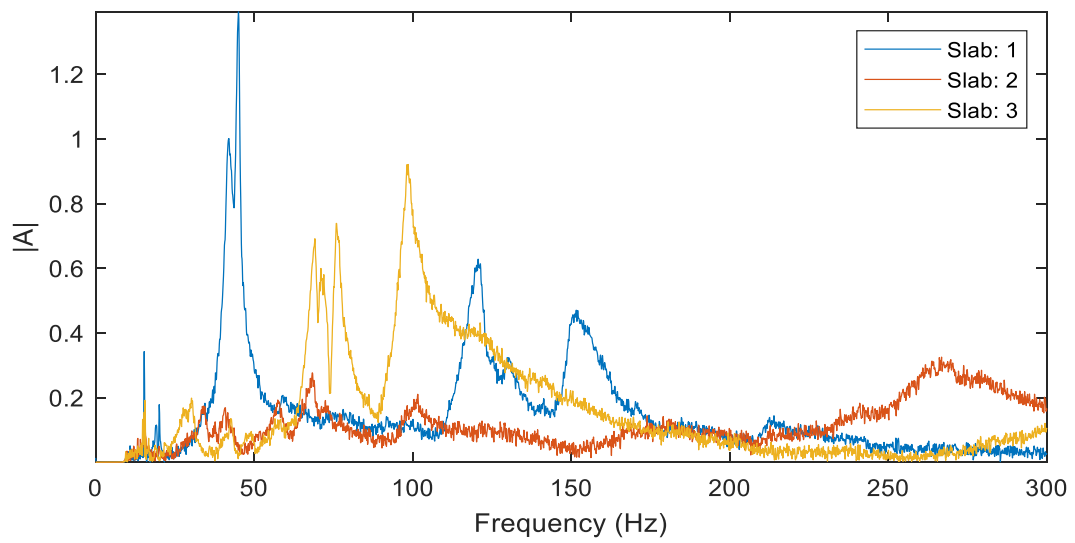


FIGURE 83: ACCELERANCE PLOT OF THE AVERAGE OF THE FIVE HITS ON POSITION 2 FOR THE THREE SLABS

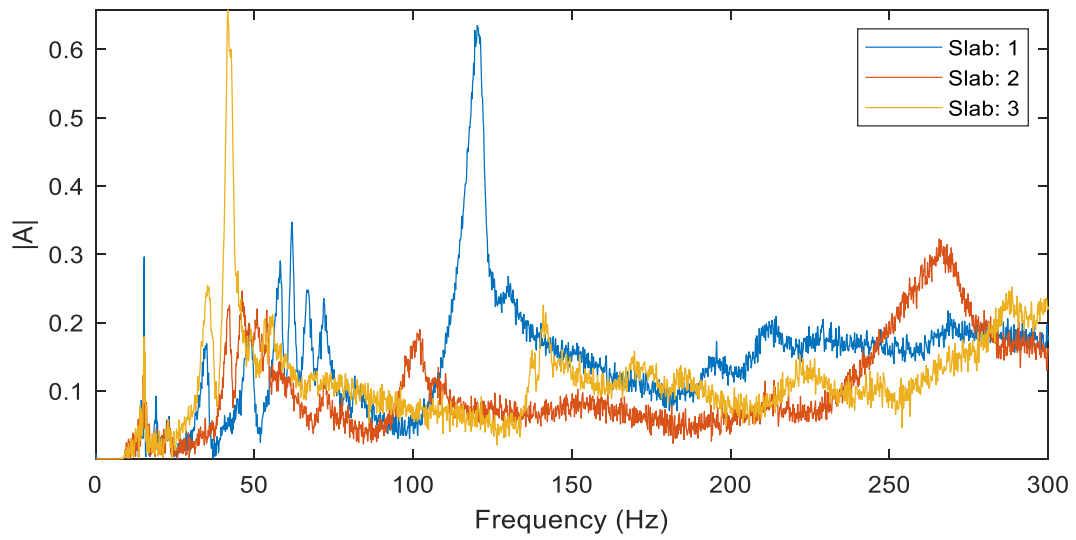


FIGURE 84: ACCELERANCE PLOT OF THE AVERAGE OF THE FIVE HITS ON POSITION 3 FOR THE THREE SLABS

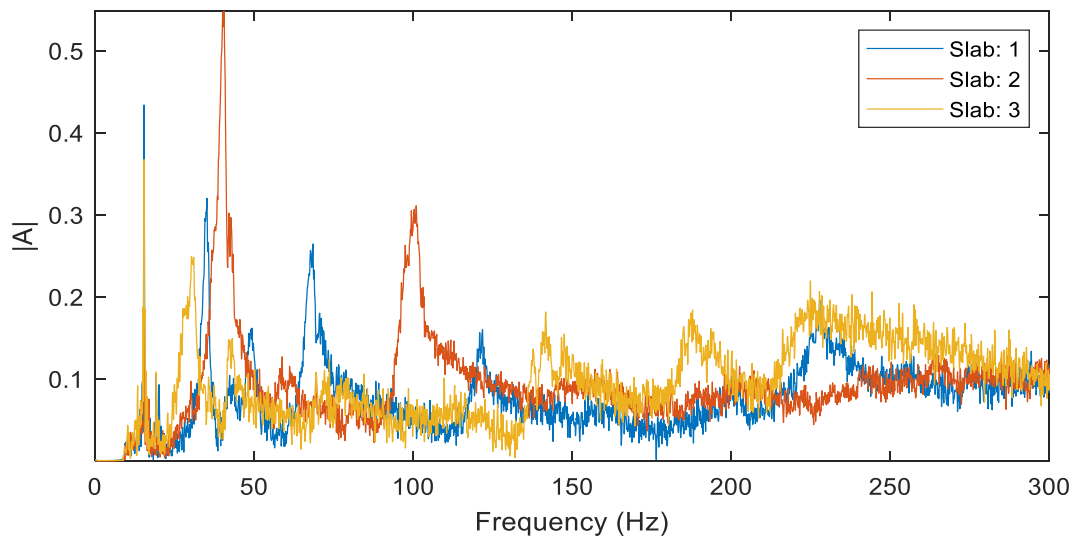


FIGURE 85: ACCELERANCE PLOT OF THE AVERAGE OF THE FIVE HITS ON POSITION 4 FOR THE THREE SLABS

Appendix B: MATLAB scripts

Appendix B.1: Main script and functions

Main script for logging signals and data post-processing using the impulse response method:

```
clear; clc;

% ---- Plotting options ----
Opt.Plot.max_freq = 100; % [Hz]
%Opt.Plot.max_freq = 1000; % [Hz]

% -----

% ---- Input ----
%Slab1= healthy
%Slab2=15mm
%Slab3=30mm
% Experiment title
MyInput.Save.title = 'Slab_1_Position3';
% MyInput.Save.title='Slab_2';
% MyInput.Save.title='Slab_3';
% Folder name
%MyInput.Save.folder = '20181008 Signal adquisition test';
% MyInput.Save.folder = 'TestDay_BlueCap';
MyInput.Save.folder = 'Prova';
% Destination path
MyInput.Save.partial_path = 'C:\Users\PC\OneDrive\Documents\NTNU\BachelorTHESIS\tests';

% How long (Duration of the measurements)
%MyInput.Test.T = 1; % [s]
MyInput.Test.T = 5; % [s]

% How many signals
MyInput.Test.num_signals = 2;

% Module and channel
MyInput.ModCh_num.signal(1,:) = [1, 1];
MyInput.ModCh_num.signal(2,:) = [1, 2];

% MyInput.ModCh_num.signal(3,:) = [1, 3];
% MyInput.ModCh_num.signal(4,:) = [1, 4];
% MyInput.ModCh_num.signal(5,:) = [2, 1];
% MyInput.ModCh_num.signal(6,:) = [2, 2];
% MyInput.ModCh_num.signal(7,:) = [2, 3];
```

```

% Sensors code in database
MyInput.Sensor(1).code = 'HAM#01';
MyInput.Sensor(2).code = 'ACC#02';

save ('SelectedSensors','MyInput');
% MyInput.Sensor(1).code = 'HAM#01';
% MyInput.Sensor(2).code = 'ACC#01';
% MyInput.Sensor(3).code = 'ACC#02';
% MyInput.Sensor(4).code = 'ACC#03';
% MyInput.Sensor(5).code = 'ACC#04';
% MyInput.Sensor(6).code = 'MIC#01';
% MyInput.Sensor(7).code = 'MIC#02';

MyInput.Test.nhits = 2;
%MyInput.Test.nhits = 2;

% Sensors Database
%MyInput.Load.SD.path = 'C:\Users\danielc\Documents\Measurements\00 Sensors calibration
data\SensorsDatabase.mat';
MyInput.Load.SD.path = 'D:\NTNU\BachelorTHESIS\New script\00 Sensors calibration
data\SensorsDatabase.mat';

% -----

% Loading Sensors database
B03_LoadSensorDatabase;

% Folder operations
[MyInput] = B04_FolderOperations(MyInput);

% DAQ Session-Based interface
[Session,Calc] = B05_DAQ_Session(MyInput);

%Logging the data
[c_table] = B06_logging_measurements(MyInput,Session,Opt,Calc)

c_table=0;

%Running A02 and saving figure
A02(MyInput,c_table);

disp ('PROGRAM FINISHED');
% ---- End of script ----

```

Function B04_FolderOperations:

```
function [MyInput] = B04_FolderOperations(MyInput)

% Checks if mat files exist in the destination folder

% Destination folder
MyInput.Save.path =
[MyInput.Save.partial_path, '\', MyInput.Save.folder, '\', MyInput.Save.title];

% Folder operations
if ~.isdir(MyInput.Save.path)

    % Creating folder if it doesn't exist
    mkdir(MyInput.Save.path);

else

    % Checking if *.mat files exist
    listing = dir([MyInput.Save.path, '*.*mat']);
    if size(listing,1) > 0
        disp('WARNING: The specified folder contains mat files');
        answer = input('Press any key to cancel, or "Y" to delete files and continue: ','s');
        if strcmp(answer, 'Y')
            disp('Deleting files ...');
            for file_num = 1:size(listing,1)
                mydelete([MyInput.Save.path, '\', listing(file_num).name]);
            end % for file_num = 1:size(listing,1)
            fprintf('\b'); disp(' DONE');
        else
            error('Process cancelled by user');
        end % if strcmp(answer, 'Y')
    end % if size(listing,1) > 0
end % if ~.isdir(MyInput.Save.path)

% ---- End of script ----
```

Function B05_DAQ_Session:

```
function [Session,Calc] = B05_DAQ_Session(MyInput)

% Creates the DAQ Session-Based interface
% Adds the channels to the session
% Creates additional variables

% -----
% ---- Input ----
% MyInput
% ---- Output ----
% Session
% Calc
% -----

% Finding supported hardware available
disp('Finding supported hardware available ...');
Devices = daq.getDevices;
fprintf('\b'); disp(' DONE');

% Create session for National instruments
Session = daq.createSession('ni');

% Adding the channels (also naming and giving sensitivity)
for signal_num = 1:MyInput.Test.num_signals
    mod_num = MyInput.ModCh_num.signal(signal_num,1);
    ch_num = MyInput.ModCh_num.signal(signal_num,2);

    Session.addAnalogInputChannel(Devices(mod_num).ID,Devices(mod_num).Subsystems.ChannelNames(ch_num),...
        MyInput.Sensor(signal_num).measurementType);
    Session.Channels(signal_num).Name = MyInput.Sensor(signal_num).code;
    Session.Channels(signal_num).Sensitivity = MyInput.Sensor(signal_num).Sensitivity.value;
end % for signal_num

% Output generation
Session.DurationInSeconds = MyInput.Test.T;
Calc.numChannels = length(Session.Channels);

% ---- End of script ----
```

Function B06_logging_measurements:

```
function [c_table] = B06_logging_measurements(MyInput,Session,Opt,Calc)
```

```
% Logs the signals from all channels defined in the Session
```

```
% -----  
% ---- Input ----  
% ---- Output ----  
% -----
```

```
counter = 0;  
c=0;  
nhits = MyInput.Test.nhits;  
b=1;  
% Hit number loop  
measurenr = 0;  
% measurenr=2;  
% while measurenr<=nhits+1; %when measuring positions 3 and 4  
while measurenr <= nhits-1
```

```
    measurenr = measurenr + 1;  
    counter = counter + 1;  
    save_measurement = 0;
```

```
% Preperation of logging  
Session.prepare;
```

```
% Information display  
disp(['** Measurement number = ',num2str(measurenr)]);  
input(['Press ENTER to log ',num2str(MyInput.Test.T),'s ']);  
disp(['Now recording for ',num2str(MyInput.Test.T),'s ...']);
```

```
% Logging data  
[data,time,triggertime] = Session.startForeground();  
fprintf('\b'); disp(' DONE');
```

```
% Plot logged series  
if counter == 1  
    h = figure;  
    myFigMaximize;  
end % if counter == 1  
for ch = 1:Calc.numChannels  
    sub_data = data(:,ch);  
    subplot(4,4,ch);  
    plot(time,sub_data); axis tight;  
    xlabel('Time (s)');  
    ylabel_text = Session.Channels(ch).Name;  
    ylabel_text(ylabel_text=='_') = ' ';  
    ylabel(ylabel_text);  
    sub_data = detrend(sub_data);
```

```

subplot(4,4,ch+8);
[PSD_x,PSD_y] = myPSD(sub_data,1/time(2));
inds = and(PSD_x>0,PSD_x<=Opt.Plot.max_freq);
plot(PSD_x(inds),PSD_y(inds)); axis tight;
    xlabel('Frequency (Hz)');
    ylabel('PSD');
    set(gca,'YScale','log');
end % for ch = 1:Calc.numChannels
shg;

% Asking user if measurement should be saved
user_input = input('Keep signals? Press "y"+ENTER = yes; other key = no => ','s');
if user_input == 'y'
    save_measurement = 1;
else
    save_measurement = 0;
end % if user_input == 'y'

if save_measurement == 1
    % Saving data
    disp('Saving ...');
    format shortg;
    c_dec=clock; %Taking the clock value
    c=fix(c_dec); %Removing decimals for the seconds
    c_table(b,:)=c;
    filename =
[MyInput.Save.title,'_',num2str(c(1:3)),'_',num2str(c(4:6)),'_number',num2str(measurenr),'.mat'];
    filename(filename==' ') = [];
    timestamp = trigger_time;
    save([MyInput.Save.path,'\',filename],'data','time','timestamp');
    fprintf('\b'); disp(' DONE');
    b=b+1;
else
    % Repeating measurement
    measurenr = measurenr - 1;
end % if save_measurement == 1

end % for measurenr = 1:MyInput.Test.nhits

disp('All measurements finished');

% Closing figure
try
    close(h);
end % try

% ---- End of script ----

```

Function A02:

```
function [] = A02(MyInput,c_table)

% filename =
[MyInput.Save.title,'_',num2str(c(1:3)),'_',num2str(c(4:6)),'_position',num2str(measurenr),'.mat'];
hits=size(c_table,1);
count=1;
while count<=hits

% data_test=
[MyInput.Save.partial_path,'\',MyInput.Save.folder,'\',MyInput.Save.title,'\',MyInput.Save.title
,'_',num2str(c_table(count,1:3)),'_',num2str(c_table(count,4:6)),'_number',num2str(count),'.mat'];

% data_test(data_test==' ') = [];
data_test=['C:\Users\PC\OneDrive\Documents\NTNU\BachelorTHESIS\tests\TestDay\Slab_1_P
osition1\Slab_1_Position1_20191129_10376_number1.mat']

% C:\Users\PC\OneDrive\Documents\NTNU\Bachelor THESIS\tests\20191113 test\Slab_1
data_sensor='C:\Users\PC\OneDrive\Documents\NTNU\BachelorTHESIS\Matlab files\00
Sensors calibration data\SensorsDatabase'

% %-----
% %Loading data and sensor proprieties
load (data_test);
load (data_sensor);
load('SelectedSensors.mat');
disp 'data loaded succesfully';

% %Selecting force and accelerometer data (column 1 and 3)
test.force=data(:,1);
test.acceleration=data(:,2);

%%Selecting the first 0,5001 sec aprox of the signal to make a "calibration signal"
Calibration_period=(1:827);
timecal=time(Calibration_period);
test.forcecal=test.force(Calibration_period);
test.accelerationcal=test.acceleration(Calibration_period);

test.forceavg=mean(test.forcecal);
test.accelerationavg=mean(test.accelerationcal);

test.forceok=test.force-test.forceavg;
test.accelerationok=test.acceleration-test.accelerationavg;
% figure;
% plot(time,test.forceok);
% figure;
% plot(time,test.accelerationok);
```

```

%Making the vectors longer up to 15 s
calc.last_time=length(time);
time_add=(time(calc.last_time):time(2):9);
time=[time',time_add];
time=time';
calc.zeros_length=length(time_add);
test.forceok=[test.forceok',zeros(1,calc.zeros_length)];
test.forceok=test.forceok';
test.accelerationok=[test.accelerationok',zeros(1,calc.zeros_length)];
test.accelerationok=test.accelerationok';
%Calculating signals with sensitivity
B09_sensitivity(test,MyInput,SD);
%FFT of the signals and plotting
[f.freq,test.force_t]=B07_TestSignal(time,test.forceok,'Force');
[f.freq,test.acc_t]=B07_TestSignal(time,test.accelerationok,'Acceleration');
%%Cumulative integral for obtaining velocity
test.velocity=cumtrapz (test.accelerationok);
%Filtering velocity to remove low frequencies
[test.velocity]=HighpassFilter(test.velocity,30,1/time(2));
[f.freq,test.velocity_t]=B07_TestSignal(time,test.velocity,'Velocity');
%Calculating the transfer function  $H(w)=(at*fct)/(ft*fct)$ 
%complex conjugate
test.forceconj=conj(test.force_t);
%transfer function
calc.num=test.velocity_t.*test.forceconj;
calc.den=test.force_t .* test.forceconj;
h.h=calc.num./calc.den;
calc.crop=length(h.h);
calc.sel=20
h.zeros=zeros(calc.crop-calc.sel,1)
h.h2=[h.h(1:calc.sel,1)',h.zeros'];
h.h=h.h-h.h2';
B08_TestNoFFT(f.freq,h.h,'H');
%Calculation of average mobility, dynamic stiffness, mobility slope
%and Voids index (v)
f.lowrange=[0,40];
f.mediumrange=[0,100];
f.highrange=[100,800];
f.low=f.freq(f.freq>=min(f.lowrange) & f.freq<=max(f.lowrange));
f.medium=f.freq(f.freq>=min(f.mediumrange) & f.freq<=max(f.mediumrange));
f.high=f.freq(f.freq>=min(f.highrange) & f.freq<=max(f.highrange));
f.lowlength=length(f.low);
f.mediumlength=length(f.medium);
f.highlength=length(f.high);
%Searching for the values in the borders of the range
f.h0=f.low(1);
f.h1=f.low(f.lowlength);
f.h2=f.medium(f.mediumlength);
f.h3=f.high(1);
f.h4=f.high(f.highlength);
% %Once I have the border values for the frequency, now I can search for the
% %position of this values in the freq matrix, and then find this position in

```



```

% %the h matrix to know the range of values of h that we want.
f.posfh0=find(f.freq==f.h0);
f.posfh1=find(f.freq==f.h1);
f.posfh2=find(f.freq==f.h2);
f.posfh3=find(f.freq==f.h3);
f.posfh4=find(f.freq==f.h4);
%Searching the values in the absolut h matrix
h.abs=abs(h.h);
h.low=h.abs(f.posfh0:f.posfh1);
h.med=h.abs(f.posfh0:f.posfh2);
h.high=h.abs(f.posfh3:f.posfh4);
%linear regressions
calc.fit1=fit(f.low',h.low,'poly1');
calc.slope=calc.fit1.p1;
result.kd=(1/calc.slope);
result.fit1=calc.slope*f.low+calc.fit1.p2
% figure;
% plot(f.low,h.low,f.low,result.fit1);
f.high_plot=f.high-f.high(1);%setting frequesncy to 0
calc.fit2=fit(f.high_plot',h.high,'poly1');
result.fit2=(calc.fit2.p1)*f.high_plot+calc.fit2.p2
% figure; plot(f.high,h.high,f.high,result.fit1);
%Calculating average mobility
result.avgmob=mean(h.high);
result.avgmobgraph=0*f.high+result.avgmob;
%Calculating peak mean mobility ratio
calc.medpeak=max(h.med);
result.voidsindex=calc.medpeak/result.avgmob;
if result.voidsindex>2.5
    result.delamination='DELAMINATION DETECTED';
else result.delamination='NO DELAMINATION DETECTED';
end %if delamination
plot_mob=figure;
plot(f.freq,h.abs,'LineWidth',1.5); hold on; box on;
plot(f.high,result.fit2); hold on; box on;
plot(f.high,result.avgmobgraph,'--'); hold on; box on;
title('Mobility plot');
xlabel('Frequency (Hz)');
ylabel('Mobility ( )');
lgd_mob=legend({'Mobility','Mobility slope','Average mobility','Location','northeast'});
str1=['Dynamic stiffness=',num2str(result.kd)];
str2=['Voids index=',num2str(result.voidsindex)];
str3=[result.delamination];
annotation('textbox',[.905 .5 .1 .2],'String','Results:','EdgeColor','none');
annotation('textbox',[.905 .45 .1 .2],'String',str1,'EdgeColor','none');
annotation('textbox',[.905 .40 .1 .2],'String',str2,'EdgeColor','none');
annotation('textbox',[.905 .35 .1 .2],'String',str3,'EdgeColor','none');
save_plot=[MyInput.Save.partial_path,'\',MyInput.Save.folder,'\',MyInput.Save.title,'\','plot',n
um2str(count),'.fig'];
savefig(gcf,save_plot);
disp(['RESULTS']);
disp(str1);

```

```

disp (str2);
disp(str3);
count=count+1;
% close all;
end %While
end %function

```

Appendix B.2: Accelerance script

```

clear;clc;
%-----
number=5;
position=4;
i=1;
for slab=1:3
    for pos=1:position
        for num=1:number

data_test=['C:\Users\PC\OneDrive\Documents\NTNU\BachelorTHESIS\TEST\TestDay\Slab_',num2str(slab),'_Position',num2str(pos),'\Slab_',num2str(slab),'_Position',num2str(pos),'_',num2str(num),'.mat'];
        data_sensor='C:\Users\PC\OneDrive\Documents\NTNU\BachelorTHESIS\Matlab files\00 Sensors calibration data\SensorsDatabase'
            % %-----zº-----
            % %Loading data and sensor propierties
            load (data_test);
            Alphabet = 'ABCDEFGHIJKLMNOPQRSTUVWXYZ';
            slb = Alphabet (slab);
            posi = Alphabet(pos);
            numb = Alphabet(num);
            %position.hitnumber
            datos.(slb).(posi).(numb)=data;
            current_data=datos.(slb).(posi).(numb);
            load (data_sensor);
            load('SelectedSensors.mat');
            disp 'data loaded succesfully';

            % %Selecting force and accelerometer data (column 1 and 3)
            test.force=current_data(:,1);
            test.acceleration=current_data(:,2);

            %%Selecting the first 0,5001 sec aprox of the signal to make a "calibration signal"
            Calibration_period=(1:827);
            timecal=time(Calibration_period);
            test.forcecal=test.force(Calibration_period);
            test.accelerationcal=test.acceleration(Calibration_period);
            test.forceavg=mean(test.forcecal);
            test.accelerationavg=mean(test.accelerationcal);
            test.forceok=test.force-test.forceavg;

```

```

test.accelerationok=test.acceleration-test.accelerationavg;
%Making the vectors longer up to 15 s
calc.last_time=length(time);
time_add=(time(calc.last_time):time(2):9);
time=[time',time_add];
time=time';
calc.zeros_length=length(time_add);
test.forceok=[test.forceok',zeros(1,calc.zeros_length)];
test.forceok=test.forceok';
RES.force.(slb).(posi).N(:,num)=test.forceok;
test.accelerationok=[test.accelerationok',zeros(1,calc.zeros_length)];
test.accelerationok=test.accelerationok';
[test.accelerationok]=HighpassFilter(test.accelerationok,10,1/time(2));
RES.acc.(slb).(posi).N(:,num)=test.accelerationok;
%Cumulative integral for obtaining velocity
test.velocity=cumtrapz (test.accelerationok);
%Cleaning velocity
test.velocitycal=test.velocity(Calibration_period);
test.velocityavg=mean(test.velocitycal);
test.velok=test.velocity-test.velocityavg;
% Filtering velocity to remove low frequencies
% [test.velok]=HighpassFilter(test.velok,30,1/time(2));
RES.velok.(slb).(posi).N(:,num)=test.velok;
% Calculating signals with sensitivity
B09_sensitivity(test,MyInput,SD);
%FFT of the signals and plotting
[f,force_t]=myfft(time,test.forceok);
[f,acc_t]=myfft(time,test.accelerationok);
[f,vel_t]=myfft(time,test.velok);
RES.acc_t.(slb).(posi).N(:,num)=force_t;
RES.acc_t.(slb).(posi).N(:,num)=acc_t;
RES.vel_t.(slb).(posi).N(:,num)=vel_t;
% % %Transfer function H2=acc/Force
h2=acc_t./force_t;
RES.h2.(slb).(posi).N(:,num)=h2;
end %for number
end %for position
end %for slab
% leng=length (f);
% crop=4000;
% final_len=leng-4000;
% f=[(f(:,1:4000)),zeros(1,final_len)];
RES.h2.A.A.N(:,4)=[];
for slab=1:3
    for pos=1:4
        Alphabet = 'ABCDEFGHJKLMNOPQRSTUVWXYZ';
        slb = Alphabet(slab);
        posi = Alphabet(pos);
        if slab==1 && pos==1
            for i=1:4
                RES.h2.(slb).avg(:,pos)=mean(RES.h2.A.A.N(:,i),2);
                RES.integral.(slb).(posi)=(trapz(abs(RES.h2.(slb).avg(:,pos))))^2;
            end
        end
    end
end

```

```

%     =integ;
    end%for
else
for i=1:5
    RES.h2.(slb).avg(:,pos)=mean(RES.h2.(slb).(posi).N(:,i),2);
    RES.integral.(slb).(posi)=(trapz(abs(RES.h2.(slb).avg(:,pos))))^2;
end%for
end%if
end%for pos
end %for slab

figure;
i=1;
for slab= 1:3
    subplot(2,2,slab);
%   maintxt=['Average transfer function',' ', 'Slab',num2str(slab)];
    for pos=1:4
        Alphabet = 'ABCDEFGHIJKLMNOPQRSTUVWXYZ';
        slb = Alphabet(slab);
        posi= Alphabet(pos);
        plot (f,abs(RES.h2.(slb).avg(:,pos)));hold on;axis tight;
        txt_legend(pos,:)=['Position: ',num2str(pos)];
%   current_energy=num2str(RES.integral.(slb).(posi).N(:,i));
%   txt_legend3(pos,:)=['Energy: ',(current_energy)];
%   Energy: ,num2str(RES.integral.(slb).(posi).N(:,i))
    end%for position
    %TEXTBOXX
%   title(maintxt);
    myFigSqueeze;
    xlim([0,300]);
    xlabel('Frequency (Hz)');ylabel('|A|');
lgd_acccomp=legend({(txt_legend(1,:)),(txt_legend(2,:)),(txt_legend(3,:)),(txt_legend(4,:))},'Location','northeast');
end%for slab

figure;
for pos=1:4
    subplot(2,2,pos);
%   maintxt=['Average transfer function',' ', 'Position',num2str(pos)];
    for slab=1:3
        Alphabet = 'ABCDEFGHIJKLMNOPQRSTUVWXYZ';
        slb = Alphabet(slab);
        plot (f,abs(RES.h2.(slb).avg(:,pos)));hold on; axis tight;
        txt_legend2(slab,:)=['Slab: ',num2str(slab)];
    end%for position
%   title(maintxt);
    myFigSqueeze;
    xlim([0,300]);
    xlabel('Frequency (Hz)');ylabel('|A|');
lgd_acccomp=legend({(txt_legend2(1,:)),(txt_legend2(2,:)),(txt_legend2(3,:))},'Location','north east');
end%for slab

```

Appendix C: Concrete recipe

Proporsjonering på volumbasis

Initialparametre	Verdi	Enhet	k
Mengde sementlim	287	l/m ³	-
v/(c+Σkp)	0,48	-	-
s/c	0,0	%	1,00
fa/c	0,0	%	0,20
Tilsetningsstoff	% av C	% av S	
RMC-420	0,69	0,00	
	0,00	0,00	
	0,00	0,00	
	0,00	0,00	
Luftinnhold (%)	2,0	%	
Matriksmengde	316	l/m ³	

Proporsjonert betong

Ønsket Oppnådd

Materialer	kg/m ³	kg	kg
Norcem Standard FA	349,2	12,2	94,8
Silikastøv	0,0	0,0	0,0
Flyveaske	0,0	0,0	0,0
Fritt vann	174,8	6,1	56,9
Absorbert vann	9,2	0,3	3,6
Årdal 0-8 mm	1102,2	38,6	308,1
Årdal 0-2 mm MS (v)	0,0	0,0	0,0
Årdal 8-11mm	734,8	25,7	116,2
Årdal 11-16 mm	0,0	0,0	116,2
	0,0	0,0	0,0
	0,0	0,0	0,0
	0,0	0,0	0,0
	0,0	0,0	0,0
	0,0	0,0	0,0
	0,0	0,0	0,0
RMC-420	2,41	0,08	0,38
0,0	0,00	0,00	0,00
	0,00	0,00	0,00
	0,00	0,00	0,00
Prop. betongdens. (kg/m ³)	2371		

Absorbert fukt, tilslag (%)	
Årdal 0-8 mm	0,5
Årdal 0-2 mm MS (v)	0,8
Årdal 8-11mm	0,5
Årdal 11-16 mm	0,5
	0,0
	0,0
	0,0
	0,0
	0,0
	0,0

Materiale	Densitet	Tørrestoff
Sement	2950	-
Silika	2200	-
Flyveaske	2200	-
RMC-420	1080	18
0	1200	100
	1200	100
	1000	100

Fersk betong

Egenskap	
Ønsket volum	35,0
Innveid volum (l)	298,6
Luftinnhold (%)	2,0
Målt betongdensitet (kg/m ³)	2319,9
Effektivt v/(c+Σkp)	0,598

Volumkorreksjon

	korr.luft	korr.dens	Korrigert
	-0,2	-1,2	316,1
	0,0	0,0	0,0
	0,0	0,0	0,0
	-0,1	-0,7	188,9
	0,0	0,0	12,1
	-0,5	-3,8	1027,5
	0,0	0,0	0,0
	-0,2	-1,4	387,6
	-0,2	-1,4	387,6
	0,0	0,0	0,0
	0,0	0,0	0,0
	0,0	0,0	0,0
	0,0	0,0	0,0
	0,0	0,0	0,0
	0,0	0,0	0,0
	0,0	0,0	0,0
	0,0	0,0	1,26
	0,0	0,0	0,00
	0,0	0,0	0,00
	0,0	0,0	0,00
	-1,2	-8,6	2320

Kommentarer:

Gule felt fylles ut, grønne beregnes.

Når fukt i tilslaget er bestemt på basis av ovnstørt tilslag skal absorbert fukt angis med målt verdi. Tilhørende densitet skal da også være basert på tørt tilslag . Dersom fukt i tilslaget er gitt på

SSD-basis settes absorbert fukt lik 0. I så fall skal densitetene også angis som SSD-densitet.

TSS angis i våt vekt. Ved beregning av volum, densiteter og masseforhold regnes vanninnholdet i TSS med i den fri vannmengden. Dette gjelder også korrigert resept. Dersom innveid mengde TSS avviker fra proporsjonert mengde korrigeres masseforhold og mengde fritt vann i korrigert resept automatisk.

Blandeskjema

Blandevolum:	35 liter
Dato:	2, mars 99 Bland6
Tidspunkt for vanntilsetning	
Ansvarlig:	Terje K.
Utført av:	ALLE

Materialer	Resept kg/m ³	Sats kg	Fukt %	Korr. kg	Oppveid kg
Norcem Standard FA	349,2	12,222			12,222
Silikastøv	0,0	0,000			0,000
Flyveaske	0,0	0,000			0,000
Fritt vann	174,8	6,118		-1,149	4,969
Absorbert vann	9,2	0,321			0,321
Årdal 0-8 mm	1102,2	38,577	2,8	1,080	39,657
Årdal 0-2 mm MS (v)	0,0	0,000	0,0	0,000	0,000
Årdal 8-11mm	734,8	25,718	0,0	0,000	25,718
Årdal 11-16 mm	0,0	0,000	0,0	0,000	0,000
	0,0	0,000	0,0	0,000	0,000
	0,0	0,000	0,0	0,000	0,000
	0,0	0,000	0,0	0,000	0,000
	0,0	0,000	0,0	0,000	0,000
	0,0	0,000	0,0	0,000	0,000
RMC-420	2,4	0,084	82	0,069	0,084
0	0,0	0,000	0	0,000	0,000
	0,0	0,000	0	0,000	0,000
	0,0	0,000	0	0,000	0,000

5,290

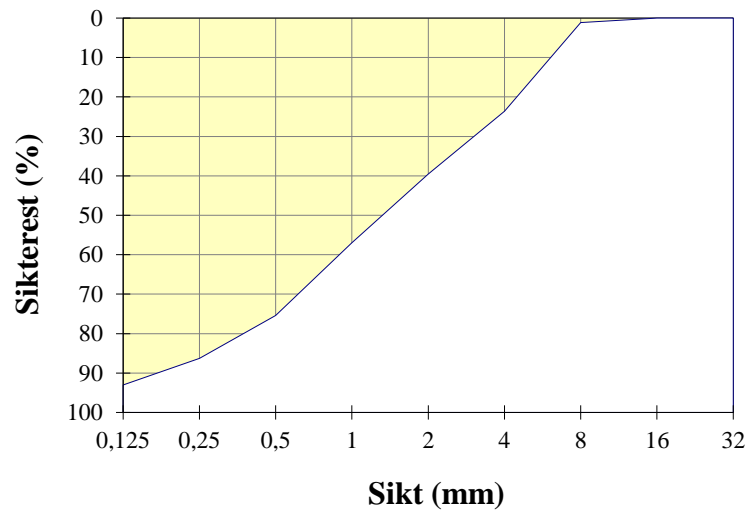
Fersk betong						
Tid etter vanntilsetning						
Synkmål						
Utbredelsesmål						
Luft						
Densitet						

Prøvestykker (antall)						
Utstøpningstidspunkt						
Terninger	3					
150x300 sylindre	0					
100x200 sylindre						

Fraksjon I

Type:	Årdal 0-8 mm
Dato:	97-11-24
FM =	3,29

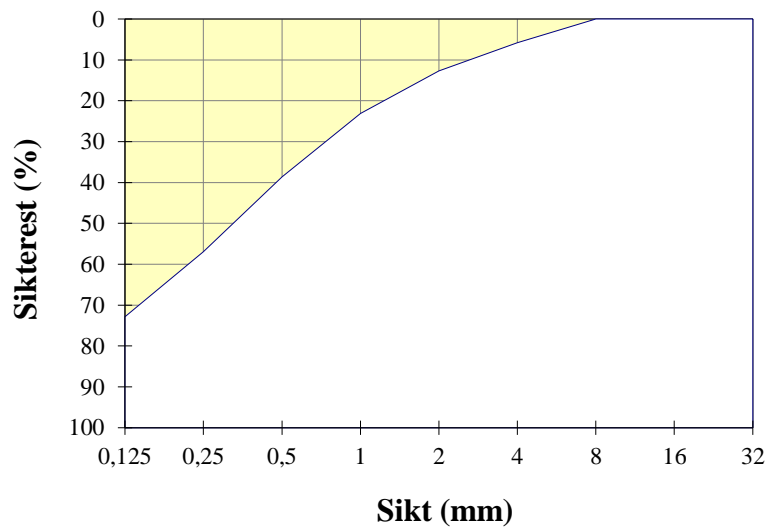
Åpning	Sikterest (g)		Sikterest (%)
	1	2	
32	0	0	0,0
16	0	0	0,0
8	9,5	13,1	1,1
4	259	213	23,6
2	431	360	39,6
1	608	532	57,0
0,5	781	727	75,4
0,25	874	852	86,3
0,125	933	927	93,0
Bunn	1000	1000	



Fraksjon II

Type:	Årdal 0-2 mm MS (v)
Dato:	97-11-22
FM =	1,74

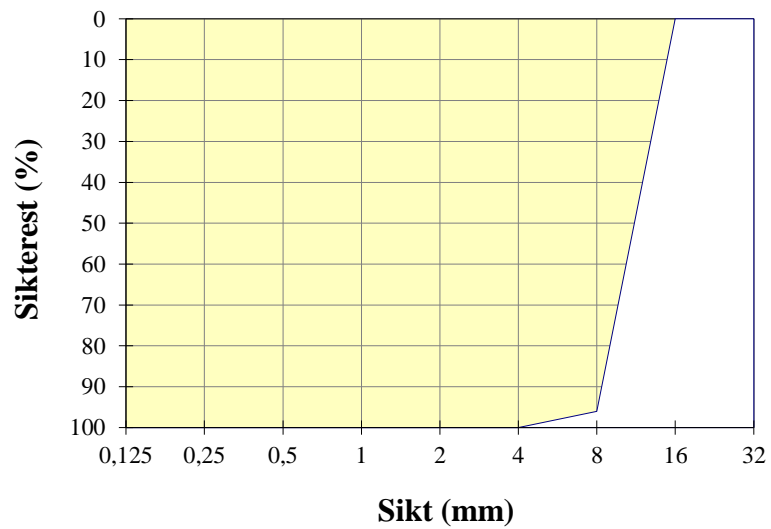
Åpning	Sikterest (g)		Sikterest (%)
	1	2	
32	0	0	0,0
16	0	0	0,0
8	0	0	0,0
4	29,2	28,8	5,8
2	63,9	62,4	12,7
1	115,4	115	23,1
0,5	191,9	193,4	38,6
0,25	282,6	285,1	56,9
0,125	362	364	72,8
Bunn	498	499	



Fraksjon III

Type:	Årdal 8-11 mm
Dato:	97-11-22
FM =	6,46

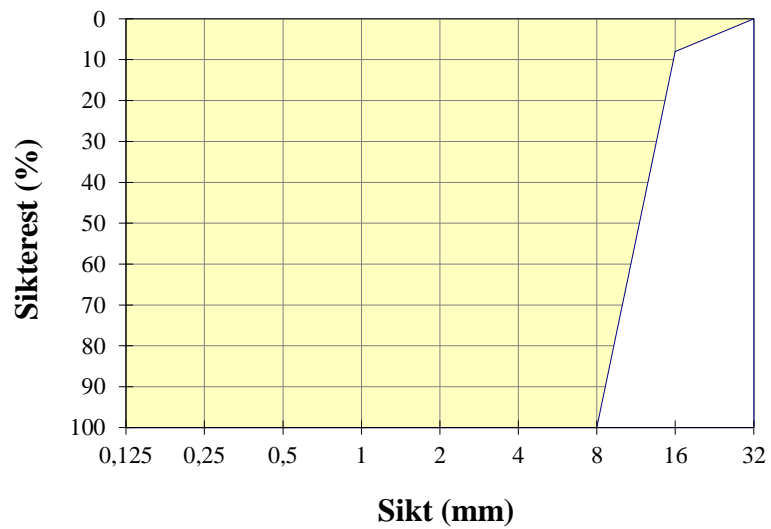
Åpning	Sikterest (g)		Sikterest (%)
	1	2	
32	0	0	0,0
16	0	0	0,0
8	96	96	96,0
4	100	100	100,0
2	100	100	100,0
1	100	100	100,0
0,5	100	100	100,0
0,25	100	100	100,0
0,125	100	100	100,0
Bunn	100	100	



Fraksjon IV

Type: Årdal 11-16 mm
Dato: 97-11-21
FM = 6,58

Åpning	Sikterest (g)		Sikterest (%)
	1	2	
32	0	0	0,0
16	8	8	8,0
8	100	100	100,0
4	100	100	100,0
2	100	100	100,0
1	100	100	100,0
0,5	100	100	100,0
0,25	100	100	100,0
0,125	100	100	100,0
Bunn	100	100	



Matriks (foreløpig versjon)

©ss 96-02-
27

Parameter	Verdi	Enhet	k
$v/(c+\Sigma kp)$	0,22	-	-
s/c	20	%	1
fa/c	0	%	0,25
f/c	0	%	-
TSS1	0	%	-
TSS2	4	%	-
Ønsket volum	0,5	l	

Delmateriale	Densitet	Fukt	Mengde
Sement	3,150	-	0,729
Silikastøv	2,200	-	0,146
Flyveaske	2,200	-	0,000
Filler	2,700	-	0,000
Vann	1,000	-	0,175
TSS1	1,200	60	0,000
TSS2	1,200	60	0,029
Matriksdensitet (kg/dm ³)	2,158		

- Masseforhold angis i forhold til valgte virkningsfaktorer
- Silikastøv, flyveaske og filler angis i prosent av sementmengde
- Tilsetningsstoffer angis som våt vektprosent av sement
- Densitet av tilsetningsstoff er densitet av tørrstoff
- I resepten angis silikastøv i tørr vekt

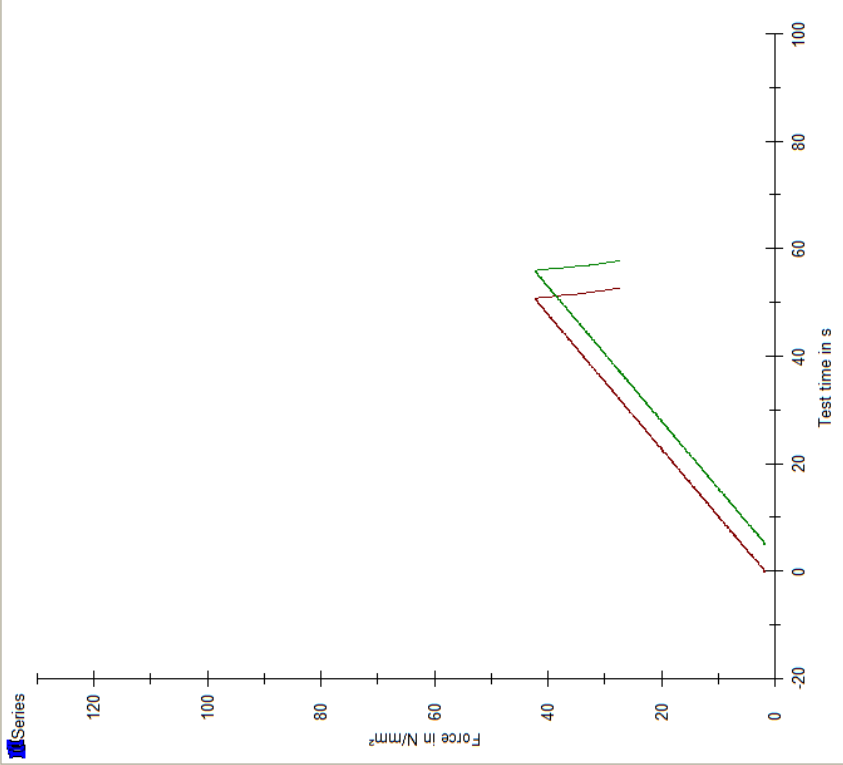
Appendix D: Concrete weight and strength measurements

File Machine Specimen management Inputs Configuration Options Help

Machine SKIFT+F2 Pos. down Pos. up Remote cor F=0 Open Entries STOP F10 Wizard CTRL+F1

Nr	Datum	ID	a	b	A	h	Weight	ρ	F_m	σ_m
			mm	mm	mm ²	mm	kg	g/cm ³	kN	MPa
1	29.11.2019	Cube-1	100,0	100,0	10000,0	100,0	2,4	2,40	421,78	42,18
2	29.11.2019	Cube-2	100,0	100,0	10000,0	100,0	2,4	2,40	422,00	42,20

Series	n	a	b	A	h	Weight	ρ	F_m	σ_m
		mm	mm	mm ²	mm	kg	g/cm ³	kN	MPa
X	100,0	100,0	100,0	10000,0	100,0	2,4	2,40	421,89	42,19
S	0,0	0,0	0,0	0,000	0,0	0,000	0,00	0,15	0,02
V	0,00	0,00	0,00	0,000	0,00	0,000	0,00	0,04	0,04



Next specimen: Mandatory inputs

Specimen ID

Specimen shape for cross-section calculation

Specimen thickness a mm

Specimen width b mm

Specimen height h mm

Weight of the specimen kg

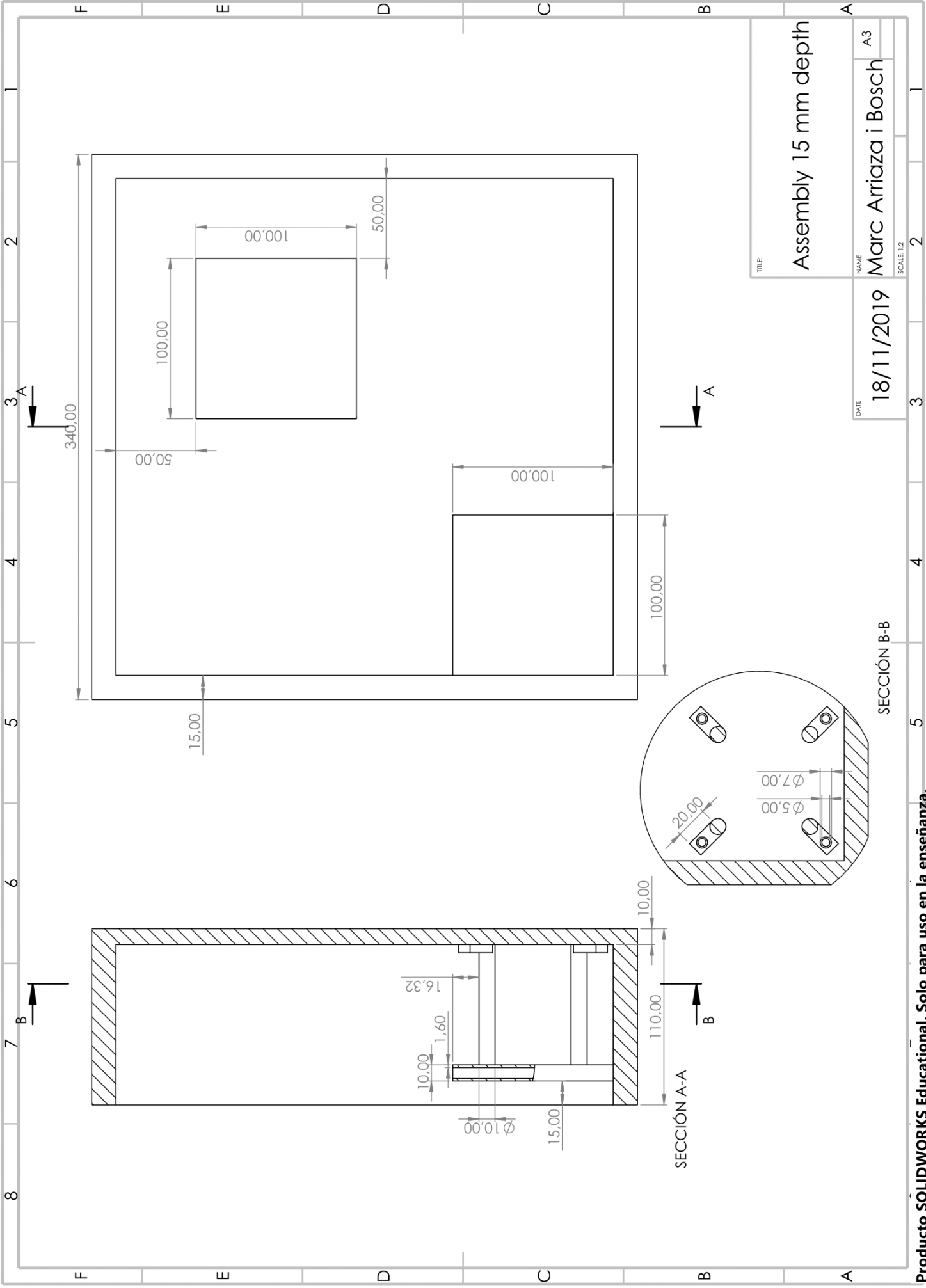
Age T

Tester

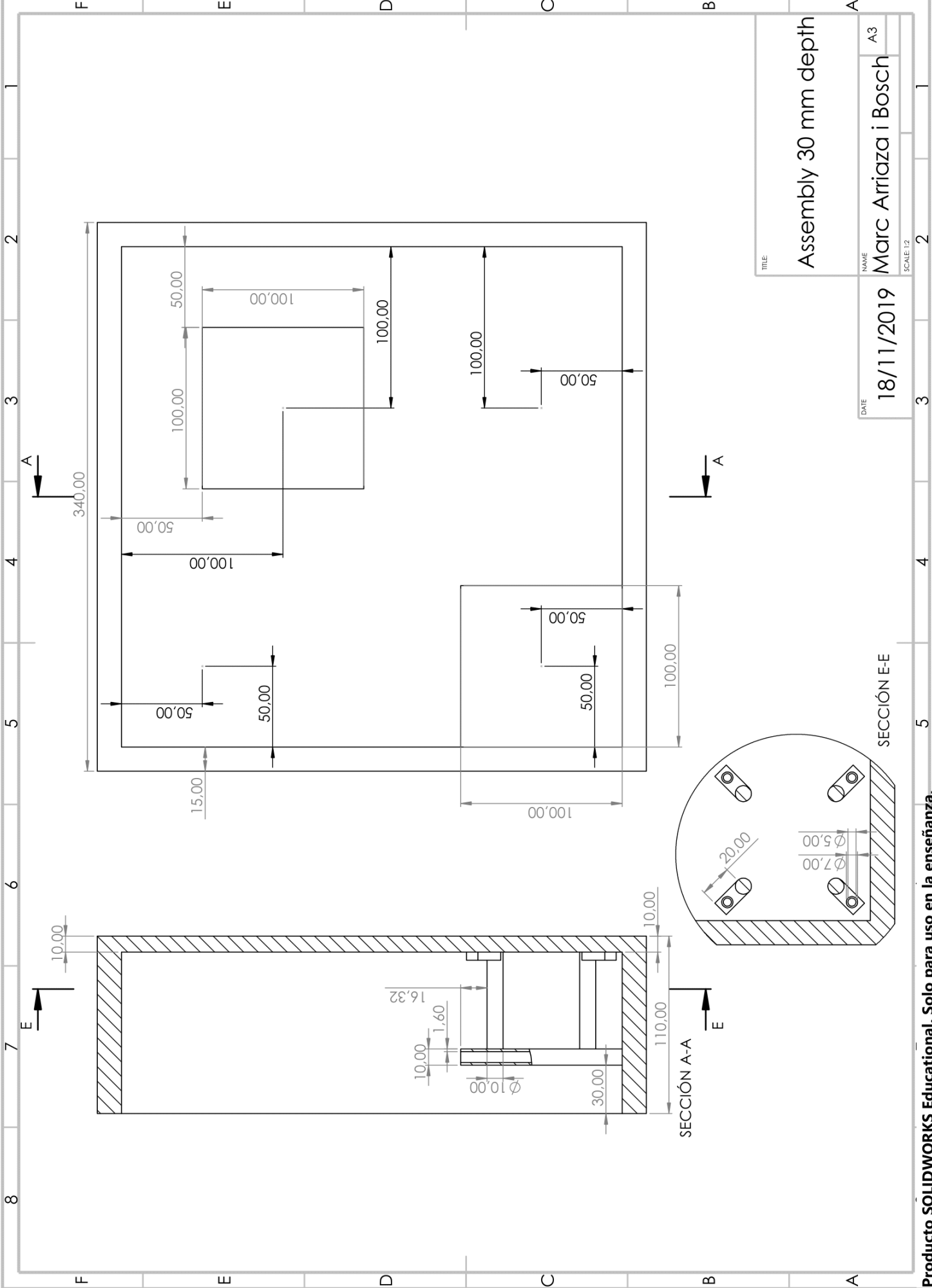
Toni Technik F [kN] S abs [mm] Frame [] 1,000

-0,17

Appendix E: Drawings of the 3D printed pieces and the moulds



TITLE	Assembly 15 mm depth
NAME	Marc Arriaza i Bosch
DATE	18/11/2019
SCALE	1:2
	A3



TITLE	Assembly 30 mm depth
NAME	Marc Arriaza i Bosch
DATE	18/11/2019
SCALE: 1:2	A3

